Studies on Cross-tier Interference Mitigation for Small Cell Networks Overlaid onto Macrocell

Thesis by

Massa Ndong

Department of Electronic Engineering

The University of Electro-Communications

This thesis is submitted for the degree of

Doctor of Philosophy

March 2015

I would like to dedicate this thesis to my dear parents, brothers and sisters, uncles and aunts... To my family, in the African sense of the word "family".

Declaration

I hereby declare that except where specific reference is made to the work of others, the contents of this dissertation are original and have not been submitted in whole or in part for consideration for any other degree or qualification in this, or any other university. This dissertation is the result of my own work and includes nothing which is the outcome of work done in collaboration, except where specifically indicated in the text. The dissertation of Massa Ndong is approved by the following committee members:

- Professor Takeo Fujii, Supervisor
- Professor Yoshio Karasawa, Member
- Professor Takeshi Hashimoto, Member
- Professor Yasushi Yamao, Member
- Associate Professor Toshiharu Kojima, Member

The University of Electro-Communications
Chofu, Tokyo

Massa Ndong
March 2015

Acknowledgements

And I am deeply indebted to a number of individuals who assisted me all along the research presented in this paper was going on. To the following people, for their support beyond university activities, I owe what I don't know how to pay back:
- my supervisor, Professor Fujii Takeo
- Professor Yasushi Yamao from AWCC
- Mr Moriyama for the Japanese translations
- The university staff
Appreciation and thanks go also to all the members of the Advanced Wireless Communication research center (AWCC) for their constant support in the laboratory and academic activities.
Finally, recognition is hereby expressed to my family for understanding and advices.

Abstract

The huge number of mobile terminals in use and the radio frequency scarceness are the relevant issues for future wireless communications. Frequency sharing has been considered to solve the problem. Addressing the issues has led to a wide adoption of small cell networks particularly femtocells overlaid onto macrocell or small cells implemented with the support of distributed antenna systems (DASs). Small cell networks improve link quality and frequency reuse.

Spectrum sharing improves the usage efficiency of the licensed spectrum. A macrocell underlaid with femtocells constitutes a typical two-tier network for improving spectral efficiency and indoor coverage in a spectrum sharing environment. Considering the end-user access control over the small cell base station (SBS), with shared usage of the macrocell's spectrum, this dissertation contribution is an investigation of mitigation techniques of cross-tier interference. Such cross-tier interference mitigation leads to possible implementation of multi-tier and heterogeneous networks.

The above arguments underpin our work which is presented in the hereby dissertation. The contributions in this thesis are three-fold.

Our first contribution is an interference cancellation scheme based on the transmitter symbols fed back to the femtocell base station (FBS) undergoing harmful cross-tier interference. We propose a cross-tier interference management between the FBS and the macrocell base station (MBS) in uplink communications. Our proposal uses the network infrastructure for interference cancellation at the FBS. Besides, we profit from terminal discovery to derive the interference level from the femtocell to the macrocell. Thus, additionally, we propose an interference avoidance method based on power control without cooperation from the MBS.

In our second contribution, we dismiss the use of the MBS for symbol feedback due to delay issues. In a multi-tier cellular communication system, the interference from one tier to another, denoted as cross-tier interference, is a limiting factor for the system performance. In spectrum-sharing usage, we consider the uplink cross-tier interference management of heterogeneous networks using femtocells overlaid onto the macrocell. We propose a variation of the cellular architecture and introduce a novel femtocell clustering based on interference cancellation to enhance the sum rate capacity. Our proposal is to use a DAS as an

interface to mitigate the cross-tier interference between the macrocell and femtocell tiers. In addition, the DAS can forward the recovered data to the macrocell base station (MBS); thus, the macrocell user can reduce its transmit power to reach a remote antenna unit (RAU) located closer than the MBS. By distributing the RAUs within the macrocell coverage, the proposed scheme can mitigate the cross-tier interference at different locations for several femtocell clusters.

Finally, we address the issue of cross-tier interference mitigation in heterogeneous cognitive small cell networks comparing equal and unequal signal-to-noise ratio (SNR) branches in multi-input multi-output (MIMO) Alamouti scheme. Small cell networks enhance spectrum efficiency by handling the indoor traffic of mobile networks on a frequency-reuse operation. Because most of the current mobile traffic happens indoor, we introduce a prioritization shift by imposing a threshold on the outage generated by the outdoor mobile system to the indoor small cells. New closed-form expressions are derived to validate the proposed bit error rate (BER) function used in our optimization algorithm. We propose a joint transmit antenna selection and power allocation which minimizes the proposed BER function of the outdoor mobile terminal. The optimization is constrained by the outage at the small cell located near the cooperating transmit relays. Such constraint improves the initialization of the iterative algorithm compared to randomly choosing initial points. The proposed optimization yields a dynamic selection of the relays with power control pertaining to the outdoor mobile terminal performance.

Table of contents

List of figures

List of tables

Chapter 1

Introduction

1.1 Overview

Due to the high demand in mobile communications and the need to improve spectral efficiency, small cell networks particularly femtocells overlaid onto macrocell or/and small cells implemented with the support of distributed antenna system (DAS) have been actively considered. Classic cellular systems have a large coverage spanning beyond 1 km of radius. Such deployment is subject to large scale fading with received power decaying as the distance between transmitter and receiver increases. In addition, multipath propagation generates fading which reduces capacity and spectral efficiency. Small cells are mainly indoor systems operating in a range below 50 m. Thus, they are small networks which improve link quality and spatial frequency reuse.

Femtocells are small cellular networks overlaid onto macrocells [1]. A femtocell is a low cost access point (AP) operating in a frequency-reuse with the macrocell. A femtocell base station has the same maximum transmit power as a macrocell outdoor mobile user equipment. Thus it is a low powered hotspot. Femtocells are connected to the operator backhaul via optical line or Digital Subscriber Line (DSL). Femtocells are deployed indoor in standards such as the 3rd Generation Partnership Project (3GPP) Long Term Evolution (LTE) and the Worldwide Interoperability for Microwave Access (WiMAX or IEEE 802.16e) [2].

A femtocell is basically constituted by a femtocell base station (FBS) and a few number of mobile users denoted as femtocell user equipment (FUE). A femtocell is operating in an open regime if any outdoor mobile user equipment can do a handover to the FBS without being a registered user. In contrast to open regime operation, in close regime operation, a mobile user equipment has to be registered with the FBS to be granted communications with it. Either mode of operation has been considered in the literature along with hybrid operation in which opportunistic schemes are defined for the FBS to operate in both modes [3]. A

communication system of femtocells overlaid onto macrocells constitutes a typical two-tier network for improving spectral efficiency and indoor coverage. In contrast to classic cellular system which are owned and controlled by telecommunications operators, a femtocell is owned by the end-user who can switch it on and off deliberately.

Similarly to femtocell, small cells based on Distributed Antenna System (DAS) has been considered. A DAS is a network of several radio heads (RAU) located separately from each other and sharing a common source (CPU). Each RAU cover a small area. An RAU can be an indoor or outdoor equipment. The distribution of the RAUs ensures an effective coverage of several small areas. However, this is achieved at the cost of a complex system architecture. DAS is promoted by the HetNet forum which was formerly the DAS forum [4]. The base station of the small cell network (SCN) is a remote antenna unit (RAU) connected via optical line to a Central Processing unit (CPU). The RAU is a simple radio frequency (RF) head devoid of any signal processing ability. Several RAUs can be connected to a CPU. A number of 6 RAUs sharing a CPU is considered in [5]. The CPU bears all signal processing such as modulation and demodulation, resource allocations for the RAUs and ensures connectivity between RAUs and with the backhaul. The DAS-based small cell can be deployed outdoor or indoor. Several works have considered the cooperation of the RAU to propose network-Multiple Input Multiple Output [6] schemes and received signal recovery via multiple antenna processing. Indeed, as the CPU is a common interface connected via a wire to several RAUs differently located, received signals at the RAU can be sent to the common CPU for network coding [7], interference cancellation [8].

In this paper, indoor deployment of small cell networks is considered. Both femtocells and DAS-based small cell are considered in this study. We will generally use the term small cell network to refer to a femtocell or DAS-based small cell network.

1.2 Motivation

Due to the current drastic growth of the indoor communication occurrences with mobile equipment such as laptops, smartphones and tablets, there is a need to address such data-craving demand by innovative and modern approaches which can fill the gap left by the conventional methods. Laptops, smartphones and tablets are end-user controlled terminals. Their communication occurrences are usually modelled by a Poisson distribution. Small cell networks are user friendly small networks which can be easily deployed according to end-user needs. The motivation in this dissertation is to develop small cell network deployment schemes which ensures that mobile terminals served by small cells can achieved their targeted data rates while sharing frequency with the legacy macrocell.

The coexistence between small cell networks and legacy macrocell raises the issue of cross-tier interference mitigation. Cross-tier interference is the electromagnetic impedance occurring from the macrocell/femtocell tier to the femtocell/macrocell tier. The macrocell tier as the primary system constituted by the macrocell base station (MBS) and the mobile user equipment (MUE) connected to the SBS. Usually, the MUEs are outdoor mobile equipment. The femtocell tier is a secondary system overlaid onto the macrocell tier and is constituted by the SBSs and the indoor MUEs connected to SBSs. For instance, in uplink operation, the interference from an outdoor MUE transmitting from a far distance to the MBS can drastically generate outage at nearby cochannel SBSs especially if the SBSs are operating in close regime [9].

Considering the end-user access control over the small cell base station (SBS), with shared usage of the macrocell's spectrum, this dissertation investigates mitigation techniques of cross-tier interference. As previously mentioned, the number of mobile users supported by a single SBS is small compared to a tower macrocell which covers large areas. Thus, customized interference mitigation schemes can be adopted for small cell networks. Such techniques can be implemented on chosen SBSs in desired areas. Another reason for such approach to handle small cell deployment is the fact that the cross-tier interference has a different impact on each SBS or each small cell user equipment (SUE) in the case of interference from the MBS or the MUE to the SCN. By choosing a modularity approach to solve the cross-tier interference, virtual small cell clusters can be formed to adopt a proposed scheme as illustrated in Chapter 3. We advocate control schemes which enable the SBS to individually cancel cross-tier interference and transmit with optimal powers. The control schemes can be implemented at the SBS to allow cross-tier interference aware self-access control and self-connectivity. Addressing cross-tier interference mitigation in a distributed manner is crucial to the offload role of small cell networks as the data rate of the SCN should remain unaffected while the addition of the SCNs has to be seamless and devoid from harmful interference to the macrocell tier. Such mitigation leads to possible implementation of multi-tier and heterogeneous networks based on small cell networks.

1.3 Thesis Presentation and Contributions

This dissertation has the following contributions:

- Our first contribution is an interference cancellation scheme based on the transmitter symbols fed back to the femtocell base station (FBS) undergoing harmful cross-tier interference. We propose a cross-tier interference management between the FBS and the macrocell base station (MBS) in uplink communications. Our proposal uses the

network infrastructure for interference cancellation at the FBS. Besides, we profit from terminal discovery to derive the interference level from the femtocell to the macrocell. Thus, additionally we propose an interference avoidance method based on power control without cooperation from the MBS.

- In our second contribution, we dismiss the use of the MBS for symbol feedback due to delay issues. In a multi-tier cellular communication system, the interference from one tier to another, denoted as cross-tier interference, is a limiting factor for the system performance. In spectrum-sharing usage, we consider the uplink cross-tier interference management of heterogeneous networks using femtocells overlaid onto the macrocells. We propose a variation of the cellular architecture and introduce a novel femtocell clustering based on interference cancellation to enhance the sum rate capacity. Our proposal is to use a (DAS) as an interface to mitigate the cross-tier interference between the macrocell and femtocell tiers. In addition, the DAS can forward the recovered data to the macrocell base station (MBS); thus, the macrocell user can reduce its transmit power to reach a RAU located closer than the MBS. By distributing the RAUs within the macrocell coverage, the proposed scheme can mitigate the cross-tier interference at different locations for several femtocell clusters.

- Finally, we address the issue of cross-tier interference mitigation in heterogeneous cognitive small cell networks comparing equal and unequal signal-to-noise ratio (SNR) branches in multi-input multi-output (MIMO) Alamouti scheme. Small cell networks enhance spectrum efficiency by handling the indoor traffic of mobile networks on a frequency-reuse operation. Because most of the current mobile traffic happens indoor, we introduce a prioritization shift by imposing a limitation on the outage generated by the outdoor mobile system to the indoor small cells. New close-form expressions are derived to validate the proposed bit error rate (BER) function used in our optimization algorithm. We propose a joint transmit antenna selection and power allocation which minimizes the proposed BER function of the outdoor mobile terminal. The optimization is constrained by the outage at the small cell located near the cooperating transmit relays. Such constraint improves the initialization of the iterative algorithm compared to randomly choosing initial points. The proposed optimization yields a dynamic selection of the relays with power control pertaining to the outdoor mobile terminal performance.

Fig. 1.1 shows the current and "future" state of cellular system given the ubiquitous communications among mobile equipment. Both hardware design limitation and misuse of spectrum have led to the inability of the current wireless system to satisfy the demand in mobile

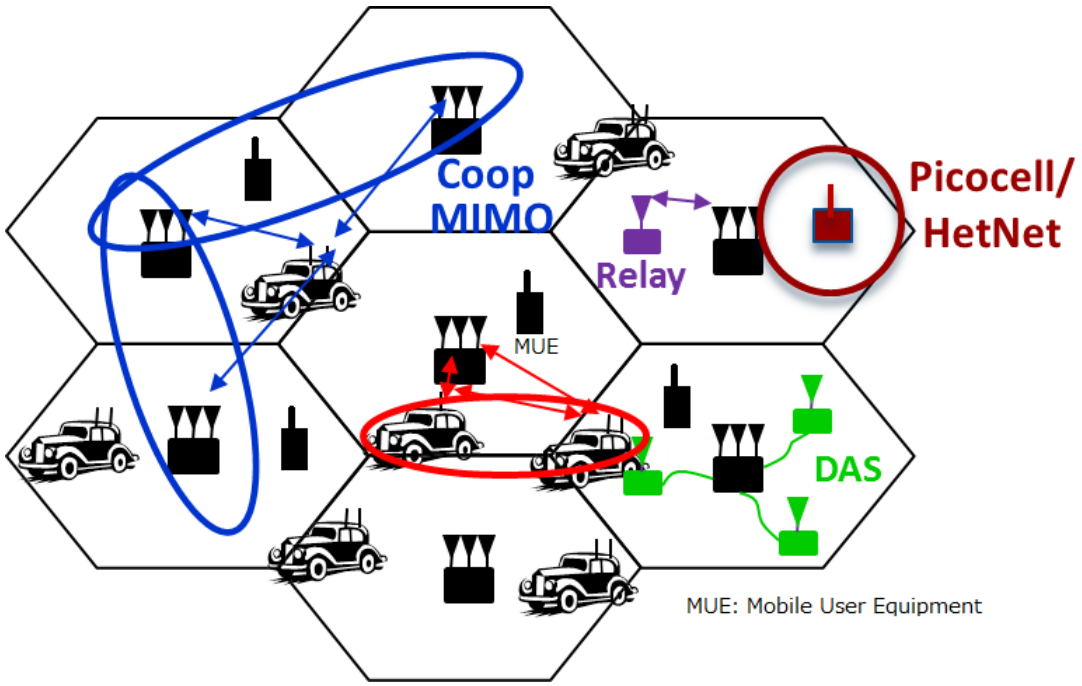

Fig. 1.1 Heterogeneous wireless communication coexistence as future wireless cellular system.

data traffic. The cellular systems reuse frequency to maximize capacity. Frequency, timeslot and code are different degrees of freedom reused at spatially-separated locations to improve the cellular system capacity. To keep up with the user demand and future capacity requirements, the current design of cellular system is driven by interference mitigation techniques. An interference-limited design is required for gains in capacity or coverage. The cooperation of heterogeneous wireless systems, as introduced in chapter 4, is shown as the solution to current cellular issues. Such solution requires effective interference reduction for reliable implementation. Fig. 1.1 presents the exploitation of cooperative multi-input-multi-output (MIMO) over different multi-antenna transceivers spatially separated over differen cells. The cells are implemented with distributed antenna system (DAS), relaying and small cells. Introducing relays in a cell changes it boundaries while the small cell creates a cell within a cell. Considering Fig. 1.1, we focus on the design of future cellular underpinned by interference mitigation.

This dissertation is presented as follows. In Chapter 2, we present the state of art research current progress on femtocells and DAS-based small cell networks. Chapter 3 presents an interference cancellation scheme for LTE-based femtocell which uses information feedback via the backhaul from the MBS. In Chapter 4, we leverage the interference cancellation scheme discussed in Chapter 2 to propose a distributed cross-tier interference management

using multicast feedback information to a virtual femtocell cluster which can perform interference cancellation. Chapter 3 and 4 system models are based on uplink transmission. In Chapter 5, we use a new approach to cross-tier interference mitigation by proposing a joint relay selection and adaptive power allocation for cognitive small cell networks in downlink. Chapter 6 presents the conclusion of this dissertation along with the future work.

Chapter 2

Spectrum sharing with small cell overlaid onto macrocell

2.1 Background

Early radiocommunications are known from works from *Marconi* and *J.C.Bose* since 1895 [10, 11]. Long range (up to 100 *km*) radiocommunications were possible with the use of low frequency spectrum (15 *khz*), and higher frequency were used later for short range communications where directivity and security were sought after [10]. Since then, it has received a huge attention from wireless communications academia. The performance limit of wireless channels hit a milestone in 1948 with *Claude Shannon's* work [12] in information theory defining the capacity of a wireless channel in function of the channel bandwidth, noise at the receiver and fading. As mentioned in [13, 14], cellular systems have to reuse their allocated spectrum at different areas (spatially-separate locations) to improve spectral efficiency.

Early cellular systems were GSM, GPRS and EDGE. GPRS and EDGE are evolved implementations of the GSM offering a higher bit rate. The main transmission technologies were CDMA and WCDMA. The 3*rd* generation of cellular networks or 3*G* adopted OFDM as a transmission technology. The first OFDM system was described in [15] and consisted of a basic multi-band transmission scheme. The works in [16, 17] show how the Fourier mathematical analysis can be used to implement the multi-band modulation. The implementation of the OFDM system using the fast Fourier transform proposed by Cooley and, the introduction of the use of guard interval by *Tristan de Couasnon* to address the issue of frequency selective channels led to the industrial adoption of OFDM as the main cellular system transmission technology. OFDM has been shown to be the main multi-band systems suitable to address the requirements of future wireless systems considering conception and

design evolution of multi-carrier systems. As currently adopted by cellular system operators, OFDM symbol multiplexing on a bandwidth divided into multi-carrier outperforms the $1st$, $2nd$ and $3rd$ generations of cellular system based on WCDMA.

In mobile environment, signals undergo several impairments due to buildings, Non Line Of Sight (NLOS), reflexion, refraction, transceiver motion, etc. With such propagation space, signals propagating via multipath is a phenomenon very likely to occur. When signal multipath occurs, the received signal becomes a summation of several versions of the initially transmitted signal, each version with a phase affected by its delay. Such delay is due to the several paths used by a signal components to reach their destination. Destructive additions of such signals worsen the ability of the wireless communications system to recover the transmitted signal at the receiving side.

Fading is a random fluctuation of a signal in wireless communications of its phase, amplitude or frequency. The factors which underpin such changes in the signal power are scatterers or reflecting objets such as man made constructions (buildings,...), motion of a transceiver such as mobile phone,etc. The basics mechanisms that affects mobile propagation are :

$*$ reflection: This phenomenon occurs if an electromagnetic wave reflects on a surface wider than the carrier wavelength.

$*$ diffraction: Diffraction occurs when the transmitted signal reaches the receiver by propagating through shadowing objects without LOS. The shadowing objects have dimensions larger than the wavelength. Diffraction is also called Shadowing.

$*$ scattering: A signal scatterer(lamppost, street sign, foliage) which has dimensions in the order or less of the wavelength of the transmitted signal, causes the signal to spread out (scatter) after impingement against the scatterer surface.

Current cellular systems are mainly based on LTE, WiMAX and DAS which are supported by the $3rd\ Generation\ Partnership\ Project$ ($3GPP$), IEEE 802.16 and the HetNet-Forum standards respectively. OFDMA has been adopted as the transmission technology by contemporary cellular systems. However, in LTE, OFDMA is adopted on the downlink while SC-FDMA is adopted in the uplink. Considering a general approach to small cell networks, we adopt OFDMA in this thesis. We believe that our proposal can be easily adapted for LTE or WiMAX specifications.

OFDMA is a multiple access scheme based on OFDM. Considering random phases, two signals' frequencies have to be separated by at least the inverse of the symbol period to be orthogonal. Users are allocated time slots to use the available spectrum. A slot in OFDMA is a data region within the radio resource assignment structure. OFDMA divides the FFT size into subchannels which are sets of subcarriers. The structure of the sets depends on the

permutation mode; the subcarriers within a subchannel may be adjacent or not. The number of subcarriers within a subchannel is also variable pertaining to whether the permutation mode is PUSC, AMC, FUSC [18]. In addition to the FDMA feature of OFDMA, a time dimension is included to the radio resource allocation. In fact the slot allocated to a user is defined as a set of subcarriers during a period of time. Thus a slot can be defined as a set of subcarriers and a number of OFDMA symbols.

The legacy macrocell architecture is basically constituted of a tower-mounted base station transmitting and receiving from mobile handsets. In urban area, the communications between the macrocell base station (BTS) and a mobile equipment is seldom a line-of-sight exchange. Indeed, at the receiver (BTS or mobile equipment), the received signal is the result of aggregated signals which have experienced different delays and fading. The fading in such none line-of-sight environment is called multipath fading or small scale fading because the channel fluctuations occurs within ms-range of time intervals. In addition to small scale fading, large scale fading is one of the parameters which decreases the received power of a transmitted signal in cellular networks. From [14], the received power decreases as the distance between transmitter and receiver increases. Such power decaying with distance law and multipath fading have prompted the adoption of small cell networks which average operating range is less than 50 m. The classic macrocell radius spans over 1000 m. The adoption of small cell networks enables the operation of a high density of mobile equipment. The traffic of the BTS can be offloaded by the small cells specially in indoor communications.

2.2 Current advances in cellular systems regarding spectrum sharing and small cell networks

Current wireless systems are cellular systems, wireless local area networks, WiGig and mmWave communications, cognitive radios, satellite systems and, Bluetooth and Zigbee radios.

The ICT-Befemto project extends the concept of femtocell by deploying femtocell-based network using LTE-Advanced (LTE-A) [19]. In ICT-BeFemto, as shown on Fig. 2.1, terms such as Fixed relay femto, Mobile Femto, stand-alone Femto and Networked femto are coined to mean an FBS serving as a relay, a moving femtocell such as a hotspot in a vehicle, a fixed femtocell base station in an end-user premises and a network whose backhaul is constituted by connected femtocell base stations respectively. The ICT-Befemto promotes the implementations of self-organized/self-optimised (SON) femtocell. In the literature doci-

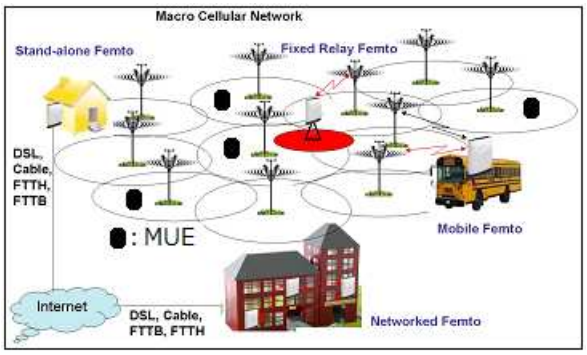

Fig. 2.1 Femtocell concept based on 3*GPP* LTE.

tive [20] and cognitive femtocell [21] performance improving schemes are considered.

Current $4G-LTE$ cellular system has a data rate spanning between 50 $Mbps$ and 100 $Mbps$. It has a flexible use of a bandwidth of 100 MHz with a 20 $4MHz$ common spectrum allocation. The packet latency is low (below 5 ms). The core network is an all IP network [2]. The $3GPP/LTE$ standard has develop a type of SCN denoted as SON. The architecture presents a SON server integrated in the core network which communicates with the macrocells and femtocells via a wired backhaul. Each FBS is connected to an MBS via a wired link (denoted by $X2$ in LTE). After installation and initial measurements, the SBS can perform self-configuration, self-healing from interference and self-optimization to avoid causing outage to nearby SONs. Small cells create a cell within a cell. The SBSs can cooperate to act as relays, or in a virtual MIMO or network coding schemes. Small cells are currently advocated as the solution to increase cellular system capacity [22] by resorting to spatial frequency reuse.

In small cell networks overlaid onto macrocells, spectrum sharing techniques are either universal [23] or fractional frequency [24] reuses. In universal frequency reuse, the SCN uses the whole bandwidth available to the macrocell tier while fractional frequency reuse (FFR) divides the bandwidth into subbands which are fractionally accessible to a SCN. The physical and MAC layer design is based on orthogonal frequency division multiple access. The network topology of two-tier networks constituted by SCNs overlaid onto macrocell is mathematically based on the pioneering work on Poisson Point Process (PPP) [25, 26]. Current academic theory leverages the work in [25, 26] to present analyses of twin-layer wireless networks using stochastic geometry [27–29]. In the PPP model, stochastic geometry is used to model the locations of the SBSs, SUEs, MBS and MUEs in the area occupied by the two-tier network. Such model yields a mathematical framework for cross-tier interference analysis [30]. The cross-tier interference framework analysis developed using stochastic geometry based on PPP leads to the computation of key performance metrics

such as coverage probability and average rate [30]. It also provides insights into heterogeneous network interference. In Chapter 4, we use the protective zone (or guard zone) defined in [31] to enable a perfect reception of the signal which should be multi-cast to the virtual cluster for interference cancellation. The analysis and configuration parameters of the protective zone are defined using stochastic geometry and PPP. The work in [30] presents a Gamma approximation of the Rayleigh fading component to evaluate coverage probability success and average data rate of the assumed interference-limited system. Considering cross-tier interference outside protective zone, the co-channel interference can be modelled into two components: a dominant interference and a lower interference. Such heterogeneous interference characterisation is difficult to analysis without stochastic geometry modelling because of tractability issues. An overview of the use of stochastic geometry for modelling, analysis and design of multi-tier (such as SCNs overlaid onto macrocells) and cognitive cellular wireless networks is considered in [28].

As a secondary system coexisting with the legacy macrocell, the SCN operates in frequency sharing usage. The issue widely considered in the literature is which portion of the macrocell spectrum can be accessed by the SCN without degrading the performance of the macrocell tier. The femtocell concept is similar to cognitive radio. FFR schemes has been widely considered given that LTE-A and WiMAX are based on orthogonal frequency division multiple access (OFDMA). The use of OFDMA defines subchannels which can be accessed according to some scheduling algorithms. Therefore, many studies present FFR based spectrum sharing schemes. The work in [32] casts of the universal frequency sharing usage into a non-cooperative (selfish) and hierarchical game theory approaches. In information theory, it has been shown that hierarchical cooperation achieves optimal capacity scaling in Ad Hoc networks [33]. In [32], the hierarchical approach consists of prioritising the macrocell tier as a primary system over the femtocell. The cooperation consists of information exchange between the MBS and the Small cell Base Stations (SBSs), and the SBSs have to minimize their interference on the MBSs. The authors used Stackelber equilibrium to derive the MBS transmit power in the hierarchical strategy and Water-filling for the selfish game. A third strategy denoted as centralised strategy is devised in [32] where the channel state information between tiers is known at both tiers. The centralised presents a higher network sum-rate than the hierarchical scheme which outperforms the selfish scheme. As in [32], the spectrum allocation for non-game theory based frequency sharing in two-tier networks, the spectrum access is based on the cognitive concept that the femtocell tier interference to the macrocell has to be mitigated efficiently. The signal-to-noise-plus-interference ratio (SNIR) is the main parameter chosen to evaluate the probability of outage in either tier [24, 34].

The concept of Heterogeneous Networks (HetNets) is based on a conglomerate of heterogeneous low-power infrastructure elements such as microcells, picocells, femtocells and DASs using RAUs [35–38]. The special features are their small coverage area, backhaul connectivity and propagation characteristics [35]. DAS cooperation for SCN successful coexistence with legacy macrocell and future HetNets deployment is considered in [36] and Chapter 4. Cell throughput maximization is considered. In [37]DAS is used to improve the coverage at cell edge and coordinated multipoint (COMP) cooperation with the base station in universal and FFR schemes. The deployment of DAS RAUs at the cell edge provides a shorter link to the MUE and multiplexing gain by exploiting the angular separation of the mobile users. With the DAS cooperation, without COMP, a throughput of 6.61 $bits/symbol$ is achieved. Such results invite to the implementation of HetNets-based small cells using DAS. As mentioned in Chapter 4 the cooperation of DAS systems with macrocell system can involve several operators. The technical aspects of sharing small cells and spectrum by multiple operators are studied in [39]. Several deployment are presented using DAS and femtocells respectively.

This thesis considers universal frequency reuse and evaluates the performance of multi-tier networks considering the issue of cross-tier interference mitigation. In Chapter 3, we propose an interference cancellation scheme at the SCN base station with information feedback from the MBS.

Chapter 3

Cross-tier interference cancellation for small cell networks in spectrum sharing with macrocell

Contemporary wireless operators are in the process of deploying short range cellular systems called femtocells. Such deployment occurs within an already existing wider cell denoted macrocell. Embedding a femtocell in a macrocell induces a cellular system structured as a two-tier network. The femtocell tier is made of the femtocell base station (FBS) and its connected mobile terminals called femtocell user equipments (FUEs). The MBS and its related mobiles denoted as MUEs constitute the macrocell tier. The communication between the FBS and the MBS goes through a wired backhaul. Femtocells may be embedded into a macrocell to improve the spectral efficiency of the resulting two-tier network's area [40]. Femtocells are deployed to satisfy the increasing demand of indoor data rate. As an end-user-owned cellular system for the next generation of femtocells, the FBS and the FUEs should be endowed with advanced decentralisation features to handle cross-tier interference management.

3.1 Introduction

Works related to femtocell deployment in co-channel operation with macrocells have focused on power control through cooperation between the FBS and its femto-connected FUEs, and partitioned spectrum usage. As an underlaid system to the macrocell, it is necessary for the femtocell to avoid impeding the MBS. To address the issue, sensing and adaptive

power allocation are additional considerations urged by cross-tier interference management. In [41], a rate optimization has been considered with a power control and a soft sensing by a Secondary System (SS) terminal to avoid any impairments at a Primary System (PS) base station. The coexistence between PS and SS has been an incentive for our considered macrocell embedded with a femtocell. Indeed, in a universal frequency reuse, we consider that the femtocell should avoid impeding the macrocell while mitigating the cross-tier interference from the macrocell to the femtocell. Optimizing the subchannel allocation in a decentralised frequency planning macrocell embedded with femtocells is considered in [34]. The power control in [42] defines utility functions that ensures that the MUEs and FUEs transmit at a maximum power under SINR constraints. In [34, 42], interference avoidance is advocated to mitigate the cross-tier interference from both tiers by transmit power limitation and different spectrum allocation between the two tiers. While considering universal frequency reuse in this chapter, we propose a decentralized interference avoidance method from the femtocell to the macrocell. Cross-tier interference mitigation methods in both uplink [43, 44] and downlink [45] leads to throughput gains and per subchannel sum-rate maximization in orthogonal system such as WiMAX and LTE. Channel information from the mobile terminals is required and the power limitations are exerted on FUEs to reduce their interference level. However, the interference mitigation method leads to a lower throughput performance than in an overall spectrum sharing. Macrocell overlaid with femtocell remains a cross-tier interference limited system as stipulated in prior work [9, 46, 47] where the cross-tier interference to the femtocell from the MUE random position has to be addressed.

This chapter considers Uplink spectrum sharing usage between a PS constituted by an MBS and its connected MUE, and an SS constituted by an FBS and its connected FUE. We assume that the femtocell operates in a closed access, i.e. only a FBS registered FUE is allowed to communicate with the considered FBS. We propose an interference cancellation and a power control schemes which applied together implement an advanced scheme to enhance small cell networks performance. Our contributions herein are of two folds:

- In a macrocell embedded with a femtocell, the MUE can be transmitting to the MBS while in the vicinity of the FBS, such that the symbols transmitted from the FUE are not resolvable at the FBS; an illustrating situation is given by a visiting MUE to the home sheltering the FBS which operates in a closed access regime. Considering that such drastic interference situation occurs randomly in spectrum shared femtocell networks, we propose an interference cancellation at the FBS using the macrocell information feedback through the two-tier network infrastructure. The interfering MUE's symbols are fed back by the MBS to the FBS to mitigate the interference from the macrocell tier to the femtocell tier. We assume that the backhaul connecting the

femtocell and macrocell networks can be used to ensure such feedback. The symbols sent by the FUE can be recovered from the interfered signal enhancing the femtocell throughput to the extent of cancelling out the interference from the MUE.

- To avoid the interference from the femtocell tier to the macrocell tier, we propose the following power control scheme: the FBS uses its received power measurements to adapt its operating parameters concordant with the interactions with the PS. Assuming the knowledge of geographical positions of the terminal in the two-tier network, we derive the suitable transmit power for the FUE to ensure interference avoidance from the FUE to the MBS.

We confirm through computer simulations that the throughput and BER are substantially improved in our cross-tier interference cancellation scheme using network infrastructure feedback, and the range of transmit powers which avoid the interference to the PS is determined for the FUE. Therefore, the PS can operate seamlessly as before the introduction of the femtocell. The reminder of this chapter is organised as follows : section 3.2 gives some incentives for considering our work, section 3.3 describes our underlaid two-tier network model, section 3.4 is dedicated to the proposed interference cancellation at the FBS, section 3.5 emphasises on the proposed power control scheme at the SS, section 3.7 discusses the self management obtained from our combined proposals, section 3.6 depicts the simulation results and the related discussion, and this chapter ends with concluding remarks in section 3.8.

3.2 Background and General Contribution

The current state of the art about femtocell has been depicted through tutorial, research papers and related technical surveys[9, 40, 46, 48]. The femtocell concept is clearly an asset to satisfy indoor coverage with high data rate. It can contribute in the implementation of ubiquitous network and the emerging paradigm, HetNets[49]. While a promising concept, the deployment of femtocells is constrained by its inherent cross-tier interference particularly in a universal frequency reuse environment. The main solution to mitigate the cross-tier interference has been focused on interference avoidance or partitioned spectrum usage. This requires highly adaptive spectrum and power allocation due to the randomness of the position of the mobile terminals connected to the macrocell. The network architecture offered by the macrocell embodying the femtocell can be used to bring performance improvement which can satisfy the rising demand in wireless communication throughput. Through the use of the two-tier network infrastructure in our proposed system, universal frequency reuse

can be applied in the drastic uplink interference scenario considered in [9, 48] where the MUE penetrates the area around the FBS in which its transmission to the MBS create a dead zone at the femtocell. The cooperation between the MBS and the FBS can be utilised to cancel out the cross-tier interference from the MUEs located in the vicinity of the femtocell. In a macrocell embedded with a femtocell, the MUE can be located anywhere while the FUE is confined in the femtocell premises. In addition, the macrocell is the primary network to outdoor mobile terminals. Such cooperation adds a degree of freedom to the two-tier network, thus improving its performance. Our additional proposal which mitigates the cross-tier interference from the femtocell to the macrocell is driven from the works in [50–52]. Neighbors discovery at the base station and the positions of the terminals can be used to enhance the self organizing scheme of the femtocell for interference avoidance at the macrocell base station.

Our general contribution in this chapter is a solution to the deployment of small cells such as femtocells in a universal frequency reuse environment considering the small size of the femtocell radius ($\sim 20m$). Interference alignment, interference cancellation and distributed or network Multiple Input Multiple Output (MIMO) are the current key concepts to breaking the interference barrier in wireless communications. Our proposal focuses on interference cancellation applications and improvements for future small cell networks. Our main proposal is the interference cancellation scheme as interference from the MUE to the femtocell has been emphasized in the literature as a limiting factor to small cell deployment [9]. It takes into account the possibility of an MUE entering a femtocell premises then restricting its operations to its registered FUEs. The novelty lays in the use of the direct link connecting the MBS to each FBS. Nonetheless, as a secondary system to the macrocell, a femtocell has to avoid interfering with the MBS; thus we additionally propose an interference avoidance scheme to the MBS managed by the femtocell. In the context of small cells coexisting with a macrocell, we can consider our combined proposals as a contribution for small cell implementation.

Computational complexity and latency can be considered as drawbacks for our proposed interference cancellation scheme at the FBS. The system model in [53] is an orthogonal frequency division multiple access (OFDMA) based cellular system such as Network MIMO which is a common cells cooperating system considered in the literature [53, 54]. The cited drawbacks are taken into account in [53] through the throughput evaluation and discussed considering Network MIMO. The computational complexity involving multi-antenna processing is of the same order as non-cooperative successive interference cancellation which is practically used in CDMA systems. The Network MIMO processes vectors whose lengths increase with the number of cooperating base stations for the matrix inversion while the

information exchanges use the data of the strongly interfering terminal [53]. The matrix inversion in our proposed interference cancellation depends on the data exchanged and the number of interferers. However, considering more than one strong interferer induces a need for interference management at the MBS for MUEs. The decoding latency is in the order of $1 \sim 3$ ms for $3GPP-LTE$ while the backhaul latency can be made acceptable by an optical link envisioned for the next generation of cellular systems [53]. Using a buffer at the FBS can mitigate the latency effect of the backhaul. The proposed interference cancellation decoding complexity reduces to the MMSE [55] processing as described in section 3.4 as it uses the internet connection between the FBS and MBS. Each FBS uses the feedback signals from the MBS if necessary, and retrieves its desired signals without involving other FBSs.

3.3 Macrocell Embedded with Femtocell Underlaid Network Model

Our network model is an underlay system. The PS is represented by the *Macro-tier* while the *Femto-tier* illustrates the SS. A view of such coexistence is given in Fig.3.1. Uplink transmission is considered and the interference is defined as follows: the transmission from the FUE intended to the FBS interferes at the MBS if the FUE's transmit power is not regulated pertaining to its position; the cross-tier interference from the macrocell to the femtocell is illustrated by the transmission of the MUE intended to the MBS which can be close enough to the FBS to create a dead zone at the femtocell. The channel gains are denoted as h_{ps} between MUE and FBS, h_p between MUE and MBS and h_s between FBS and FUE; S_p and S_s respectively stand for the transmitted symbols from the MUE and the FUE; D is the distance between FBS and MUE, and d, is the distance between FBS and FUE. The product of the path loss and Rayleigh fading component represents the magnitude of the channel gain at arbitrary values of the mobile terminal positions.

We consider spectrum sharing between the two tiers, and the femtocell operates in a closed regime i.e. the femtocell owner does not allow a non registered mobile to be connected to the FBS. We propose to combine an interference cancellation at the SS which cancels out the signals received from the MUE at the FBS and power control. The power control can be seen as an interference avoidance scheme mitigating the interference from the FUE to the MBS. The illustration is given in Fig.3.1 by the crossing of the line representing the transmission from the FUE to the MBS; it derives a suitable FUE's transmit power under a given threshold based on the terminals positions and power parameters.

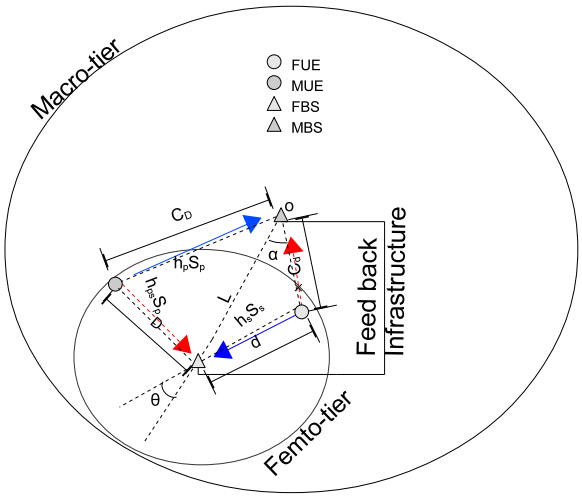

Fig. 3.1 Macrocell embedded with femtocell in Uplink interference.

3.4 Proposed Interference Cancellation at the FBS

In this mitigation scheme, we address the cross-tier interference from the MUE to the FBS. In contrast to prior work [46, 47], we consider that the MUE can penetrate in the FBS minimal operating region. The FBS minimal operating region has been defined in [46, 47] as the vicinity of the FBS where MUE transmission to the MBS induces outage at the FBS. We define the signal to interference ratio (SIR) in this section as the ratio between the FUE's average symbol energy and the MUE's, i.e. SIR stands for signal (of the FUE) to interference (from the MUE) ratio. The network infrastructure offers wired communications between the FBS and the MBS. Wireless over cables architecture have been utilized to propose a decode-forward scheme with relay for multi-user access, and protocols are designed for the combined use of the wireless and cable links embedded in femtocell networks [52]. Indeed, the signal of the MUE received at both the FBS and the MBS can be fed back from the MBS to the FBS through the network infrastructure. The gateway connecting the FBS to the operator network is an optional and transparent gateway connecting the FBSs to the core network. It can support a large number of connection interfaces to the core network. The use of a certain number of such interfaces can be dedicated on demand to cross-tier interference cancellation through symbols forwarding similar to the process of FBSs exchanging messages to control inter-cell interference. We assume that the connections suffer delays of the order of $1 \sim 10$ *ms* similar to the coherence time of small-scale fading components.

Such delay can be compensated by the storage of the interfered signals of the MUE and FUE received at the FBS. After reception of the MUE symbols at the FBS, the interference cancellation can be performed. The combined signals of the FUE and the MUE at the FBS are used with the feedback to recover FUE's signal at the femtocell.

For this study, the feedback signal is considered without noise at the reception, however it is taken into account at the same receiver for the reception of the signal-plus-interference resulting from the combination of the FUE and the MUE transmitted signals. We assume a cellular model with OFDMA. We implement the MMSE through the RLS algorithm for user signal separation at the femtocell base station if plural terminals' signals are received simultaneously. Pilot symbols are used for the training necessary to the RLS to estimate the channel for the FUE in the spectral domain, and a hard decision is performed at the MBS to recover the MUE symbols before performing the feedback. The MMSE is used for the estimation of the channel of the FUE. Our proposed interference cancellation consists of using the symbol feedback to derive an estimate of the FUE channel. The use of the MMSE is done through the RLS algorithm. Since the RLS adopts an optimization of a least square criterion, we use pilot symbols as data sequence for the estimation of the FUE channel.

The synchronization issue between the macrocell and femtocell tiers can be achieved as follows: the FBS listens to the MUE signaling destined to the MBS because the MUE is interfering at the FBS; the convex combination algorithm in [56] can be used to update the FBS timing.

In addition to the pure path loss (no shadowing), we consider flat fading in our channel model as in the related work [24, 40]. There is no consideration of Doppler effect. We propose interference cancellation with multiple interfering MUEs and one FUE transmitting the symbol X_1 on the channel with fading coefficient h_1. For the purpose of the analysis, we consider the following notations: $M-1$ stands for the number of MUEs, h_i is the channel gain between the FBS and the ith MUE modeled as an independently and identically distributed (i.i.d) Gaussian random variable with zero mean and unit variance and estimated from pilot symbols where $i = 2, ..., M$ and $Y = \begin{bmatrix} y_1 & y_2 & y_3 & ... & y_M \end{bmatrix}^T$ is the received vector at the FBS, where $[.]^T$ indicates vector transpose. y_1 is the combination of the FUE and MUEs signals while the y_i for $i = 2, ..., M$ are the fed back signals from the MBS.

Using matrix notation, we have at the FBS:

$$\begin{pmatrix} y_1 \\ y_2 \\ y_3 \\ \dots \\ \dots \\ \dots \\ y_M \end{pmatrix} = \begin{pmatrix} h_1 & h_2 & h_3 & . & . & . & h_M \\ 0 & 1 & 0 & . & . & . & 0 \\ 0 & 0 & 1 & . & . & . & 0 \\ 0 & 0 & 0 & 1 & . & . & 0 \\ . & . & . & . & . & . & . \\ . & . & . & . & . & . & . \\ . & . & . & . & . & . & . \\ 0 & 0 & 0 & 0 & 0 & 0 & 1 \end{pmatrix} \begin{pmatrix} X_1 \\ X_2 \\ X_3 \\ . \\ . \\ . \\ X_M \end{pmatrix} + \begin{pmatrix} n \\ 0 \\ 0 \\ . \\ . \\ . \\ 0 \end{pmatrix},$$

where X_i is the transmitted symbol from the ith user and n is an AWGN. By using the notation

$$Y = HX + N, \tag{3.1}$$

we let

$$H = \begin{pmatrix} h_1 & h_2 & h_3 & . & . & . & h_M \\ 0 & 1 & 0 & . & . & . & 0 \\ 0 & 0 & 1 & . & . & . & 0 \\ 0 & 0 & 0 & 1 & . & . & 0 \\ . & . & . & . & . & . & . \\ . & . & . & . & . & . & . \\ . & . & . & . & . & . & . \\ 0 & 0 & 0 & 0 & 0 & 0 & 1 \end{pmatrix},$$

$$X = \begin{bmatrix} X_1 & X_2 & X_3 & . & . & . & X_M \end{bmatrix}^T$$

and

$$N = \begin{bmatrix} n & 0 & 0 & . & . & . & 0 \end{bmatrix}^T.$$

The diagonal elements of H being non zero, H is non singular. Besides, it is upper triangular. H being non singular and triangular, it admits an inverse matrix H^{-1} which is upper

triangular as well:

$$H^{-1} = \begin{pmatrix} \frac{1}{h_1} & \frac{-h_2}{h_1} & \frac{-h_3}{h_1} & . & . & . & \frac{-h_M}{h_1} \\ 0 & 1 & 0 & . & . & . & 0 \\ 0 & 0 & 1 & . & . & . & 0 \\ 0 & 0 & 0 & 1 & . & . & 0 \\ . & . & . & . & . & . & . \\ . & . & . & . & . & . & . \\ . & . & . & . & . & . & . \\ 0 & 0 & 0 & 0 & 0 & 0 & 1 \end{pmatrix}$$

The directions of arrival constituted by the channel of each transmitted signal in the

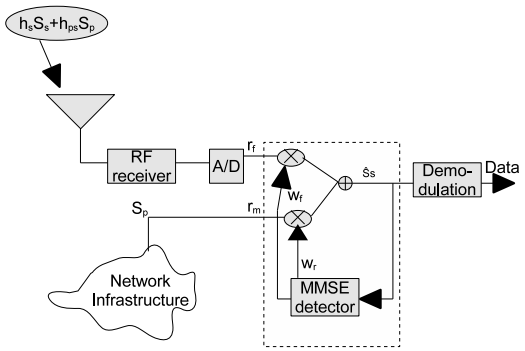

Fig. 3.2 Proposed FBS receiver structure.

columns of H are linearly independent vectors. The signal space is then M and the receiver can differentiate between the signals. The utilization of the network infrastructure feedback offers signaling space design. While the signals from the wireless channel interfere with each other, the feedback makes them separable at the FBS. Therefore, the FBS is able to invert H in order to recover the desired symbol which is X_1 in this case. Each column of H is the channel matrix of one user. Since the columns are linearly independent, single-symbol detection can be performed. X_1 can be extracted from the first component of $H^{-1}Y$, resulting into $X_1 + \frac{n}{h_1}$.

We consider in the following analysis the particular case of one FUE under one MUE. The proposed FBS receiver structure is illustrated in Fig.3.2. The noise added interfered received signal $h_{ps}S_p + h_sS_s$ is converted in the analog to digital converter (A/D). The resulting digital signal r_f and the network infrastructure signal r_m are the inputs to the detector module encompassed in the dashed line box in Fig.3.2:

$$r_f = h_sS_s + h_{ps}S_p + n, \tag{3.2}$$

$$r_m = S_p, \tag{3.3}$$

where n is an additive white Gaussian noise (AWGN). The fading coefficients h_s and h_{ps} are i.i.d with zero mean and unit variance. Using matrix notation, we can write the received signals as a received vector R:

$$R = \begin{pmatrix} r_f \\ r_m \end{pmatrix} = \begin{pmatrix} h_s & h_{ps} \\ 0 & 1 \end{pmatrix} \begin{pmatrix} S_s \\ S_p \end{pmatrix} + \begin{pmatrix} n \\ 0 \end{pmatrix},$$

which can be rewritten as:

$$R = HS + N, \tag{3.4}$$

where

$$H = \begin{pmatrix} h_s & h_{ps} \\ 0 & 1 \end{pmatrix}, S = \begin{pmatrix} S_s \\ S_p \end{pmatrix}, N = \begin{pmatrix} n \\ 0 \end{pmatrix}.$$

The decoupling of the two symbols is given by:

$$H^{-1}R = S + \frac{1}{h_s}, \begin{pmatrix} n \\ 0 \end{pmatrix},$$

where

$$H^{-1} = \frac{1}{h_s} \begin{pmatrix} 1 & -h_{ps} \\ 0 & h_s \end{pmatrix}.$$

If we denote by $\hat{r}_f$ the first component of $H^{-1}R$, we obtain:

$$\hat{r}_f = S_s + \frac{n}{h_s}. \tag{3.5}$$

Denoting by N_0 the variance of n, the second term of $\hat{r}_f$ has the variance $E\left\{\left|\frac{n}{h_s}\right|^2\right\}$:

$$E\left\{\left\|\frac{n}{h_s}\right\|^2\right\} = \frac{N_0}{|h_s|^2}; \tag{3.6}$$

$\hat{r}_f$ can be rewritten as:

$$\hat{r}_f = S_s + \frac{z}{|h_s|}, \tag{3.7}$$

where z has zero mean and its variance is N_0. Scaling $\hat{r}_f$ by the factor multiplying z gives

the following:

$$r_f' = |h_s| S_s + z. \tag{3.8}$$

We can notice that the scalar $|h_s|$ in (3.8) is Rayleigh faded such as in a 1×1 channel [57]. Considering the two transmitters as mutually interfering users, single-symbol detection is equivalent to nulling out the interference.

To avoid noise enhancement while mitigating the interference, we propose to use Wiener combining techniques [58] in the spectral domain to provide the linear output estimating S_s with Minimum Mean Square Error (MMSE) which is more tolerant to noise. Denoting by $\hat{S}_s$ the estimated value of S_s and d_s as the desired chosen signal correlated with the inputs of the equalizer, we can obtain:

$$\hat{S}_s = w_f^* r_f + w_m^* r_m, \tag{3.9}$$

where $(.)^*$ denotes the complex conjugate vector, and w_f and w_m are the weights minimizing the error: $E\{\left(\hat{S}_s - d_s\right)^2\}$. The MMSE equalization optimally trades off mitigating the noise and the interference. Denoting by W the weights matrix derived from the equalization, from [55] we have:

$$W^H = \left(H^H H + N_0 I\right)^{-1} H^H, \tag{3.10}$$

where $(.)^H$ denotes the complex conjugate transpose vector and I is the unit matrix having the same dimension as H. The estimated signal $\hat{X}$ for the general analysis or $\hat{S}_s$ in the application involving the FUE and the MUE is obtained from the MMSE equalization as follows:

$$\hat{X} = W^H Y = \left(H^H H + N_0\right)^{-1} H^H Y, \tag{3.11}$$

which shows that if the noise variance N_0 is high compared to the estimated signal, then the MMSE reduces to a matched filter. The weights can be generated through the recursive least square technique which avoids direct matrix inversion. The demodulation of $\hat{S}_s$ gives the data symbols of the FUE.

The issue addressed with our proposed interference cancellation is a limiting factor to small cell performance. Thus our proposal can be considered for future small cell deployment and HetNets. The implementation can be done in future HetNets with a coordinator connecting the core network and managing the interference cancellation at each FBS in need of cross-tier interference mitigation incurred by an MUE transmission in the femtocell minimal operating region. Such coordinator insertion can reduce the feedback delay and enhance the MBS offload. The feedback delay can be compared to the listening time for an FUE to find a channel free from the PS transmission in cognitive radio underlay system [44, 47]. In such system, the SS can be denied transmission because the PS is occupying

the available channel or the SS transmitting terminal is in the minimal operating region of the PS receiver. The MUE symbols fed back to the FBS are directly inserted to the signal processing module as illustrated in Fig.3.2. For security concern, the feedback is enabled without any opportunity to use MUE data besides the recovery of the FUE symbols. In a closed access regime, we advocate that the FBS be configured to only decode its FUEs at the bit level.

A femtocell is an additional entity pertaining to the macrocell. Therefore, it can send and decode the synchronization sequence available in the broadcast channel allocated for symbol synchronization. As simultaneous synchronization and symbol decoding is enabled in the macrocell, the FUE can achieve synchronization with an MUE while regulating its FUE transmission to support the necessary coordination to interference cancellation as explained in our proposal.

3.5 Decentralised Power Control for Cross-tier Interference avoidance at the MBS

Considering the spectrum sharing two-tier network system, we propose an interference avoidance from FUE to MBS to complement the proposed interference cancellation. The proposed power control at the FBS regulates the FUE transmit power using the parameters described in the system model as follows. Considering [46], we assume that the FBS acquires the positions of the MUE and the FUE through the references signals used in the macrocell for localization services.

We derive the SIR at the MBS using the signal strengths of both MUE and FUE. The SIR is defined as the ratio of the symbol power of the MUE over the FUE. The channel gains are represented by h_{C_d} (resp. h_{C_D}) between the FUE (resp. MUE) and the MBS. The SIR is represented as:

$$SIR = \frac{P_h \left|h_{C_D}\right|^2 C_D^{-ml} K_m}{P_m \left|h_{C_d}\right|^2 C_d^{-hl} K_f}, \tag{3.12}$$

where $|.|$ indicates the amplitude, ml and hl are respectively the macrocell and the femtocell path loss components, P_h (resp. P_m) is the transmit power of the FUE (resp. MUE), K_f (resp. K_m) is the constant power loss for the FUE (resp. MUE) and C_d (resp. C_D) is the distance between FUE (resp. MUE) and the MBS. Since h_{C_d} and h_{C_D} are not correlated, Jensen's

inequality provides a lower bound of the average SIR:

$$E\left[SIR\right] \geq \frac{P_h E\left[\left|h_{C_D}\right|^2\right] C_D^{-ml} K_m}{P_m E\left[\left|h_{C_d}\right|^2\right] C_d^{-hl} K_f}, \tag{3.13}$$

where $E(.)$ indicates ensemble average. From the assumption that $E(\left|h_{C_d}\right|)^2 = E(|h_{C_D}|)^2 = 1$. Assuming an interference limited system, we approximate the SIR by its average to derive the proposed power control scheme:

$$\hat{SIR} = \frac{P_h C_D^{-ml} K_m}{P_m C_d^{-hl} K_f}. \tag{3.14}$$

Given an SIR constraint on FUE's transmit power, we can derive the suitable transmit power for the FUE to avoid its interference at the MBS. At each base station, we have an interfering and a desired signals following [34] :

- at the FBS: we denote by I_m the interference from the MUE located at distance D from the FBS.

$$I_m = P_m - 10ml\log 10(D) - Pl - 37, \tag{3.15}$$

  where Pl is the indoor penetration loss, and by R_f the received power from the FUE located at distance d from the FBS:

$$R_f = P_h - 10hl\log 10(d) - 37, \tag{3.16}$$

- at the MBS: we denote by I_f the interference from the FUE located at distance C_d from the MBS.

$$I_f = P_h - 10hl\log 10(C_d) - Pl - 37, \tag{3.17}$$

  and by R_m the received power from the MUE located at distance C_D from the MBS:

$$R_m = P_m - 10ml\log 10(C_D) - 30\log 10(f_c) + 71, \tag{3.18}$$

Replacing the constant loss terms k_f and k_m from the interference patterns, we obtained the approximate SIR:

$$\hat{SIR} = \frac{P_h C_D^{-ml} - 30\log 10(f_c) + 71}{P_m C_d^{-hl} - Pl - 37}. \tag{3.19}$$

Our proposed power control at the femtocell is based on:

$$\hat{SIR} \geq P_{th}, \tag{3.20}$$

where the constraint is restrictive in the sense that we consider only two users mutual interference. From this model, the interference level of neighboring base station can be known to the FBS. After characterizing such interference as a fixed loss varying at a large scale, the random cross-tier interference is left to be dealt with. Therefore, from (3.20) we derive the maximum transmit power of the FUE denoted as Pt_{fmax}:

$$\begin{aligned} Pt_{fmax} = P_{mt} - 10log10(C_D) - 30log10(f_c) + 71 \\ - (P_{th} - 10log10(C_d) - 37 - P_l). \end{aligned} \tag{3.21}$$

If P_{th} decreases, the performance of the MUE improves as D increases. Corrections of P_{th} can be done by requesting received power at the MBS from the FUE which can be forwarded to the FBS through infrastructure network. This cooperation is similar to [59] where the macrocell base station assigns additional resources to the femtocell base station through the backhaul. We avoid the use of the backhaul for in this section and define a restriction on the FUE to guarantee cross-tier interference avoidance to the MBS. Besides, our proposed interference avoidance is solely managed by the FBS; thus enhancing the decentralization feature in small cell networks.

3.6 Results and Discussion

3.6.1 Simulation Methods

We used the C language for deriving the simulation results presented in this chapter. The channel model is a 5 paths exponential Rayleigh fading combined with path loss. The noise is generated randomly as an AWGN variable with mean 0 and variance 1. Each user transmits using QPSK modulation to generate the symbols from the binary output of the convolutional encoder. Then OFDM is applied before entering the channel. A guard interval of 20% is considered in the OFDM system. The details of the OFDM modulation are given in Table 3.1.The noise is added to the interfered signal at the receiver illustrated in Fig. 3.2. The interfered signal is the addition of the MUE and FUE signals. Noise is not added to the signal fed back to the FBS. We use the RLS algorithm to recover the data at the receiver for the interference cancellation scheme. The transmit power and positions of each user are given in Table 3.2. The details of the distance path loss model are given in Table 3.2. A

Table 3.1 Simulation conditions

Parameters	Value
Bandwidth	5MHz
Number of subcarriers	512
Useful symbol time	6.4E-6s
Guard interval	1.25E-6s
Data modulation	OFDM QPSK
small scale channel model	Rayleigh flat fading
Weight estimation algorithm	RLS
Noise	AWGN
Convolutional code rate	1/2
Convolutional code constraint length	7

Table 3.2 FUE and MUE cellular parameters.

Parameters(Variable)	Value
Macrocell radius (R_c)	1000m
femtocell radius (R_f)	30m
normalized distance from FBS to MBS (L)	0.95
Carrier Frequency (f_c)	2500 MHz
Wall penetration loss (P_l)	5dB
Mobile maximum transmit power (P_{tmax})	23dBm
Macrocell path loss (m_l)	3.8
femtocell path loss (h_l)	3
SIR threshold(P_{th})	10,16dB
MUE_angle	$\frac{\pi}{4}$
FUE_angle	$0 \ldots \frac{\pi}{4}$

fixed loss is chosen instead of considering random lognormal shadowing in this chapter.

The BER is evaluated by the ratio of the correctly received bits over all transmitted bits. The PER is the ratio of the correctly received packets over all transmitted packets. The throughput formula which utilises the PER is derived from [60].

3.6.2 Femtocell Performance Evaluation with the Proposed Interference Cancellation

In this section, the simulation results illustrate the performance obtained solely from the proposed interference cancellation scheme with varying D and d and Rayleigh fading. We

consider Fig.3.1 for the numerical results obtained from our proposed interference cancellation and its related conventional scheme. The varying SIR between the FUE and MUE terminals is obtained in Fig.3.3 through each terminal's average symbol energy variation. Both terminals have the same data modulation. The simulation parameters related to the macrocell-femtocell two-tier network are represented in Table 3.1. Our simulation uses the packet error rate to estimate the throughput denoted by T [60] :

$$T = (1 - P_e) r N_{sub} N_{sym} n_{mod} / T_s, \tag{3.22}$$

where P_e is the packet error rate, N_{sub} is the number of subcarriers, N_{sym} is the number of data symbols, n_{mod} is the number of bits per data symbol, r is the channel coding rate and T_s is the symbol time. The MMSE uses pilot symbols to minimize the square of the difference between the estimated the reference symbols at the MMSE detection block.

3.6.3 Performance Evaluation Including the Proposed Power Control

The throughput in Fig.3.3 illustrates the interference cancellation performance. The SIR variation in *"conventional"* and *"with interference cancellation"* are obtained by varying d and D. In this evaluation, the noise power has been independently generated at the receiver. Each transmitter signal's path loss varies solely based on D or d which are normalized distances chosen randomly between 0 and 1. Negative and low SIRs represent the presence of the MUE in the femtocell minimal operating region or an MUE transmitting in the vicinity of the FUE while being far apart from the MBS. Compared to the conventional method, the interference is canceled out by the proposed interference mitigation leading to a throughput curve remaining horizontal for the proposed method at the maximum level permitted by the noise power.

In Fig.3.4, the BER performance is evaluated. The *"conventional"* and *"with interference cancellation"* curves respectively represent the BER of the FUE for the conventional and proposed schemes. The *"with interference cancellation"* steadiness below the *"conventional"* illustrates the interference cancellation effect.

The interference of the FUE is maintained negligible at the MBS through the power control. In Fig.3.5, the throughput performance of the combined proposals is represented. *"with interference cancellation"* illustrates the FUE performance with the interference cancellation without the effect of the power control. The effect of the power control is illustrated by *"with interference cancellation and power control"*. With the conventional scheme, the FUE performance is given by *"conventional"*; the combined proposals leads to a similar improved throughput for both FUE and MUE singly. We can notice that the power control

affects the performance of the FUE through transmit power reduction. Future work will consider real case where the SIR is higher than -20dB.

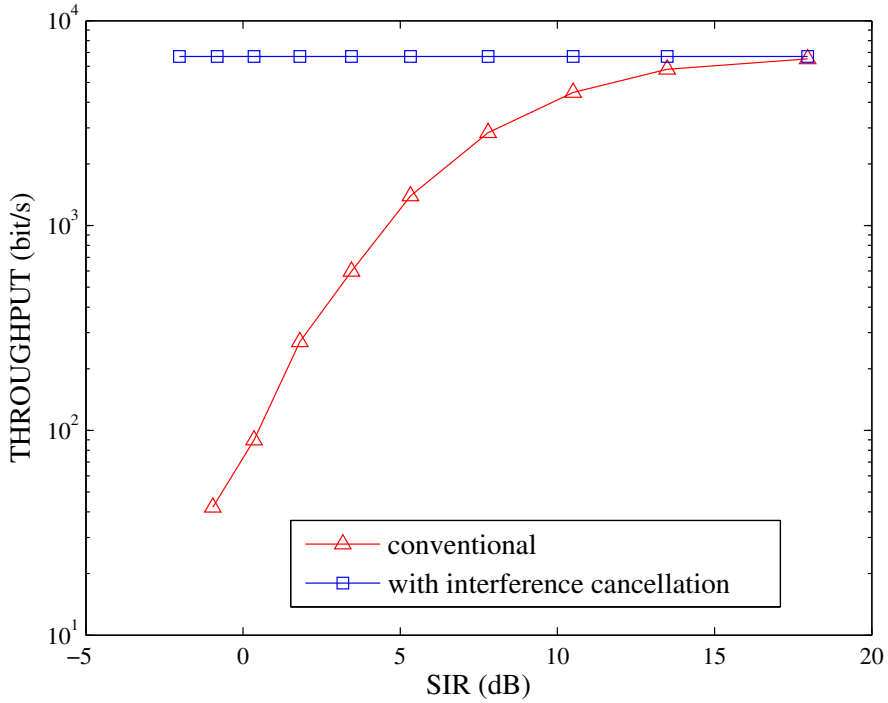

Fig. 3.3 Throughput performance of the FUE under an MUE with variable d and D.

3.6.4 Angular effect

In this section we propose an application of the power control scheme as explained in section 3.5. From the parameters given in the description of the system model, we derive the dependency of the distances on the angles in the following equations. Such dependency affects the derived power control, and thus the results which include the constrained transmit power of the FUE such as in the performance illustrations including the proposed power control.

Given the parameters d, L and θ are available at the FBS, we can derive C_d and C_D:

$$d\sin(\theta) = C_d \sin(\alpha), \tag{3.23}$$

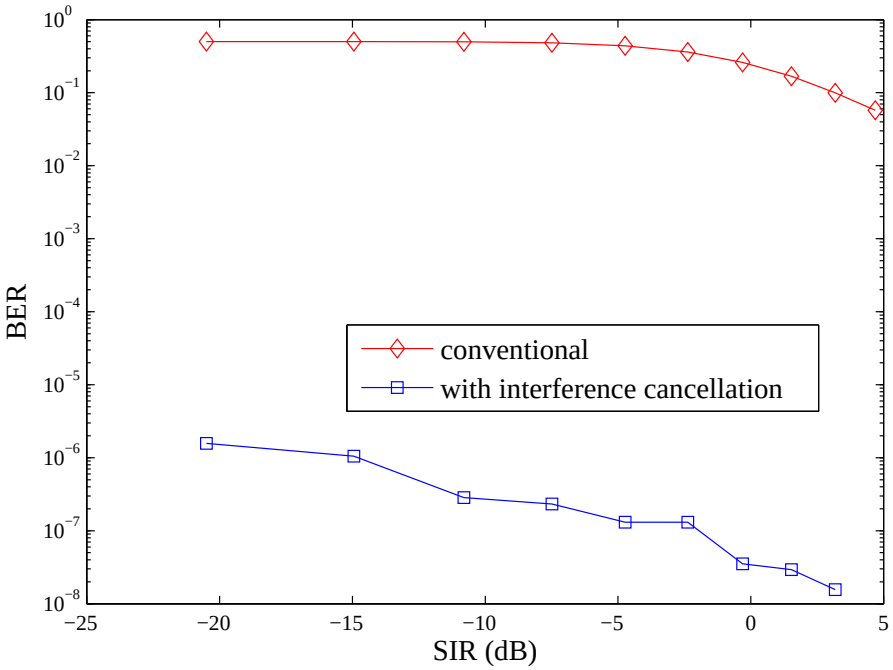

Fig. 3.4 FUE's BER under an MUE with variable d and D.

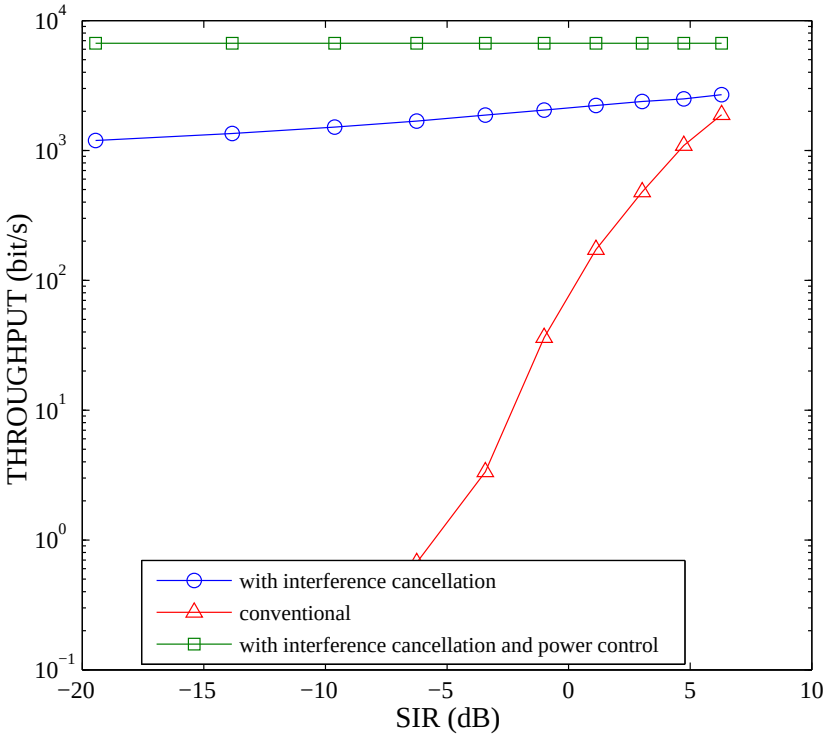

Fig. 3.5 FUE's throughput from power control by the femtocell.

where α is the angle at the vertex O, considering the triangle formed by O at the MBS, FUE and FBS. This leads us to:

$$(d\sin(\theta))^2 = {C_d}^2 - (L - d\cos(\theta))^2. \tag{3.24}$$

C_d is therefore obtained as:

$$C_d = \sqrt{L^2 - 2Ld\cos(\theta) + d^2}. \tag{3.25}$$

Following the same derivation method with α at the MBS and θ at the FBS in the triangle formed by MBS, MUE and FBS, we have:

$$C_D = \sqrt{L^2 - 2LD\cos(\theta) + D^2}. \tag{3.26}$$

We consider the effect of the variation of the angle positioning the interfering terminal on the proposed interference scheme. The angular effect is obtained through evaluation of the BER and throughput of the FUE at different "$FUE\_angle''s$. Following the power control scheme, the transmit power of the FUE depends on the "FUE_angle'' θ which provides the position of the FUE to the FBS. Thus we evaluated such effect of the power control through the variation of θ in Fig.3.7 and BER in Fig.3.6 illustrating the performance of the FUE. As θ increases, the interference decreases at the MBS. From the power control scheme, we derived the transmit power without considering a BER threshold. The BER of about $10^{-2} \sim 10^{-1}$ illustrates the effect of constraining the transmit power of the SS by the protection of the PS. The low SIR represented in the horizontal axis of Fig.3.6 is a part taken from the conventional system of Fig.3.4. We can notice that the SIR spreads about $-5dB \sim -4dB$. Therefore, to improve the BER, we can resort to the proposed interference cancellation or reduce the interference of the PS.

As for obtaining the angle θ several methods can be advocated from the literature. In the femtocells realm, the E-plane horns based reconfigurable antenna presents low power side lobe and dynamically switchable main beam. Its half power-bandwidth can span within $\frac{\Pi}{12}$ radians and the beam can be switched to the user location. Therefore, in addition to increasing femtocell capacity [51], it can be utilized to estimate the angles used for the purpose of our interference avoidance to the MBS. In [43] the position of the femtocell base station is given w.r.t the macrocell base station by its distance and direction angle. Therefore the angle utilized in this chapter can be inferred considering a certain error in the measurement related to the equipment accuracy. The need for advance cognitive radio networks to take into account the angle of arrival is expressed in [44].

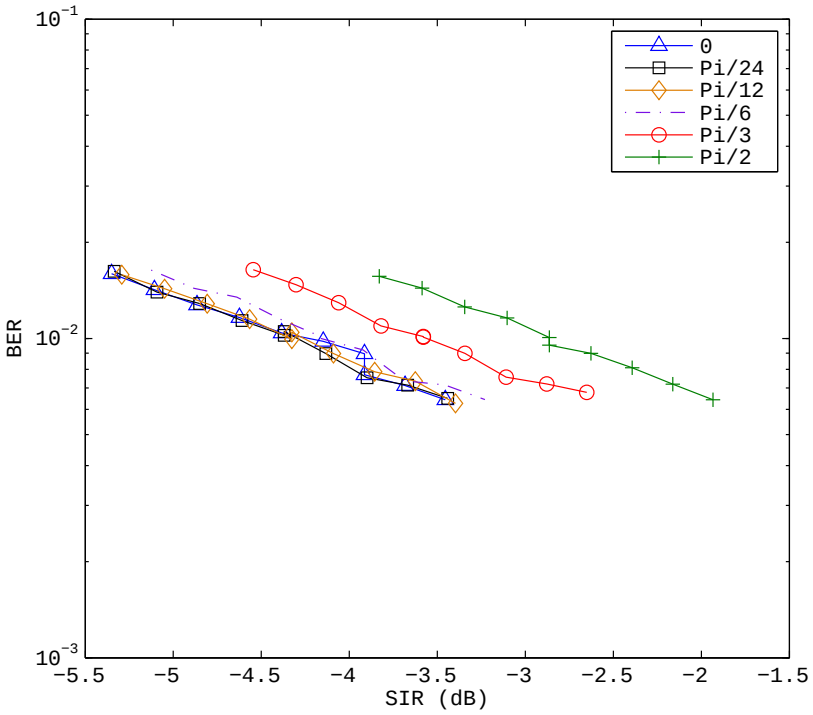

Fig. 3.6 BER with power control by the femtocell under varying FUE's angle.

3.7 Femtocell Autonomous Management

The combination of the interference cancellation and power control offers to the underlaid system the ability to operate seamlessly w.r.t the state of the macrocell before the introduction of the femtocell. Taking into account the proposed power control, we also evaluated the interference of the FUE under the constraints of not interfering to the PS through *Fig*.3.4 and *Fig*.3.5.

The interference cancellation scheme provides a resilient interference mitigation scheme which prevents the occurrence of dead zone at the FBS. In addition, given that the primary cellular network for both the FUE and MUE is the macrocell, it waives the restriction of the macrocell user to a minimal operating region whence its interference to the femtocell is negligible. Such restriction is advocated in [46, 47]. With our combined proposals, we manage to reduce the cross-tier interference at an insignificant noise level at the MBS side and cancel it out at the FBS side. In a conventional system, pairs of terminals pertaining to a tier schedule their transmissions using the available degrees of freedom. However, with universal frequency reuse, cross-tier interference becomes a capacity limiting variable to the competition for spectrum between tiers. Our proposed small cell network design resolves

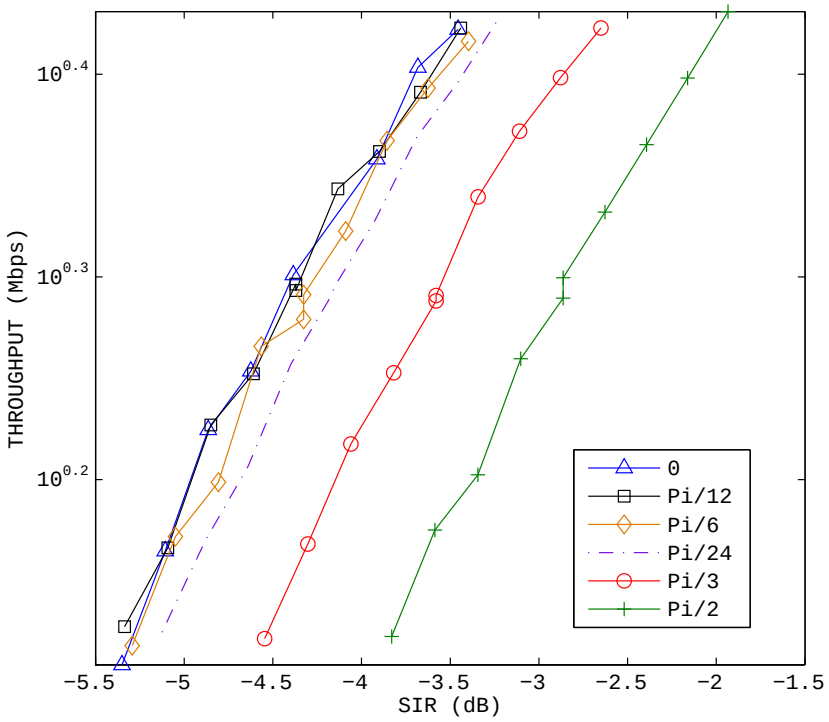

Fig. 3.7 Throughput with power control by the femtocell under varying FUE's angle.

such limitation and mainly assigns the task of handling the cross-tier interference from both tiers to the femtocell which is the "intruding element to the previously existing system, the macrocell". The macrocell can then operate as the femtocell was not embedded without interference to the femtocell.

Femtocells are small cells of radius around $\sim 20m$. The number of simultaneously supported users is therefore limited to one or two FUEs. We assume that OFDMA can be used for such number. As for higher number of users, we would like to address the task in future work.

3.8 Conclusion

The next generation cellular system gains in area spectral efficiency with the deployment of femtocells into macrocell in a spectrum shared usage. Nevertheless, the random positions of mobile terminals connected to either tier generate a cross-tier interference issue which has to be handled for a successful implementation of femtocells. This chapter has addressed the design for future small cell network by handling the cross-tier interference from both tiers

mainly by the means of the femtocell. From the macrocell, the proposed interference cancellation effectively mitigates the impedance from the MUE to the FBS. It uses the backhaul to feedback the MUE's symbols to the FBS which can then recover its signal of interest from the received aggregated signals of the FUE and MUE. From the femtocell side, we proposed a power control which limits the hindrance of the FUE to the MBS receptions. It defines a range of transmit powers of the FUE by means of direct power measurements and the use of localizations services to avoid the interference to the MBS. The simulation results confirm the resilience of the cross-tier overall operative mitigation.

Chapter 4

Cross-tier interference management with a distributed antenna system for multi-tier cellular networks

Next-generation wireless communication demands enhanced cooperation at the multi-tier level to improve the end-user data rate. In [33], cooperation between wireless systems presents a better performance. Contemporary novel wireless network concepts such as heterogeneous networks (HetNets) and multi-tier networks such as femtocells overlaid onto the macrocells, require advanced management of the cell load, cross-tier interference mitigation and user access to the spectrum. The adoption of spectrum sharing adds to the complexity of wireless system design; thus the emergence of these networks require more investigation on the implementation methods which provide end-user satisfaction. This implementation of system cooperation requires the design of spectrum-sharing self-enforcing rules compatible with each individual system [61]. Considering the near-far problem and adaptive transmit power in two-tier networks [62], our proposal contributes to the design of a coordinator between the two systems, which manages the cross-tier interference and enhances the ergodic sum-rate capacity scaling.

4.1 Introduction

In this chapter, we focus on managing the cross-tier interference between a PS and an SS in a spectrum-shared usage scenario. The PS or macrocell tier consists of an MBS and the mobile users that communicate directly with it by default, denoted as MUEs. The SS or femtocell tier consists of femtocells. A femtocell is a low-powered user-deployed base station

(FBS) that operates in frequency-reuse with the macrocell to deliver high spectral efficiency in closed- or open-access regime [62] to one or two indoor mobile users, denoted as FUEs. The femtocell tier defines the architecture of the core of small cell networks [63–65]. In [66], self-configuration and self-optimization protocols are detailed for LTE networks and a mobility load balancing is proposed to address the random occurrences of mobile users in cellular networks which can create base station overload in the network.

Femtocells are deployed within with the macrocells operating area and reuse the macrocell allocated spectrum. Because each FBS is exclusively powered on/off by its end-user, managing the cross-tier interference coordination similarly to that in traditional cellular networks (individually handled by the operators) becomes difficult. Furthermore, the backhaul exchange information between the MBS and the FBSs becomes tedious for a large number of femtocells because the MBS communicates with the femtocells through a gateway (LTE-A). Our proposal addresses these challenges by leveraging advanced HetNets schemes and innovative femtocell clustering consequent to the proposed introduction of distributed antenna system (DAS).

This chapter considers the DAS presented in [5]. A DAS has signal processing modules and remote radio-frequency (RF) antenna element modules. We denote the RF elements as remote antenna units (RAUs). Multiple RAUs share the same signal processing unit denoted as common processing unit (CPU). Each RAU is connected to a CPU by a high data rate physical link such as optical fiber. The RAUs are located nearby premises which shelter FBSs. Therefore, different RAUs can cover several small areas in a heterogeneous coverage while sharing the same processing unit. We assume that the communication between the DAS backhaul and the RAUs presents a negligible error rate and delay. The DAS has a common platform role, because it can accommodate different wireless service operators and different protocols (see HetNetForum). Thus, the DAS is an asset for heterogeneous small cell deployment and can be functionally compared to a radio-access network (RAN) aggregation system [67]. RAN aggregation between operators is considered in [67] to improve throughput and spectrum efficiency; this study considers femtocells overlaid onto a macrocell with a DAS interface to mitigate the cross-tier interference between the macrocell and femtocell tiers.

In this chapter, the FBSs are small base stations located within the premises of the customers. Since we assume close access operating regime, the FBSs allow communication with only their registered mobile users. The RAUs of the DAS are antenna elements located outside the premises sheltering the FBSs. We consider a path loss exponent difference between the wireless indoor communications of each FBS and its registered FUE, and each RAU and an unregistered (to the FBS) MUE.

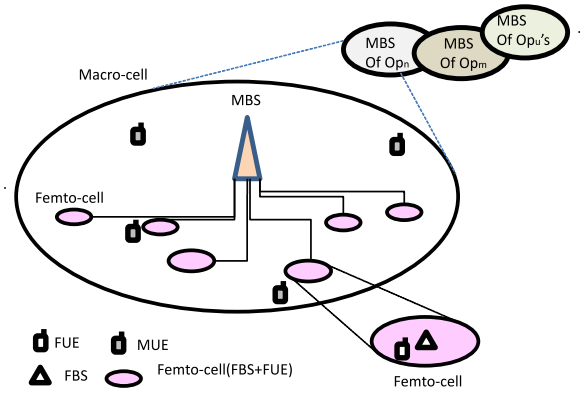

Fig. 4.1 Femtocells overlaid onto legacy macrocells.

The work in [68] is focused on a cellular architecture based on DAS to address coverage scarcity in HetNets. The results show that the sum-rate of the network improved because of the DAS. The improvement is due to the added degrees of freedom to the network resulting from the consideration of the DAS. Recently HetNets have been considered [69] to implement efficient architecture for broadband access in relation to LTE [70] where DAS is used as a HetNet technology enabling system. Interference mitigation in HetNets was considered in [71] through orthogonal resource allocation and relaying. The ergodic capacity analyses can be found in [5], where downlink DAS was considered in multicell environment. Analysis featuring cooperation between DAS antenna element modules and femtocells located in high buildings was presented in [72].

The work in [53] studies the cooperation of base stations equipped with multiple antennas within a cellular system. The proposed interference cancellation is based on multiple antenna signal processing concept. The strongly interfering terminal data is shared with the base stations where another desired received signal decoding remained unsuccessful due to the strong interference. The latter base stations perform successive interference cancellation. In [53], it is assumed that some base stations in the cell can decode multiple user signals using their multiple antennas and then share the estimated signals with the other base stations. Then, the shared signals are used for interference cancellation when the signal-to-interference-plus-noise ratio (SINR) at the femtocell due to the MUE interference is negligible.

The interference cancellation scheme in [53] reflected more of the version of the traditional successive interference cancellation combined with network MIMO. The traditional successive interference cancellation involves the extraction of the estimated interfering signal from the combined signals, and the estimation of the desired signal from the difference. The system model in [53] lacks reliability because one of the base stations could be unable

to estimate the signal of a strongly interfering terminal from the received combined signals. In contrast to [53], the study in this paper uses signaling without resorting to multiple antennas at each base station. It is difficult to apply the schemes in [53] or network MIMO to the different femtocell base stations because femtocells are indoor systems managed by their end-users. In addition, given the recent ubiquity of small cell networks [65], our proposal in this chapter effectively addresses the cross-tier interference issue in an innovative way to the best of the authors' knowledge.

Since DAS has already been introduced into cellular systems, we propose to use it as an interface between the macrocell and femtocell tiers. We consider uplink transmission and mitigation of the cross-tier interference as follows:

- The mitigation at the femtocell side considers a cluster of femtocells. Near the cluster, an MUE that transmits to its MBS drastically subjects the cluster into a high outage probability. When the DAS is connected to the MBS and to each femtocell in the cluster through the optical line, information exchange can be performed for interference cancellation. By placing an RAU in the cluster, the DAS can retrieve the symbols transmitted by the MUE and feed them back to each FBS, thus cross-tier interference can be cancelled at the FBS. The DAS can multicast the feedback to the FBSs in the cluster affected by the same MUE on the basis of each FBS request for feedback. The feedback request can be based on the evaluation of the SINR at each FBS in the cluster of femtocells.

- At the macrocell side, the interference from the MUE to the femtocells in the cluster can be mitigated by reducing the MUE transmit power because the DAS retrieves the symbols transmitted by the MUE through the nearby RAU located closer to the MUE than the MBS. Such reduction is constrained by the MUE outage probability at the RAU. The introduction of the DAS shortens the radio transmission distance of the MUE. This implies a reduction of its transmit power [73].

In addition mitigating the cross-tier interference because of the introduction of the DAS interface between the macrocell and femtocell tiers , we can derive consequent benefits from our proposal. Instead of exchanging the related information of the strongly interfering terminal as performed in [53] or resorting to network MIMO as done in [5], our proposed DAS interface directly forwards the MUE transmitted symbols where needed in femtocell clusters. The traditional MBS-FBS direct connection can be used for interference cancellation [74]; however, as the number of femtocell clusters increases, the macrocell off-loading role of the femtocells [65] is compromised by the induced traffic delay in the backhaul. Furthermore, the signal decoding complexity individually involves each femtocell that requests

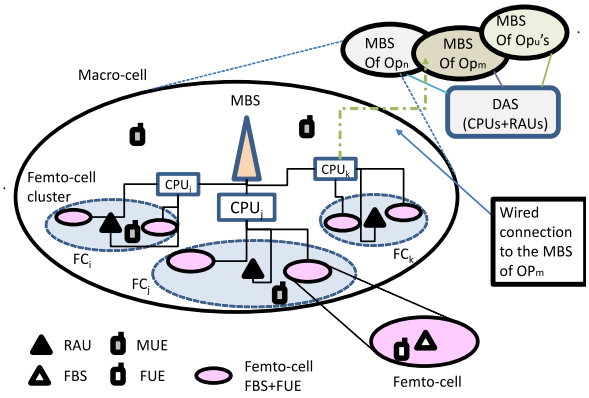

Fig. 4.2 Femtocells overlaid onto legacy macrocells in uplink interference with the added DAS.

interference cancellation. Such distributed system is not considered in [5, 53]. As stated in the outage analysis, to ensure that the feedback system retrieves the symbols of the MUE(s) causing interference at the FBSs, we propose a cross-tier interference avoidance which consists of prohibiting any FUE transmission susceptible of creating significant interference at the RAU which has the role of receiving and transmitting the feedback signals. The overall novelty and contribution of our proposal is the use of distributed direct(wired) links between the DAS (through CPUs and RAUs) and the femtocell tier (FBSs). Consequent to our proposal, the sum-rate of the small cell networks improves substantially. Such result is confirmed in this chapter by computer simulations.

Extending the above cited work and in contrast to prior works based on the knowledge of the number of terminals per unit of area [75] and area restriction of the mobile terminals[31], in a universal frequency reuse operation, we propose femtocell clustering methods based on the transmission occurrences in uplink transmission aided by the insertion of the DAS in the two-tier network. As an interface between the macrocell and femtocell tiers, the CPU-RAU virtually clusters the femtocells based on signal-to-interference-plus-noise ratio (SINR) computation at the RAU and the femtocell base stations denoted as Home nodeBs (HeNBs) (in LTE-A) to perform spatial cross-tier interference mitigation. The CPU-RAU selects the femtocells under MUE strong interference and feed them back the decoded symbol of the MUE for interference cancellation as described in [53] and extended to femtocells in [74]. The selection is based on SINR which determines the necessity for feedback and the required cell load from the CPU. The CPU-RAUs mitigate the near-far effects at random locations in the cell as considered in [74]. Such clustering enables the computation of the cardinalities of the sets of femtocells without the knowledge of terminal density per unit of area. The cardinalities of the femtocells clustering contribute to the maximization of

the sum-rate capacity which becomes a posynomial as in[76]. The simulation results show substantial capacity improvement over conventional cellular system.

The rest of this chapter is structured as follows: the system model and the proposed architecture are described in Section 4.2. The femtocell clustering concept based on the feedback request is presented in Section 4.3. Section 4.4 is devoted to the proposed interference management. The computer simulations are discussed in Section 4.5 and this chapter ends with the concluding remarks in Section 4.6.

4.2 System Model and Proposed Architecture

Figures 4.1 and 4.2 illustrate our conventional and proposed systems respectively. $Op_x, x = n, m, u$ are telecommunications operators operating in the same region, each having his own MBS. For each operator, frequency sharing between macrocell and femtocells is considered. Considering the work in [67], we assume that operators can share the DAS through wired optical links connected to the CPUs. We further assume that the RF part of the DAS sensor supports the operator frequency bands. We do not consider the situation where different MBSs share simultaneously the same RAU. Therefore, this chapter focuses on a macrocell coexistence with femtocells with regard to the cross-tier interference mitigation in presence of the DAS which is an independent interface to the operators. We assume TDD-OFDMA in this paper. The cases presented in this chapter are feasible situations for our proposal performance evaluation. As the MUEs are managed by the MBS, considering several MUEs located in the same area, the MBS allocates different frequency bands or time slots for them to communicate. Consequently we considered one or two MUEs for the cases studied in this paper since we consider frequency sharing in our system model.

4.2.1 Conventional System: Traditional Coexistence of the Femtocell and Macrocell Tiers

Each femtocell constitutes an FBS and an FUE (FUE+FBS) as shown in Fig.4.1. The FBS carries the radio access control of its FUE. Because we assume a closed regime, the MUE is unable to communicate directly on the wireless link with any FBS. The femtocell radius is on the order of $10-50m$. The macrocell tier is composed of the MBS and each MUE randomly distributed in the tier. Each MUE attempts to transmit directly to the MBS.

4.2.2 Cellular Architecture Modification

Our proposed modification of the conventional system involves the insertion of the DAS in the benchmark. The DAS is represented in Fig.4.2 by the CPUs and the RAUs. Each RAU is connected directly to a CPU, which is linked to the MBS. We assume that all RAU-CPU and CPU-MBS links are fiber optic links with negligible delay. Signal processing such as minimum mean square estimation (MMSE) implemented through recursive least square algorithm and symbol demodulation can be performed at each FBS, and each CPU. A logical implementation of a DAS that cooperates with a network operator can be found in [70].

4.3 Proposed Concept of a Femtocell Clustering aided DAS

In [74], the interference cancellation considered information exchange directly between MBS and FBS. Because of the number of femtocells in a macrocell, we consider DAS cooperation as a solution to address the drawbacks such as signal decoding complexity and the traffic constraint on a single MBS.

4.3.1 Femtocell Clustering Concept

Our proposal considers a virtual cluster concept. Our concept of "*cluster*" is defined in as an aggregation of several femtocells (FBSs+FUEs) around a DAS sensor node which assists the FBS at the femtocells in the cross-tier interference cancellation. Due to the small operating radius of a femtocell, we can obtain several femtocells that form a physical cluster in a random location in the macrocell. Figure 4.2 shows such clusters, and we denote three of them as FC_i, FC_j and FC_k associated each with at least an RAU. In FC_j, F_j is a femtocell and R_j is an RAU. Considering such cluster, we derive the following femtocell clustering concept relative to the DAS elements and the interfering MUE near the cluster. The MUE transmission generates interference at the cluster. Each FBS evaluates its SINR to assess the need to mitigate the interference. We define a femtocell in outage as a femtocell whose FBS has a SINR below a threshold above which symbol decodability is possible. The femtocells in outage can request the cooperation of the DAS for interference mitigation. The DAS selects the femtocells that request interference mitigation. This selection consists of the femtocell clustering by the DAS. The interference mitigation requires that the DAS retrieves the symbols transmitted by the MUE through its RAU(s) and feed them back to the set of selected femtocells. Thus, each femtocell in the femtocells clustered by the DAS can retrieve its desired signal by interference cancellation which uses the feedback symbols of

the interfering terminal(s). Given the distribution of the DAS elements within the macrocell-tier, such cross-tier interference management can be performed in different clusters. This concept generalizes the interference cancellation scheme in [74].

4.3.2 Interference Cancellation Patterns

The introduction of the DAS allows cross-tier interference management under different situations. The channel gains are modeled as independently and identically distributed variables with zero mean and a unit variance. The interference cancellation for the femtocells selected by the DAS is illustrated in the following cases:

- Figure 4.3 shows $MUE1$ and $MUE2$ interference at the FBS. On the wireless link, the FBS receives its desired signal S_0 weighted by the channel gain h_{ff} in addition to the signals S_1 and S_2 which are weighted by the channel coefficients h_{m1f} and h_{m2f}, respectively. Simultaneously, the feedback system constituted by $CPU1$ and $CPU2$ retrieves the symbols S_1 and S_2 through signal processing and forward them to the FBS. $CPU1$ receives $MUE1$ transmitted signal S_1 without interference from $MUE2$ assumed to be located far enough from $CPU1$. Then, it demodulates the received signal in order to forward S_1 to both the FBS and $CPU2$. After receiving S_1, $CPU2$ performs interference cancellation as detailed in Fig.4.4 in order to retrieve S_2 from the wireless signal $h_{m1R}S_1 + h_{m2R}S_2$, where h_{m1R} (h_{m2R}) is the channel coefficient between $MUE1$ ($MUE2$) and the RAU of $CPU1$. The FBS can perform interference cancellation using the forwarded symbols S_1 and S_2 to recover S_0.

- Figure 4.4 shows the feedback system composed of the MBS and an RAU, where h_{m1R} (h_{m2R}) is the channel coefficient between $MUE1$ ($MUE2$) and the RAU of the CPU, and h_{m1M} is the channel coefficient between $MUE1$ and the MBS. $MUE1$ is close to the MBS such that interference from $MUE2$ to MBS is negligible , and $MUE2$ is close to the RAU linked to the CPU. When both MUEs interfere at the RAU, the MBS can recover S_1 and forward it to the CPU, which can recover the symbol S_2 of $MUE2$. This process involves a single feedback scheme at the CPU. Then, the two MUE symbols can be forwarded at the femtocells (FBSs connected to the CPU) that experience the interference from the two MUEs.

- Figure 4.5 shows a similar situation to Fig.4.4 with the difference that the MBS in Fig.4.4 is replaced by an RAU. Owing to the presence of the two MUEs and two RAUs sharing a CPU, we propose a power control of the MUEs through the following scheme: $MUE2$ reduces its transmit power to reach its closest RAU, $RAU2$. $MUE1$

transmits to *RAU*1. The CPU can demodulate the symbol received by *RAU*1 independently of the signal received at *RAU*2. The CPU connecting the two RAUs retrieves the MUE symbols to feed them back to the FBS for interference cancellation.

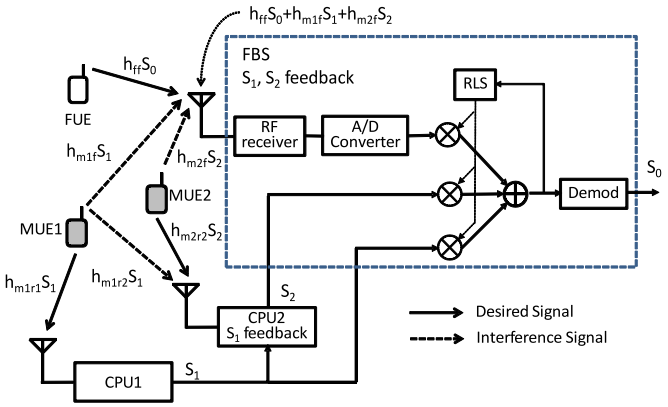

Fig. 4.3 Interference pattern and interference cancellation principle at the FBS.

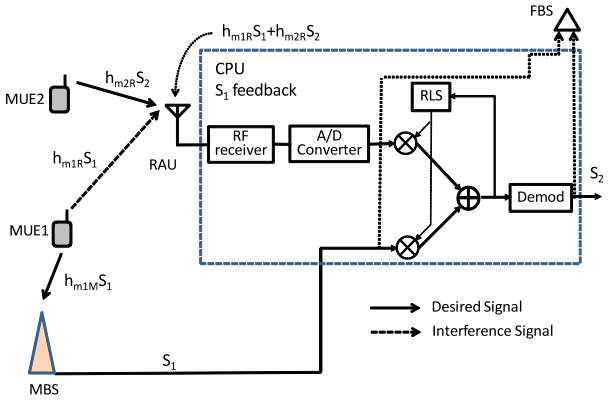

Fig. 4.4 Feedback system with CPU and MBS.

In Fig. 4.5, *RAU*1 receives the symbol S_1 without interference. Thus, the RLS module can receive the symbol S_1 after demodulation. The equation represents the signals received at the RLS input for interference cancellation. As represented in Fig. 4.5, h_{m1r1} is not required at the RLS input, therefore is not necessary in the following matrix representation of the signals for modeling the interference cancellation process. Such interference cancellation scheme has been proposed in our previous work in [74]. In Fig.4.5, the signals received by the CPU can be represented as follows:

$$\begin{pmatrix} S_2 h_{m2R} + S_1 h_{m1R} + n_R \\ S_1 \end{pmatrix} = \begin{pmatrix} h_{m2R} & h_{m1R} \\ 0 & 1 \end{pmatrix} \begin{pmatrix} S_2 \\ S_1 \end{pmatrix} + \begin{pmatrix} n_R \\ 0 \end{pmatrix},$$

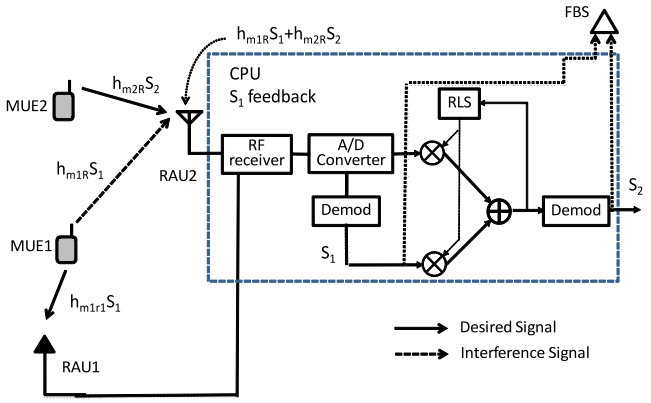

Fig. 4.5 Feedback system with two RAUs.

where h_{m2R} and h_{m1R} are the channel coefficients from $MUE2$ and $MUE1$, respectively, to $RAU2$; h_{m1r1} is the channel coefficient from $MUE1$ to $RAU1$, and n_R is an AWGN. $MUE1$ signal at $RAU1$ is received without interference. S_1 and S_2 can be independently decoded by the signal processing at the CPU because the channel matrix

$$\begin{pmatrix} h_{m2R} & h_{m1M} \\ 0 & 1 \end{pmatrix}$$

is invertible.

Considering that the feedback system can be one of the situations represented in either Fig. 4.4 or Fig.4.5, we use the notation in Fig.4.3 to effectively describe the interference management schemes for the rest of this section. FUE transmits the symbol S_0 under channel gain h_{ff} to its related FBS. S_1 and S_2 are transmitted from the two $MUE1$ and $MUE2$, respectively. h_{m1f} and h_{m2f} represent the channel gains from $MUE1$ and $MUE2$ to the FBS. We consider $MUE1$ and $MUE2$ in Fig.4.3 for the analysis of the S_0 recovery under the interference of two MUEs. We assume that the estimation process of S_0 can be performed as described in [74], by considering the signal feedback from the feedback system to the FBS that receives the combined signal $S_0h_{ff}+S_1h_{m1f}+S_2h_{m2f}$. The interference case that must be considered before the recovery of S_0 by the FBS is described as follows: $(h_{m1r2}S_1+h_{m2r2}S_2)$ represents the signal received at the RAU resulting from the transmission of the two MUEs. The feedback of S_1 from the MBS to $CPU2$ allows a single-symbol detection as in [74]. Assuming correct recovery of S_1 and S_2 at the CPU, each femtocell in the DAS femtocell cluster can perform interference cancellation using the following rela-

tionship:

$$\begin{pmatrix} S_0 h_{ff} + S_1 h_{m1f} + S_2 h_{m2f} + n_f \\ S_1 \\ S_2 \end{pmatrix} = \begin{pmatrix} h_{ff} & h_{m1f} & h_{m2f} \\ 0 & 1 & 0 \\ 0 & 0 & 1 \end{pmatrix} \begin{pmatrix} S_0 \\ S_1 \\ S_2 \end{pmatrix} + \begin{pmatrix} n_f \\ 0 \\ 0 \end{pmatrix},$$

where n_f is an AWGN. The symbols S_1 and S_2 are provided to the FBS by the CPU. The FBS can retrieve S_0 by channel matrix inversion. Such channel matrix inversion is approximated by the RLS algorithm with minimum mean square error equalization. Therefore, the FBS approximates h_{m1f} and h_{m2f} by the RLS algorithm. The detection of S_0 using the above matrices notation was explicitly derived in [74].

4.3.3 Reception at the RAUs and FBSs

On one hand, the proposed interference management based on the DAS relies on the correct reception of the interfering MUE symbols at the RAU located in the vicinity of both the femtocell cluster and the MUE. On the other hand, the inter-femtocell interference may remain at the FBS although the cross-tier interference is cancelled with our proposed feedback. The restriction on the femtocells transmission due to their closeness to the DAS sensor node is made to allow the DAS sensor node to receive the interfering MUE signal without interference from the close femtocell users.

Thus, we evaluate the probability of successful reception of the transmission of an MUE (FUE) at an RAU (FBS). This evaluation is subject to the MUE (FUE) transmit power control and the combined interference from the set of femtocells that transmit within the cluster. We denote the cardinality of this set by $|\Omega|$. We assume that the femtocells involved in the outage derivation are each located at a distance r from the RAU. Such combined interference is subject to the following analysis:

We denote the set of transmission occurrences in the vicinity of the RAU as $E = \{x_1, x_2 ...\}$. Therefore, we obtain $\Sigma = \{\emptyset, \{x_1\}, \{x_1, x_2\} ...\}$ as the set of the subsets that can be constructed from E, where $\emptyset$ is an empty set. We define the following function over Σ:

$$\begin{aligned} f : \Sigma &\rightarrow R^+ \\ \Omega &\rightarrow P(X \in \Omega), \end{aligned} \tag{4.1}$$

where Ω is the set of FUE transmission occurrences from the cluster, $P(X \in \Omega)$ is the total probability of the events constituting Ω and R^+ is the set of positive real numbers. To express $P(X \in \Omega)$, we must rely on the DAS femtocell clustering which defines the set of

femtocells that request interference mitigation. The cardinality of Ω is given by:

$$\begin{aligned} |\Omega| &= |\{X_s \in \Omega_M\}| + |\{X_n \in \Omega_c\}| \\ &= |\Omega_M| + |\Omega_c| - |\Omega_M \cap \Omega_c|, \end{aligned} \tag{4.2}$$

where $s,n \in \{1,2,..|\Omega|\}$ are the indexes, Ω_M is the set of transmission occurrences interfering at the RAU, and Ω_c is the set that requires symbol feedback from a CPU for interference cancellation. The probability of successful reception at the RAU denoted as $P_s(r,|\Omega_M|)$ is derived from [31] as follows:

$$P_s(r,|\Omega_M|) = e^{-\theta \frac{N_0}{P_{tm}} d^{\lambda_{out}}} \prod_{i=1}^{|\Omega_M|} \frac{1}{1+\frac{P_i}{P_{tm}} \frac{d^{\lambda_{out}}}{r^{\lambda_{in}}}}, \tag{4.3}$$

where P_i is the transmit power of the FUE whose transmission is received at the RAU considered in 4.3,θ is the threshold SINR for successful reception, N_0 is the noise power, P_{tm} is the transmit power of the MUE, d is the distance from the MUE to the RAU, and λ_{out} and λ_{in} are the outdoor and indoor path loss exponents, respectively.

*Proof:*The SINR of the MUE at the sensor node is expressed as

$$SINR = \frac{P_{tm} d^{-\lambda_{out}} |h_M|^2}{N_0 + \sum_{i=1}^{|\Omega_M|} P_i r^{-\lambda_{in}} |h_i|^2}, \tag{4.4}$$

where h_M is the channel coefficient between the MUE and the RAU and h_i is the channel coefficient from the ith femtocell to the RAU. The outage probability is given by

$$P(SINR < \theta) = 1 - P(SINR \geq \theta), \tag{4.5}$$

where $P((x) < (y))$ indicates the probability that x is lower than y. Furthermore,

$$P(SINR \geq \theta) = P(|h_M|^2 \geq \frac{N_0 \theta}{P_{tm} d^{-\lambda_{out}}} + \frac{\sum_{i=1}^{|\Omega_M|} P_i r^{-\lambda_{in}} |h_i|^2}{P_{tm} d^{-\lambda_{out}}}). \tag{4.6}$$

We note that $|h_M|^2$ and $|h_i|^2$ are exponentially distributed with a variance of one; thus, by computing the moment generating function [14], we can obtain

$$P(SINR \geq \theta) = e^{-\theta \frac{N_0}{P_{tm}} d^{\lambda_{out}}} M_t(Y), \tag{4.7}$$

where t is a real number parameter of the moment generating function and Y is defined as:

$$Y = \sum_{i=1}^{|\Omega_M|} P_i r^{-\lambda_{in}} |h_i|^2 . \tag{4.8}$$

$M_t(Y)$ is the moment generating function of the random variable Y and parameter t is defined as

$$\begin{aligned} M_t(Y) &= E[e^{tY}] \\ &= \prod_{i=1}^{|\Omega_M|} \int_0^{\infty} e^{-st} e^{-t} dt \\ &= \prod_{i=1}^{|\Omega_M|} \frac{1}{s+1}, \end{aligned} \tag{4.9}$$

where $s = \frac{\theta P_i r^{-\lambda_{in}}}{P_{tm} r^{-\lambda_{out}}}$ and e^{-t} is the density function of an exponentially distributed random variable with a variance of one. Replacing $M_t(Y)$ by its value in 4.9 ends the proof.

4.4 Proposed Interference Management in the two-tier Network

As $|\Omega|$ results partially from the cardinality of the terminals that interfere at the RAU, we propose to manage the interference by considering the situation where two different sets of DAS-selected femtocells are linked to different DAS elements as denoted by FC_j and FC_k where the MUE denoted by M_j interferes in both sets. Because interference cancellation can be performed at each element of the DAS femtocell clustered in $\{X_n \in \Omega_c\}$, the resulting sum-rate capacity can be written as follows:

$$C_{\Omega_c} = \sum_{n=1}^{|\Omega_c|} \log_2(1 + SINR_n), \tag{4.10}$$

where $SINR_n$ is the SINR of $X_n \in \Omega_c$. Because the feedback option is unfeasible with M_j interfering in FC_k, we propose the following time slot based orthogonal resource allocation for the MUE transmissions to improve the network sum-rate.

Considering the transmission of an FUE to its FBS, the previous analysis can be applied by substituting the MUE with the FUE and the RAU with the FBS. The set of femtocells surrounding the considered FBS can cause interference and degrade the FBS reception even

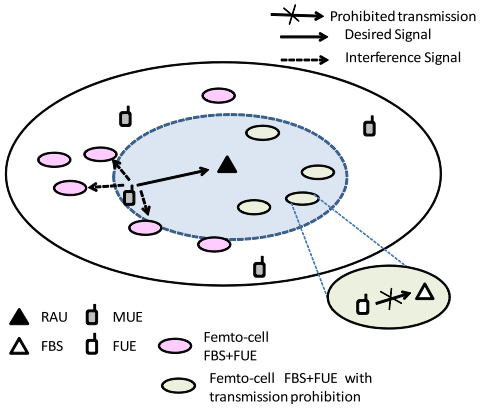

Fig. 4.6 Interference management at the reception.

in the case of feedback. Thus, for a perfect reception at the RAU, we propose to prohibit the FUE transmission close to the RAU as illustrated in Fig.4.6 used for our simulation model described in the Section 4.5.

4.4.1 Proposed Radio Resource Allocation for Cross-tier Interference Management in the two-tier network

In Fig.4.2, let's consider M_j and M_k are MUEs interfering at FC_j and FC_k, respectively. In addition, we assume that M_j interferes at F_j and F_k whereas M_k interference is restricted to FC_k. R_j and R_k are RAUs in FC_j and FC_k, respectively. F_j (resp. F_k) is a femtocell in FC_j (resp. FC_k). The interference management through feedback can be achieved as follows: R_j (resp. R_k) retrieves M_j (resp. M_k) transmitted symbols, then CPU_j (resp. CPU_k) feeds back the retrieved symbols to F_j (resp. F_k). Such feedback process is enabled by the following radio resource allocation of the MUEs. Table 4.1 lists the access of the femtocells and MUEs to FC_j and FC_k partitioned using time slots (TS). For each column, the different TSs are expressed as TS_i, $i = 1,2,3$. At each column TS_i, the simultaneously transmitting terminals are denoted as MUE and/or FUE. M_j and F_j can transmit simultaneously during TS_1 because M_j can target the MBS or the RAU. The interference of M_j at F_j can be cancelled by the feedback as illustrated by Fig.4.4 or Fig.4.5. In TS_2, the interference from M_j to F_k is avoided and a transmission similar to TS_1 can occur in M_k and F_k whereas F_j is beyond the interference range. F_j and F_k can transmit simultaneously in TS_3. The DAS enables terminal access management and permits cooperation if the MUE access to any femtocell base station is restricted. In the conventional scheme, three TSs are required to avoid interference from the base stations. Because the transmit power decays with the distance, the interference of M_k with F_j is assumed to be negligible.

4.4.2 Simultaneous Transmission without the Proposed Radio Resource Allocation

This section describes the conventional scheme of the proposal in Section 4.4.1. We consider FC_j and FC_k in the absence of the proposed radio resource allocation. We assume a simultaneous transmission of all femtocells and MUEs. Considering the DAS elements, the MUEs can transmit at minimum power to reach the RAU. Although F_j and F_k benefit from the interference cancellation from M_j and M_k,respectively, in the DAS femtocell clustering, F_k experiences interference from M_j. In the conventional system, F_j and F_k experience low SINR from the high transmit power of the MUEs.

4.5 Simulation Results and Discussion

4.5.1 Simulation Conditions

We use the C language for the simulations presented in this chapter. The channel model is a five-path exponential Rayleigh fading. The noise is generated as AWGN. Each user transmits by QPSK modulation to generate the symbols from the binary output of the convolutional encoder. Then, OFDM is applied before the signals enter the channel. The OFDM key parameters are listed in Table 4.2 and the simulation parameters related to the macrocell-femtocell two-tier network are presented in Table 4.3 which are similar to those in [62]. The noise is added during signal reception whereas the signal fed back to the base station or the DAS element is free from noise. We use the RLS based MMSE algorithm to recover the data at the receiver for interference cancellation at CPU and/or FBS. The transmit power, positions and details of the distance path loss model of each user are listed in Table 4.3. A fixed loss is chosen instead of considering a random lognormal shadowing. We use the SINR and capacity evaluation from [18]. The sum-rate is then evaluated by 4.10 whose cumulative distribution function (CDF) is used in the simulation results.

4.5.2 Performance Evaluation and Discussion

Our simulation system model is illustrated by Fig.4.6. In Fig.4.6, MUE is located at random distances from the femtocells in its vicinity. In our simulation, we consider different values of r for the variation of the distance between the MUE and different FBSs under the MUE cross-tier interference. Therefore, we evaluate the performance at the FBS with and without feedback from the feedback system. As represented in Fig.4.6, the reception of the MUE

symbols at the RAU is performed without femtocell interference. In the case of 2 MUEs, we apply the feedback system in Fig.4.4 or Fig.4.5 where the MBS or RAU(s) are protected from femtocell interference.

The performance evaluation consists of the computation of the sum-rate that considers a femtocell cluster and its neighboring MUE. The sum-rate is evaluated using 4.10 for a given number of mobile terminals. Thus, we add up the rates of the femtocells and MUEs chosen in the situations that illustrate our proposal and the benchmark. For the two MUEs and two RAUs connected to the same DAS signal processing unit, the DAS can recover the MUE transmitted symbols and forward them to the FBSs that require interference cancellation. In the case of a one-sensor node and two MUEs, one MUE can target the RAU, and the other transmits directly to the MBS. The DAS can demand data from the MBS for interference cancellation as depicted in Fig.4.4. In the presence of more than two MUEs, we assume a time slot based orthogonal resource allocation for the MUE transmissions as explained in 4.4.1. Therefore, the FBS can synchronize with the MUE scheduling. We present the results through the CDF of the capacity.

Table 4.1 Proposed orthogonal radio resource allocation for interference management.

Proposed	Conventional
$TS_1 : M_j, F_j$	$TS_1 : M_j$
$TS_2 : M_k, F_j, F_k$	$TS_2 : M_k, F_j$
$\cdots$	$TS_3 : F_j, F_k$

Table 4.2 Simulation conditions.

Parameter	Value
Bandwidth	5MHz
Number of subcarriers	512
Useful symbol time	6.4μs
Guard interval	1.25μs
Data modulation	OFDM QPSK
Small-scale channel model	Rayleigh flat fading
Weight estimation algorithm	RLS
Noise	AWGN
Convolutional code rate	1/2
Convolutional code constraint length	7

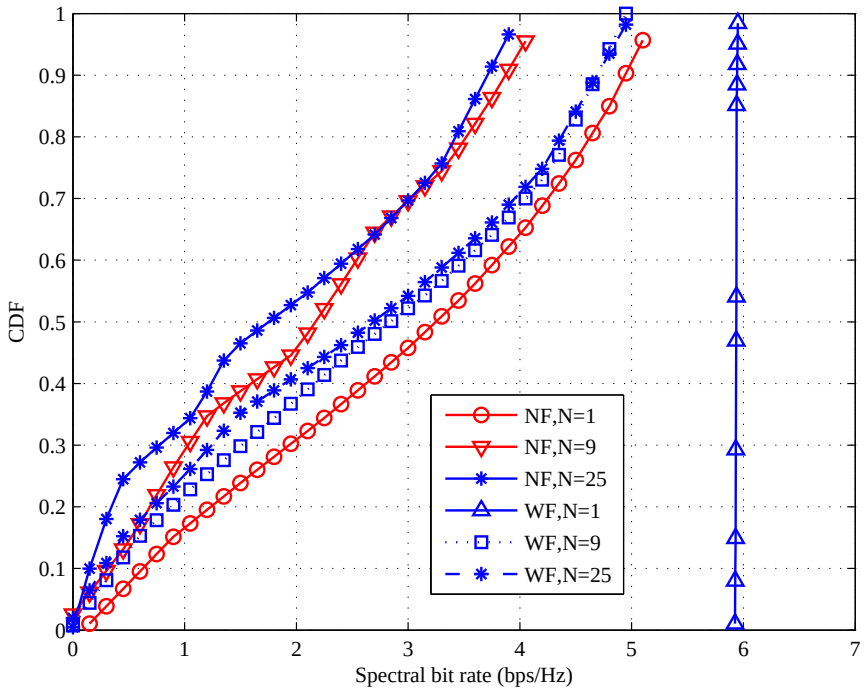

Fig. 4.7 Spectral bit rate at sensor Node and FBSs with $|\Omega_M|$.

4.5.3 Spectral Bit Rate at RAU and FBSs with $|\Omega_M|$

The capacity of the MUE at the RAU or at any FBS is subject to the interference of the surrounding femtocells. Thus, we evaluate the capacity considering the transmitting femtocells i.e. $\{X_s \in \Omega_M\}$. We present the performance of a receiver considering the presence of surrounding terminal interference and the proposed interference cancellation. In Fig.4.7, *"NF"* stands for *"No Feedback"*, i.e. there is no interference cancellation of the cross-tier interference. The curves with *"NF"* represent the benchmark. *"WF"* indicates *"With Feedback"*, i.e. the receiver performs interference cancellation using the feedback of the symbols of an interfering MUE. *"N=i"* indicates that i FUEs are interfering at the receiver as in the situation where the FBS retrieves its FUE data with the MUE symbols feedback and the interference of the neighboring femtocells. The curves with *"WF"* represent the simulations with interference cancellation by the CPU or the FBS using feedback symbols. The spectral bit rate performance improves with the reduction of the received interference power which decreases in these simulations with the path loss and the interfering terminals are farther located from the receiver.

"NF,N=1" evaluates the situation where the desired signal of one mobile equipment is received with interference. Such cases is represented in this study by an MUE transmission received at the RAU while another MUE interference occurs at the reception. Another illus-

tration of *"NF,N=1"* is the interference of an MUE at an FBS receiving the transmission of its FUE without inter-femtocell interference. *"WF,N=1"* represents the interference cancellation performance where the symbols of the single interfering terminal are fed back to the receiver. In this case, the interference is completely removed. This situation illustrates the performance of the feedback system in Fig.4.4 or Fig.4.5.

"NF,N=4" and *"NF,N=25"* evaluate each the performance at the receiver when the number of interfering mobile terminals increases and without interference mitigation. *"WF,N=4"* and *"WF,N=25"* are similar to *"NF,N=4"* and *"NF,N=25"*, respectively; with the difference that for *"NF,N=4"* and *"NF,N=25"*, the MUE interference at the FBS has its interference cancelled at the receiver whereas the interference from neighboring femtocells affects the performance. The interference mitigation effectively reduces the cross-tier interference to enhance the spectral bit rate.

4.5.4 Sum-rate Capacity by the Proposed Radio Resource Allocation

We consider two MUEs and two femtocells to evaluate the sum-rate capacity, as shown in Fig.4.2 and described in Sections 4.4.1 and 4.4.2. The situation of FC_j and FC_k requires our proposal in 4.4.1 to improve the sum rate of the two MUEs (M_k and M_j) and the two femtocells(F_j and F_k). We evaluate the CDF of the sum-rate capacity resulting from the performance of the MUEs at the RAUs and the corresponding $|\Omega_c|$ femtocells for the situation presented by FC_j and FC_k, as described in Sections 4.4.1 and 4.4.2. $conv1$ and $proposed1$ represent the performance of the conventional and proposed systems, respectively, as described in Table 4.1 and Section 4.4.1. $conv2$ and $proposed2$ represent the transmission without the proposed orthogonal radio resource allocation, i.e., MUE simultaneous transmissions presented in Section 4.4.2. In $conv2$, FC_k experiences interference from the two MUEs whereas in $proposed2$, it receives feedback from M_k.

In Fig.4.8, the intersections of $conv1$ with $conv2$, and $proposed1$ with $proposed2$ occur because of the power decay with the distance adopted for each interfering terminal, i.e. as the interfering terminal moves away from the receiving terminal, the interference effect decreases. The proposed resource allocation enhances the DAS femtocell clustering interference mitigation to reduce the combined interference in order to lower the outage probability at the RAU. With the increase in N due to the number of terminals that experience high interference mitigated by feedback, the joint interference cancellation and DAS femtocell clustering yields significant sum-rate improvement compared with the conventional system.

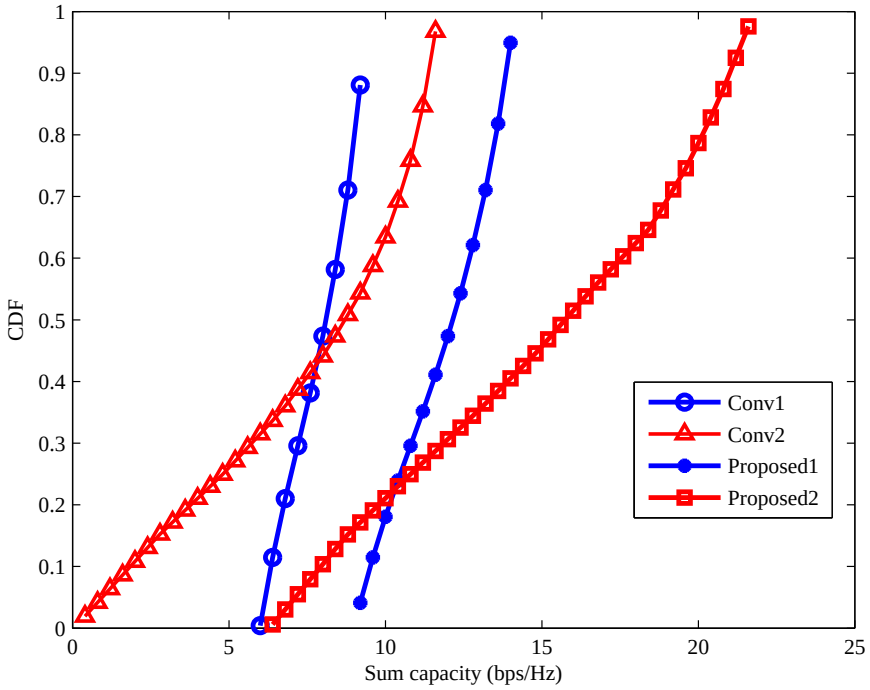

Fig. 4.8 MUE interference management spectral bit rate at RAUs and FBSs with $|\Omega_M|$.

4.5.5 Average Capacity across all Users in the Two-tier Network

This section shows the effect of inserting the DAS in the two-tier network. The performance metric used in the simulations is the average capacity across all users in the underlay system. The sum-rate capacity of the two-tier network can be re-written as:

$$C_f = \sum_{i=1}^{N_1} \log_2(1+SINR_i) + \sum_{j=1}^{N_2} \log_2(1+SINR_j), \tag{4.11}$$

where $SINR_i$ is the average SINR for each femtocell in the DAS clustering, $SINR_j$ is the SINR of an interfering MUE on the femtocells. 4.11 is an expansion of 4.10. The benchmark is the conventional system described in Section 4.5.3. We have $N_i \in \{4,14,25\}$. We use all the permutations of $\{4,14,25\}$ to evaluate 4.11 with the permutations of the $SINR_j s$. In the Fig.4.9 simulations, $N_1 = N_2 = 3$. Each element of $\{4,14,25\}$ is a number of femtocells clustered by the DAS selection described in Section 4.3.

Fig.4.9 shows the CDFs of the average capacity across all users in different scenarios. The average capacity across all users is defined by:

$$C_u = \frac{C_f}{N_1+N_2}. \tag{4.12}$$

Without the insertion of the DAS, and $N_2 > 1$, we assume that the radio resource management (by the MBS) assigns orthogonal resource blocks for the MUESs because of their direct transmission to the MBS by default. Thus, there is MUE interference avoidance from the MUEs to the MBS. Each femtocell cluster experiences the interference from one or two MUEs. *NoFeedback* and *MBSFeedback* represent each the conventional system without the DAS. With *NoFeedback*, each femtocell experiences an MUE interference without interference mitigation. *MBSFeedback* considers a feedback from the MBS; each cluster which experiences an MUE interference can receive a feedback from the MBS for interference cancellation. However, the feedback is subject to the orthogonal resource allocation applied for the MUEs directly transmitting to the MBS. Because of the MUE transmission scheduling (we assume different time slot allocation in the simulations), the sum-rate decreases with N_2. *DAS*1 and *DAS*2 represent our proposed modification of the two-tier network with the DAS insertion. With *DAS*1, the MUEs transmit to their respective RAUs. Thus, there is a simultaneous transmission of the MUEs; besides, the DAS can feedback the symbols of each interfering MUE to the femtocells which experience the interference. *DAS*2 is similar to *DAS*1 except that in *DAS*2, the interference cancellation removes all the cross-tier interference.

With *DAS*1, more than 90% of all users get each an average capacity of $2bps/Hz$, whereas with the *MBSFeedback*, almost all users get each less than $2bps/Hz$. The performance gap obtained by the insertion of the DAS can be interpreted as the traffic unmanageable by the MBS without the DAS.

A synchronization of the transmitting terminals is required in order to achieve our proposed interference cancellation scheme. The FBS and sensor node can adopt the macrocell synchronization by listening to the closest MUE signaling with the MBS. We propose the use of the convex combination algorithm in [77] to update the FBS timing to their nearest neighbors in the wireless interface. Additionally, we propose to feedback the synchronization signaling to the cluster of femtocells from the CPU as the CPU is directly connected to the femtocell cluster without intermediate node.

4.6 Conclusion

We have presented a novel femtocell clustering in a multi-tier network which was made possible using a proposed HetNet consisting of a DAS on the macrocell and femtocell tiers. We proposed the use of DAS as an interface between the two tiers to manage the cross-tier interference. Consequently, the network cross-tier interference was effectively mitigated, and the sum-rate capacity has improved substantially because the DAS femtocell cluster-

ing linearly scaled the capacity in proportion of the proposed femtocell clustering and its cardinality. The introduction of a DAS within the macrocell overlaid with the femtocells improved the cross-tier interference management and can be used as a benchmark for future HetNet.

Table 4.3 HUE and MUE cellular parameters.

Parameter(Variable)	Value
Macrocell radius (R_c)	1000m
Femtocell radius (R_f)	30m
Normalized distance (r)	$0.01 - 0.95$
Carrier frequency (f_c)	2500 MHz
Wall penetration loss (P_l)	5dB
Mobile maximum transmit power (P_{tmax})	23dBm
Macrocell path loss exponent(λ_{out})	3.8
Femtocell path loss exponent(λ_{in})	3

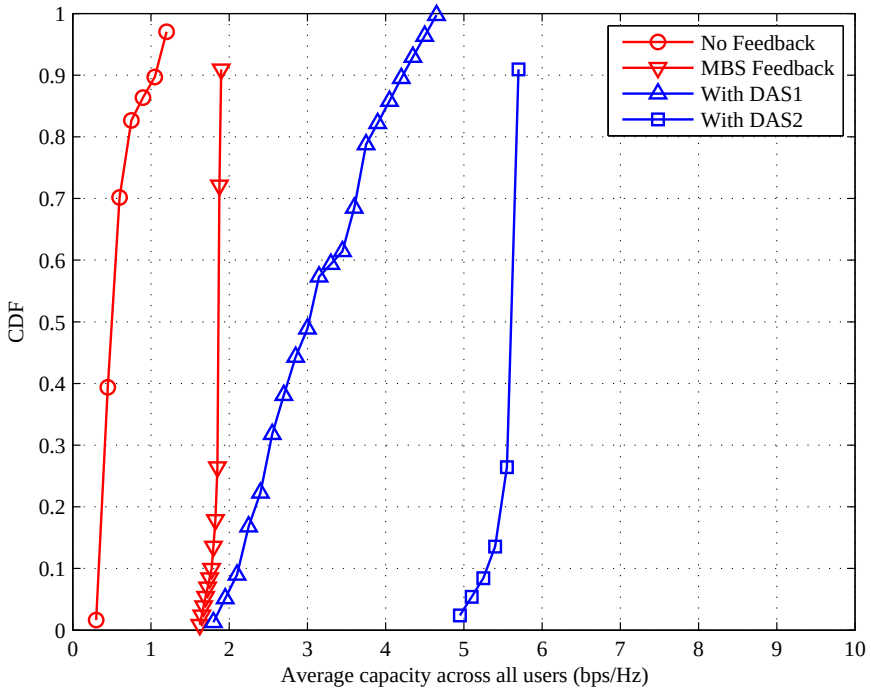

Fig. 4.9 Average capacity across all users in the underlay system.

Chapter 5

Joint antenna selection and power allocation for distributed-STBC cognitive small cell networks

Small cell networks enhance spectrum efficiency by handling the indoor traffic of mobile networks on a frequency-reuse operation. Current mobile communication researches tries to achieve co-channel deployment of small cell networks (SCNs) [78] and legacy macrocell as a response to the ever-growing demand in wireless channel capacity. In such multi-tier cellular network, transmit power allocation with regard to the outage constraint is an issue due to cross-tier interference. The complexity of the problem rises when more than one antenna transmit as in distributed space-time block code (STBC) [79–81]. Because most of the current mobile traffic happen in indoor, we introduce a prioritisation shift by imposing transmit power limitation on the outage generated by the outdoor mobile system to the indoor small cells. The prioritisation shift consists of setting an outage probability threshold limitation on the macrocell system which is classically considered as a primary system. In this chapter, we consider downlink spectrum sharing between a system consisting of small cells and a macrocell with relay network. The relays constitute a distributed-space-time block code relaying which provides the data traffic for the outdoor system terminals. New close-form expressions are derived to validate the proposed bit error rate (BER) function used in our optimisation algorithm. We propose a joint transmit antenna selection and power allocation which minimises the proposed BER function of the outdoor mobile terminal. The optimisation is constrained by the outage at the small cell located near the cooperating transmit relays. Power allocation for STBC-based transmit diversity can be achieved by selecting two relays out of all transmitters which are optimal in the sense of a dynamic power allocation for minimising the symbol error rate [79], an adaptive transmission power for minimising

the total energy transmitted [80] and the reduction of the number of relays for mitigating a total transmit power consumption in a source to destination transmission [81]. This chapter considers two-relay selection diversity based on STBC with power control.

5.1 Introduction

For two-tier networks, cross-tier interference is a limiting factor as emphasised in [82] where both intra and inter-tier interferences are considered to evaluate the optimal sensing threshold for the cognitive small cell base station (SBS). Suboptimal and near-optimum transmit power allocations are derived in [83] and [84] respectively. In addition, outage probability analysis of spatially distributed relaying based on STBC is provided for ergodic and non-ergodic channel in [83] and [84], respectively. The relaying transmit power is a function of the power allocated to the source and the number of underlying STBC matrix columns [85]. The performance of distributed-STBC in [85] is achieved by using channel state information (CSI) availability [86, 87]; in addition the difference in signal-to-noise ratio (SNR) branch due to the large scale fading environment of multi-tier cellular networks is ignored. In distributed-STBC with relaying, the two-selected transmit antennas are located at different distances from the receiver; thus, the path loss affects bit error rate (BER) performance. Furthermore, the cross-tier interference in heterogeneous small cell networks is a function of the path loss exponents of the indoor and outdoor systems. In contrast to the related work such as [80], the aforementioned considerations are taken into account in this study. Our proposal derives the two-relay transmit powers independently of CSI while considering path loss effect on unequal SNR branch.

Diversity branch with unequal SNR is studied in [13, 88, 89]. In [88], the output SNR of a selected diversity branches with unequal SNRs [13] is maximised through maximum ratio combining. The work in [89] differs from [88] by its application of unequal transmit power allocation to the Alamouti scheme [90]. However, the derived transmit powers are function of the channel gains of the diversity branches in contrast to the proposal in this paper which derives transmit power function without CSI for the two-selected relays. This paper contributes to advance the recent instance of heterogeneous networks denoted as cognitive small cell networks (CSCNs) [78, 91–93]. The probabilities of false alarm and detection are provided for a SBS in [78] pertaining to the aggregate interference at the SBS, using small cell stochastic geometry model. In [91], the SBS senses both the macrocell uplink and downlink spectra of the macrocell operating in frequency division duplex for opportunistic access. In [92], CSCN performance limits are illustrated through the user detection

becoming infeasible at the SBS under a certain interference threshold. Our proposal extends the CSCN concept in multi-tier cellular networks by leveraging relay selection to maximise macrocell user performance with respect to cross-tier interference on the small cell network.

The cognitive radio concept of our proposal consists of controlling the outage generated by the outdoor macrocell system to the small cell networks. We propose to design a modern wireless system with adjustable transmit powers which minimise the BER of the macrocell user equipment (MUE) while satisfying the outage constraint of the underlaying small cell. Considering a set of relays transmitting to the MUE, our proposal derives a novel function of the MUE BER for Alamouti encoding [90] with two selected diversity branches having unequal SNRs. The novel expression matches the RAKE maximum ratio combining performance in [13]. We additionally derive a new closed-form BER expression using the distribution of the sum of the unequal branch SNRs. The optimisation derives the set of optimal transmit powers of two relays among the candidate relays re-transmitting to the outdoor MUE while surrounding the small cell. For the selected relays, the derived outage caused by each relay to the small cell is used to define the selected relay transmit power threshold. Finally, the BER function is iteratively minimised under the outage constraints to derive the relay transmit powers. Applying this optimisation to two-relay selection yields a better BER compared to the distributed-Alamouti STBC with equal power allocation.

Due to the ad-hoc deployment of small cells, it is difficult to tailor their transmit powers to the MBS transmit power as in [83] where the relay transmit power is at most half the source transmit power.

The work in [83] derives sub-optimal relay transmit power considering distributed STBC with Alamouti encoding. Two main differences occur compared to our work. In [83], the transmit power of a relay is equal to the source transmit power divided by the number of columns of the underlying STBC matrix. In [83], this number is higher or equal to 2. Therefore, the maximum transmit power of a relay is always equal or smaller than half of the source transmit power. In our proposed strategy, a selected relay can transmit at a maximum power if it is not causing outage at the closest small cell; the relay power allocation is independent from the source power. Moreover, our allocation power is optimal with reference to the iterative algorithm.

The work in [94] considers the optimization of the Shannon capacity of the small cell while we propose to limit the outage from the macrocell tier. In [94], the FBSs use feedback information from the macrocell tier to update their transmit power using water-filling algorithms. The need to include the macrocell tier feedback into the power derivation increases in the complexity of the algorithm due to delay in receiving the feedback information. In contrast, the relay transmit power thresholds can be computed with the network parameters

given in Table 1 in this work.

In [78], the authors derive trade-offs to achieve energy-efficient cognitive small cell networks. Given the huge deployment of small cells overlaid on macrocells, we consider a prioritization of the small cell performance by limiting the relay transmit power. To compensate the transmit power reduction which affects the MUE performance, the transmit power issue has to be addressed. Conventional relay transmission is oblivious to the outage at the small cell due to the primary system (MBS, MUE, relay) because the small cell is conventionally considered as a secondary system; the relay transmit power is either high enough for the interference from the relay to the small cell to cause outage or too low for the MUE performance to be optimal. We propose a distributed-STBC scheme with two-relay selection to provide MUE optimal performance under the constraint of outage limitation at the small cell. Thus, the contribution of this work is manifold:

- The cognitive radio concept of our proposal consists of controlling the outage generated by the outdoor macrocell system to the small cell networks. Small cells are mostly self-organized as with femtocells. Such feature leaves the small cell performance dependent on the cross-tier interference in multi-tier networks. Therefore, the individual transmit power limitation derived with regards to the small cell outage reduces the performance degradation due to outer tier interference.

- We propose to design a modern wireless system with adjustable transmit powers which minimise the bit error rate (BER) of the macrocell user equipment (MUE) while satisfying the outage constraint of the underlaying small cell. Our propose STBC scheme with unequal branch signal-to-noise ratio (SNR) assigning individual transmit power limitations based on the individual outage generated at the neighboring small cell has been discussed in the literature. In addition, the use of STBC precludes the transmit power adaption based on channel state information (CSI). Most of the papers in the literature use CSI for optimal power allocation.

- Considering a set of relays transmitting to the MUE, our proposal derives a novel function of the MUE BER for Alamouti encoding [90] with two selected diversity branches having unequal SNRs. The novel expression matches the RAKE maximum ratio combining performance in [13]. We additionally derive a new closed-form BER expression using the distribution of the sum of the unequal branch SNR. The optimisation derives the set of optimal transmit powers of two relays among the candidate relays re-transmitting to the outdoor MUE while surrounding the small cell. The derived outage caused by each relay to the small cell is used to define a power threshold which limits the transmit power of the considered relay. Using the outage at the

small cell, we apply individual transmit power limitation on the selected relays. Such scheme is nonexistent in the literature.

- Finally, the novel BER function is iteratively minimised under the outage constraints to derive the two-relay transmit powers. The optimisation yields a better BER compared to the distributed-Alamouti STBC with equal power allocation.

The rest of this chapter is structured as follows: the system model is described in Section 5.2. The proposed BER for distributed-STBC with unequal branch SNR, and the joint two-relay selection and transmit power allocation are presented in Sections 5.3.1 and 5.4 respectively. The computer simulations are discussed in Section 5.5 and this chapter ends with the concluding remarks in Section 5.6.

5.2 System Model

5.2.1 Two-tier Cellular Network Topology

We consider universal spectrum sharing between a tier consisting of a single macrocell base station (MBS) and outdoor MUEs, and another of randomly distributed SBSs. Each SBS serves at least one small cell user (SCU). The downlink between the MBS and the MUEs is interfaced by a set of relays as illustrated in Fig. 5.1. The relays are equally distanced from the MBS. Both tiers can access the full spectrum and use orthogonal frequency-division multiple access (OFDMA). We assume a closed-access operation of the SBSs, i.e. a SBS is solely accessed by its registered SCUs. Such closed-access regime is detailed in [95].

5.2.2 Two-tier Cognitive Cellular Networks

We restrict this study to the second time slot where two selected relays among a total number of N_r relay the MBS data to the MUE. For instance, in Fig. 5.1, the relays R_i and R_j are selected to transmit to MUE_k. Such transmission generates different interference levels at the close SCN_k considering the variable position and transmit power of the relays. We adopt the Alamouti scheme [90] for the symbols transmitted from the two selected relays. The relays belong to the macrocell tier while the SCNs are overlaid onto the macrocell as a second tier.

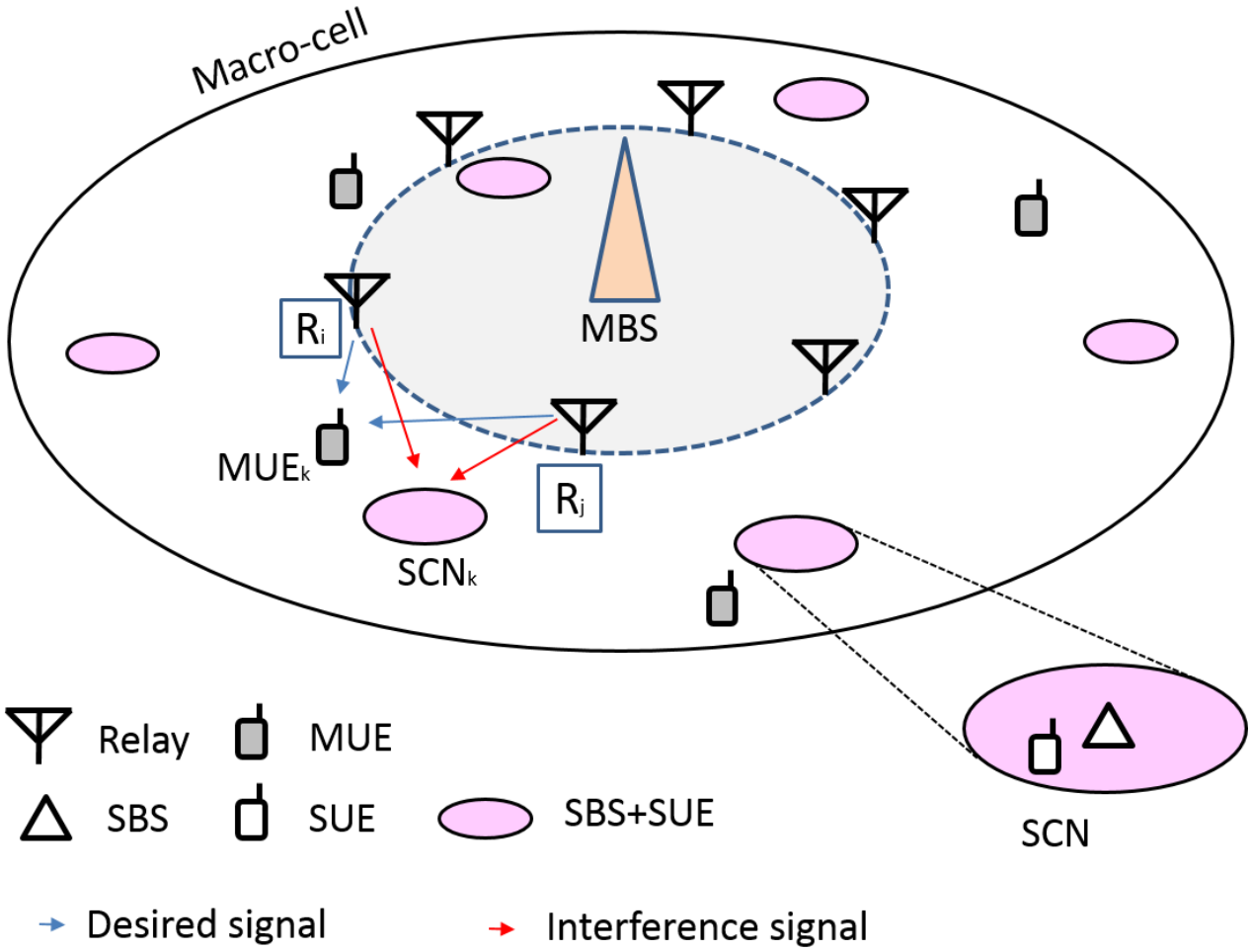

Fig. 5.1 Downlink two-tier cognitive small cell networks.

5.3 BER Functions for Distributed-STBC with Unequal Branch SNR

5.3.1 A Novel BER Function for Distributed-STBC with Unequal Branch SNR

The maximum ratio combining (MRC) for the sum of instantaneous channel to noise ratio (CNR) is studied in [96]. The sum is defined as the MRC for individual branches in a multi-branched system. We consider path loss in determining the SNR of a two branch with different SNRs in an Alamouti transmission scheme which is studied in [96].

To derive the BER function, we assume that the relays R_i and R_j have been selected to

transmit to SCN_k. For the rest of the paper, two selected relays are denoted as R_1 and R_2, and SCN_k is used without index. We denote by h_n the complex channel gain from the nth relay to the SCN, where $n = 1,2$. The channel gains $|h_1|^2$ and $|h_2|^2$ are each exponentially distributed under Rayleigh fading with 2 degrees of freedom and variance 0.5. The distance between the nth relay and the SCN is denoted as d_n, and the nth relay transmits power by P_n. We use the SNR derivation in [90] for each relay transmitting symbols according to the encoding in [90]. We omit the symbol notation in our equations as each symbol is assumed to have a unit energy. However, we consider path loss and transmit power in our analysis. Such two consideration are important to our contribution. Assuming that two relays transmit following the Alamouti [90] encoding, the SNR at the SCN denoted by γ can be written as:

$$\begin{aligned}\gamma_M &= \frac{P_1 d_1^{-\alpha_{out}}}{N_0}|h_1|^2 + \frac{P_2 d_2^{-\alpha_{out}}}{N_0}|h_2|^2 \\ &= \lambda_1|h_1|^2 + \lambda_2|h_2|^2 \\ &= X_1 + X_2,\end{aligned} \tag{5.1}$$

where λ_n is the average branch SNR of the nth relay at the SCN given by:

$$\lambda_n = \frac{P_n d_n^{-\alpha_{out}}}{N_0}, \tag{5.2}$$

X_1 and X_2 denote $\lambda_1|h_1|^2$ and $\lambda_2|h_2|^2$ respectively, and α_{out} denotes the outdoor path loss exponent. In (5.2), N_0 is the variance of the zero-mean Gaussian noise at the receiver of SCN. The transmitted symbols have unit energy. We use the moment generating function method to derive the BER function from (5.1). $\lambda_n|h_n|^2$ is an exponentially distributed random variable with parameter λ_n. Therefore γ_M in (5.1) is the sum of two exponentially distributed random variables namely $\lambda_1|h_1|^2$ and $\lambda_2|h_2|^2$. λ_1 is different from λ_2, γ_M is the sum of independent exponentially distributed random variables with different scale parameters. The distribution of γ_M is studied in [97, 98]. The moment generating function (MGF) $M_{\gamma_M}(t)$ of γ_M is given by its Laplace transform as:

$$\begin{aligned}M_{\gamma_M}(t) &= E[e^{\gamma_M t}] \\ &= \int_0^\infty p_{\gamma_M}(\gamma_M) e^{\gamma_M t} d\gamma_M \\ &= M_{X_1}(t) M_{X_2}(t),\end{aligned} \tag{5.3}$$

where $t < \frac{1}{\lambda_n}$, $E[.]$ and $e^{[.]}$ are the expectation and exponential functions respectively, and $p_{\gamma_M}(\gamma_M)$ is the probability density function (PDF) of γ_M. The independence property of

the random variables $\lambda_1|h_1|^2$ and $\lambda_2|h_2|^2$ yields the second line of (5.3). The MGF of the exponentially distributed random X_n is given by :

$$M_{X_n}(t) = \frac{\frac{1}{\lambda_n}}{\frac{1}{\lambda_n} - t}. \tag{5.4}$$

Thus, the $M_{\gamma_M}(t)$ becomes:

$$M_{\gamma_M}(t) = \frac{\frac{1}{\lambda_1}}{\frac{1}{\lambda_1} - t} \frac{\frac{1}{\lambda_2}}{\frac{1}{\lambda_2} - t}. \tag{5.5}$$

The probability of bit error for $\frac{\pi}{4} - QPSK$ denoted as P_b can be found in [99] as:

$$P_b = \int_0^{\infty} Q(\sqrt{2\gamma_M}) p_{\gamma_M}(\gamma_M) d\gamma_M, \tag{5.6}$$

where $Q(.)$ is the Q-function [99] approximated as:

$$Q(x) = \frac{1}{\pi} \int_0^{\frac{\pi}{2}} e^{-\frac{x^2}{2\sin^2(\theta)}} d\theta. \tag{5.7}$$

Inserting the Q-function approximation in (5.6) yields:

$$\begin{aligned} P_b &= \frac{1}{\pi} \int_0^{\frac{\pi}{2}} \int_0^{\infty} e^{-\frac{2\gamma_M}{2\sin^2(\theta)}} p_{\gamma_M}(\gamma_M) d\theta d\gamma_M \\ &= \frac{1}{\pi} \int_0^{\frac{\pi}{2}} M_{\gamma_M}(-\frac{1}{\sin^2(\theta)}) d\theta. \end{aligned} \tag{5.8}$$

Using software such as Mathematica, the integration of (5.8) yields the BER expression:

$$\begin{aligned} P_b =& (\sqrt{\lambda_1\lambda_2} + \sqrt{\lambda_2(1+\lambda_1)} + \sqrt{\lambda_1(1+\lambda_2)}) / \\ & 2(\sqrt{\lambda_1} + \sqrt{1+\lambda_1}) \sqrt{(1+\lambda_1)(1+\lambda_2)} (\sqrt{\lambda_2 + \sqrt{1+\lambda_2}}) \\ & (\sqrt{\lambda_2(1+\lambda_1)} + \sqrt{\lambda_1(1+\lambda_2)}). \end{aligned} \tag{5.9}$$

The partial derivatives of P_b are negatives; thus P_b is a decreasing function of λ_1 and/or λ_2 as shown in the appendix. To validate P_b, we compare it with the RAKE maximum ratio combining studied in [13] and the BER derived using the PDF of the sum of two independent exponentially distributed random variables in [97] for the SNR of a two-branch transmit diversity.

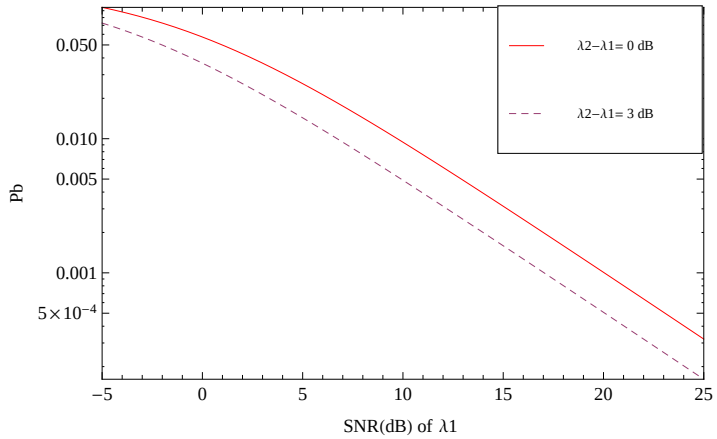

Fig. 5.2 Performance of our proposed BER function with unequal two-branch SNR.

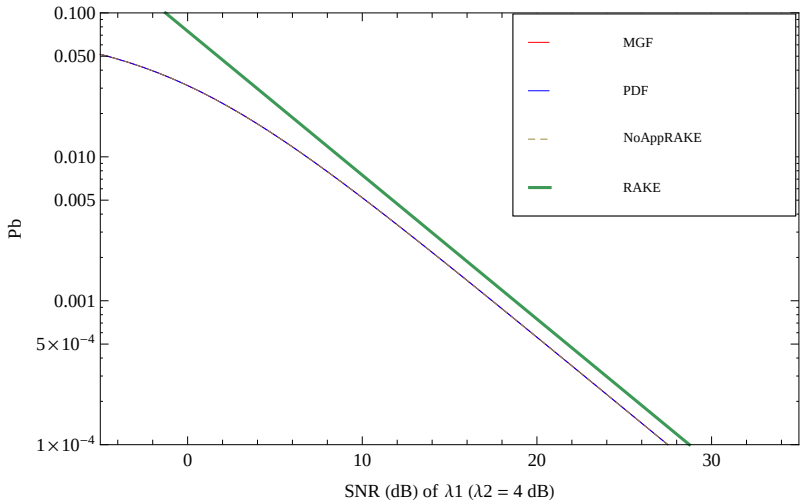

Fig. 5.3 Performance of our proposed BER function compared to the RAKE maximum ratio combining and the PDF-based methods for low SNR.

5.3.2 Theoretical Comparison of BER Derivation using the PDF in [97]

To compare P_b with related works, we use the PDF in [97] to derive the BER for STBC with unequal branch SNR. In 5.1, γ_M is the sum of two independent exponentially distributed random variables, namely X_1 and X_2 with parameters λ_1 and λ_2 respectively. The PDF of γ_M denoted as $P_\gamma(\gamma_M)$ can be written as:

$$P_\gamma(\gamma_M) = \frac{1}{\lambda_1\lambda_2}\left(\frac{e^{-\frac{\gamma_M}{\lambda_1}}}{\frac{1}{\lambda_2}-\frac{1}{\lambda_1}} + \frac{e^{-\frac{\gamma_M}{\lambda_2}}}{\frac{1}{\lambda_1}-\frac{1}{\lambda_2}}\right), \tag{5.10}$$

and used to express the BER denoted as Pb_{pdf} as follows:

$$Pb_{pdf} = \int_0^{\infty} \frac{1}{2} erfc(\sqrt{\gamma_M}) P_{\gamma}(\gamma_M) d\gamma_M, \tag{5.11}$$

where $erfc(.)$ is the complementary error function related to the Q-function [99]. Using software such as Mathematica, the integration of (5.11) yields the BER expression:

$$Pb_{pdf} = \frac{1}{\lambda_1 \lambda_2} \left(\frac{0.5(\lambda_1 - \frac{\lambda_1^{\frac{3}{2}}}{\sqrt{1+\lambda_1}})}{\frac{1}{\lambda_2} - \frac{1}{\lambda_1}} + \frac{0.5(\lambda_2 - \frac{\lambda_2^{\frac{3}{2}}}{\sqrt{1+\lambda_2}})}{\frac{1}{\lambda_1} - \frac{1}{\lambda_2}} \right). \tag{5.12}$$

To the best of our knowledge, the proposed derivation of the MUE BER using the PDF of unequal branch SNR is a novel method. Such PDF is seldom used in the literature. The results are achieved in the theoretical scenario and consequently the comparison; to derive the RAKE performance in [13], perfect channel tap weights are assumed. In practice, such approximation can be approached if the channel fading is sufficiently slow, e.g., the coherence time is about a hundred times the signaling interval. In contrast, our proposed error performance derivation is devoid of such approximation.

5.3.3 Theoretical Performance Comparison to Validate our Proposed BER Function P_b

This section presents theoretical performance comparison to validate our proposed BER function P_b. Figs. 5.3 and 5.4 illustrate respectively the low and high SNR plots of the proposed BER function P_b, the BER of the RAKE maximum ratio combining studied in [13] and the derived BER in Section 5.3.2. The proposed BER function P_b and the derived BER in Section 5.3.2 are represented by the curves "*MGF*" and "*PDF*" respectively. *NoAppRake* and *Rake* represent the RAKE maximum ratio combining studied in [13] at low and high SNRs respectively. The plots are made with $\lambda_2 = 4dB$ for Fig. 5.3 and $\lambda_2 = 10dB$ for Fig. 5.4, and λ_1 varying in the x-axis.

At low SNR, there is a match of the curves "*MGF*", "*PDF*" and "*NoAppRake*" while "*Rake*" suffers a slight performance penalty because "*Rake*" is an approximation of the RAKE maximum ratio combining for SNR values higher than $10dB$. Such approximation validity is confirmed with the high SNR plot on Fig. 5.4 where the "*MGF*", "*PDF*", "*NoAppRake*" and "*Rake*" are superposed. The matching of the curves "*MGF*", "*PDF*" and "*NoAppRake*" shows that P_b is a valid BER function to use in our optimisation in Section 5.4.

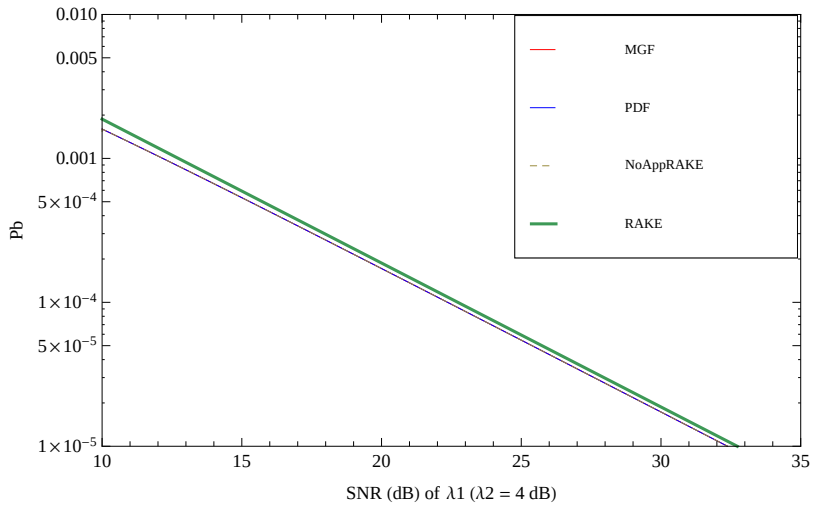

Fig. 5.4 Performance of our proposed BER function compared to the RAKE maximum ratio combining and the PDF-based methods for high SNR.

5.4 Proposed Joint two-relay Selection and Transmit Power Allocation

We propose a design of cognitive SCNs with the constraint of SCN outage threshold imposed on the relays. We achieve such objective by minimising P_b under the two constraints of maximum relay transmission and relay-wise transmit power limitation derived from the outage at the *SCN*. Thus the proposed optimisation can be expressed as follows:

$$\begin{aligned} \underset{P_1,P_2}{\text{minimise}} \quad & P_b(P_1,P_2) \\ \text{subject to} \quad & \sum_{n=1}^{2} P_n - P_{max} = 0 \\ & 0 \preceq P_n \preceq Th_n, n = 1,2. \end{aligned} \tag{5.13}$$

In (5.13), P_{max} is the total maximum transmit power of the relays and Th_n is the transmit power threshold of the nth relay derived from the outage at the *SCN* in Section 5.4.1. We solve the optimisation by using the Lagrangian $J(P_1,P_2)$

$$J(P_1,P_2) = P_b(P_1,P_2) + \beta(\sum_{n=1}^{2} P_n - P_{max}). \tag{5.14}$$

In (5.14), β is a Lagrange multiplier.

The iterative resolution of (5.13) is detailed in Section 5.4.2 with *Algorithm 1*.

5.4.1 Outage at the *SCN*

Each relay transmitting can generate cross-tier interference at the *SCN*. We use the outage probability of the *SCN* due to such interference to determine a cutoff relay transmit power value guaranteeing a better performance (compared to reception of signals with transmit power above the cutoff value) for the *SCN* receiving signals with transmit power below the cutoff value. The signal to interference (cross-tier interference) ratio (SIR) per relay at the *SCN* denoted as SIR_f is given by:

$$SIR_f = \frac{A_c P_f d_f^{-\alpha_{in}} |h_f|^2}{A_f P_n r_n^{-\alpha_{out}} |g_n|^2}, \tag{5.15}$$

where α_{in} denotes the path loss exponent of indoor small cell, A_c and A_f denote the fixed path losses for the outdoor and indoor transmissions respectively, d_f and $|h_f|^2$ are respectively the distance and the exponentially distributed channel gain with unity mean under Rayleigh fading between the *SCN* base station and its SCU, and r_n and $|g_n|^2$ are respectively the distance and the exponentially distributed channel gain with unity mean under Rayleigh fading between the SCU at the *SCN* and the *nth* relay. The probability of outage at the *SCN* denoted as P_r is defined as the probability that SIR_f falls below a threshold values denoted as T:

$$\begin{aligned} P_r(SIR_f < T) &= 1 - P_r(\frac{P_f d_f^{-\alpha_{in}}}{A_f}|h_f|^2 \geq T\frac{P_n r_n^{-\alpha_{out}}}{A_c}|g_n|^2) \\ &= 1 - P_r(\lambda_f |h_f|^2 \geq \lambda_i |g_n|^2) \\ &= 1 - \frac{1}{1+\frac{\lambda_i}{\lambda_f}}, \end{aligned} \tag{5.16}$$

where λ_f and λ_i are defined as $\lambda_f = \frac{P_f d_f^{-\alpha_{in}}}{A_f}$ and $\lambda_i = T\frac{P_n r_n^{-\alpha_{out}}}{A_c}|g_n|^2$, and $i = 1,2$. Setting P_{out} as a given probability of outage value yields:

$$P_n \leq Th_n, \tag{5.17}$$

where

$$Th_n = (\frac{1}{1-P_{out}} - 1)\frac{A_c P_f d_f^{-\alpha_{in}}}{A_f T r_n^{-\alpha_{out}}}. \tag{5.18}$$

(5.18) establishes the transmit power upper bound of the *nth* relay independently of P_{max}. The proposed dynamic transmit power allocation in Section 5.4.2 presents a method to resolve such discrepancy.

5.4.2 Proposed Relay Transmit Power Adaptation

We assume that the knowledge of the previously mentioned distances. By replacing λ_n with $\frac{P_n d_n^{-\alpha_{out}}}{N_0}$ in the optimisation problem, the transmit powers of the selected two relays can be derived in function of the large scale parameters referred in Table 5.1. Such bit error rate function is asymptotic to the x-axis. Thus the proposed minimisation algorithm converges to the largest P_n satisfying a given convergence criterion such as a fixed number of iteration or an error tolerance. This paper contribution consists of the following gradient descent algorithm to iteratively compute the transmit powers and two-relay selection:

The appendix shows that the derived BER function is convex. Thus, we have a unique solution to our proposed iterative algorithm. Since the first order derivatives are negative, the BER function is a strictly decreasing function of the SNRs. We avoid the slow convergence [100] of the classic gradient descent algorithm by setting the initial transmit power closer to the thresholds derived from the outage generated by the selected relays at the small cell in Section 4.1. The average number of iterations is 10. The number of iterations depends on the transmit power thresholds of the relays. Since each relay has a different threshold, the optimal transmit powers of the relays are different and so are the numbers of iterations. The proposed gradient descent algorithm has a similar complexity as [100] with the differences that the same power is allocated to all subcarriers per time slot in our work while in [100] power is allocated to each subcarrier. This difference occurs because we use STBC without CSI available at the transmitter. However, with CSI, *SP* can be applied for OFDM systems as in [100]. As for the relay selection, since we select the best two relays, the complexity is $\Theta(N^2)$, where N is the total number of relays. N should be small as the candidates relays are the ones located in the vicinity of the small cell.

In the proposed *SmallCell-Protected (SP)*, the individual constraint on each relay transmit power derived from the outage generated by a relay to a small cell has lead to an initialisation of the P_n in *SP*. Such initialisation reduces the delay in an iterative gradient descent computation. Furthermore, it precludes the need to consider negative powers in the iterative process given that P_b is a monotonic decreasing function of the P_n. The initialisation of the P_ns by the Th_ns ensures a rapid convergence compared to an arbitrary guess or setting to zero. $\xi = 0.99$ is an arbitrary factor to keep the initial P_n the closest to Th_n for $n = 1,2$ while $\varepsilon = 10^{-12}$ is the precision or the difference between two consecutive (in time domain) iterative powers to declare convergence. From the allocation power, we note that if a threshold Th_n is larger than P_{max}, then $P_n^\star$ gets as close as possible to the Th_n while maintaining $P_1^\star + P_2^\star \leq P_{max}$. If the threshold Th_n is lower than P_{max}, a similar reasoning applies to the optimal power solutions.

Algorithm 1 Compute initial $P_n, n = 1,2$ by the gradient descent algorithm

Computation of Th_i, $i = 1,2,\ldots,N_r$
Choosing two relays among the possible $\binom{N_r}{2}$ combinations, Indexing the two relays with 1 and 2. Choosing an arbitrary step size St and setting of the initial P_n for $n = 1,2$:
$P_n \leftarrow \xi Th_n$, $n = 1,2$
if $(Th_1 + Th_2) > P_{max}$ **then**
  $P_n \leftarrow \xi Th_n$, $n = 1,2$
  while $(P_1 + P_2) > P_{max}$ **do**
    $P_n \leftarrow \xi Th_n$, $n = 1,2$
  end while
end if
Computation of the partial derivatives $\frac{\partial P_b(P_1,P_2)}{\partial P_1}$ and $\frac{\partial P_b(P_1,P_2)}{\partial P_2}$ at the initial P_n, $n = 1,2$
Computation of the Lagrange multiplier:
$\lambda \leftarrow (\frac{\partial P_b(P_1,P_2)}{\partial P_1} + \frac{\partial P_b(P_1,P_2)}{\partial P_2})/2$
Simultaneous update of P_n for $n = 1,2$ if $P_n \neq Th_n$:
$P_n \leftarrow P_n - St(\frac{\partial P_b(P_1,P_2)}{\partial P_n} + \lambda)$
Convergence and optimisation constraint management:
if $(P_1 > 0$ and $P_2 > 0)$ **then**
  if $P_n > Th_n$, $n = 1,2$ **then**
    $P_n \leftarrow Th_n$, $n = 1,2$
  end if
end if
Augmentation of the number of iterations by a unit
if $\sqrt{(\frac{\partial P_b(P_1,P_2)}{\partial P_1} + \lambda)^2 + (\frac{\partial P_b(P_1,P_2)}{\partial P_2} + \lambda)^2} < \varepsilon$ or
the number of iterations reaches a predefined maximum number or
$(P_1 + P_2) \geq P_{max}$ or
$(P_1 + P_2) \geq (Th_1 + Th_2)$ **then**
  Declaration of convergence; optimal powers are P_n^*, $n = 1,2$
else
  Repeat the algorithm from the stage computing λ.
end if
Ordering the SNRs at the MUE:
$SNR_i = P_{ik} d_k^{-\alpha_{out}} + P_{ij} d_j^{-\alpha_{out}}$,
where $1 \leq k \leq N_r$, $1 \leq j \leq N_r$, $k \neq j$, $P_{ik} = P_k^*$, $P_{ij} = P_j^*$
$i = 1,2,\ldots,\binom{N_r}{2}$, the two largest SNR_is yield the optimal two relays.

Table 5.1 Simulation conditions

Parameters	Value
Bandwidth	$5\ MHz$
Number of subcarriers	512
Useful symbol time	$6.4 \times 10^{-6}\ s$
Guard interval	$1.25 \times 10^{-6}\ s$
small scale channel model	Rayleigh flat fading
Noise	AWGN
Data modulation	OFDM $\pi/4$-QPSK
Convolutional code rate	$1/2$
Convolutional code constraint length	7
Macrocell radius	$1000\ m$
SCN radius	$30\ m$
Carrier frequency (F_c)	$2000\ MHz$
Wall penetration loss (P_l)	$5\ dB$
Relay maximum transmit power (P_{max})	$30\ dBm$
Macrocell path loss exponent(α_{out})	3.8
SCN path loss exponent(α_{in})	3
Indoor fixed path loss (A_f)	$37\ dB$
Outdoor fixed path loss (A_c)	$30log10(F_c) - 71.0 + P_l$

5.5 Simulation Results

5.5.1 Performance evaluation at the MUE and the *SCN* considering the outage limitation

The simulation results show the BER and packet error rate (PER) of the MUE and the SCU. Additionally, the SIR at the SCU provides insight in the cross-tier interference effect on the small cell with respect to our proposal. The simulation conditions are given by the parameters shown in Table 5.1.

Our proposal is compared to the benchmark system which allocates the same power to two transmitting relays with power limitation by the constraint at the small cell. Owing to the outage constraint at the *SCN*, the lowest power derived from our proposed algorithm is assigned to both relays.

Fig. 5.5 depicts the BER of the MUE. Our proposal represented by *"Proposed"* outperforms the benchmark illustrated by *"Conventional"*. The curve *"Proposed"* has a bit error floor lower than 10^{-3} while *"Conventional"* ceiling reaches 10^{-2}. The iterations which provide the simulation results consider a distance-decay power. As shown on Fig. 5.5,

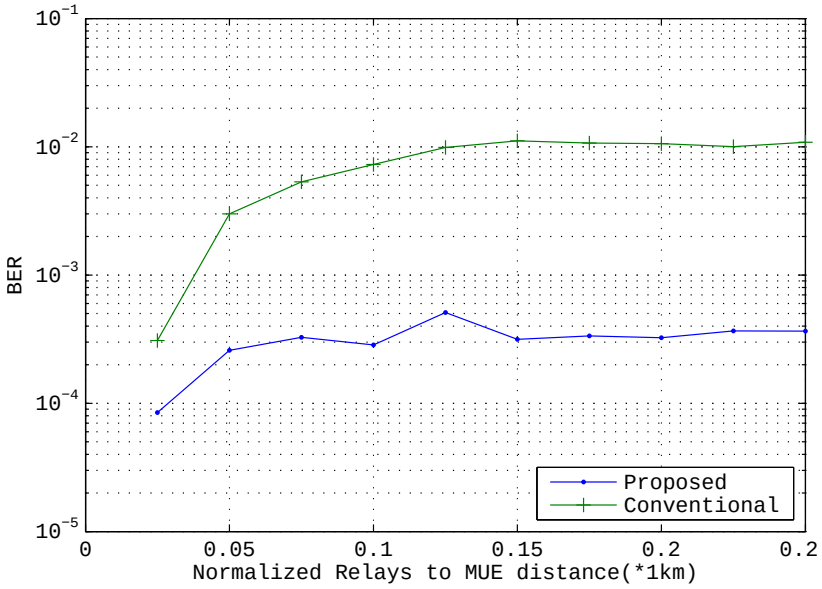

Fig. 5.5 BER at the MUE.

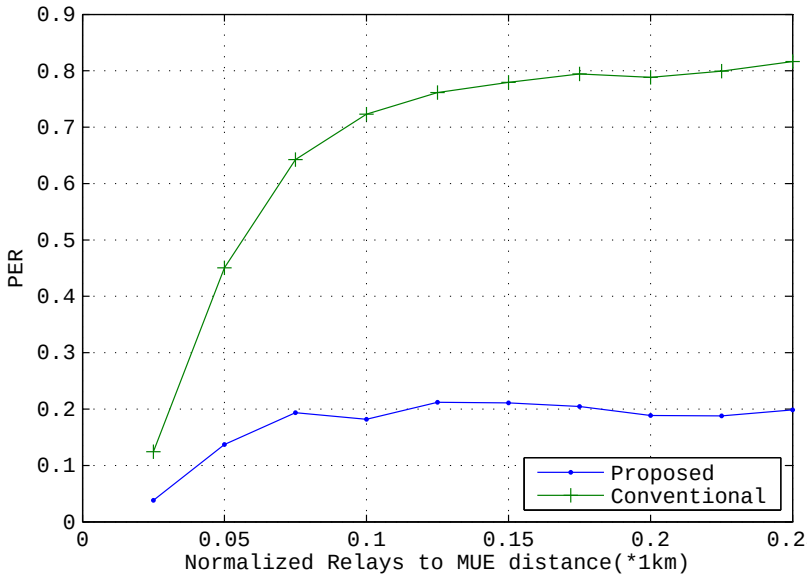

Fig. 5.6 PER at the MUE.

the BER degrades as the MUE is farther from the selected relays. From 150 m, the BER experiences an error floor. In addition to the distance, the threshold limitation affects the maximum relay transmit power. Fig. 5.6 illustrates the PER of the MUE. The proposed system curve *"Proposed"* presents a better PER than the benchmark represented with the curve *"Conventional"*; indeed the PER of the *"Conventional"* has an asymptote at 0.8 while the *"Proposed"* curve remains under 0.2. In both Figs. 5.5 and 5.6, the x-axis is the ratio of the distance between the closest transmitting relay to the MUE, and the radius of the macrocell.

We can notice that the PER and BER decrease as the MUE is farther from the transmitting two-relays. The fact that the two-relays are located at unequal distance from the MUE is an additional incentive to our proposal considering distributed-STBC and unequal branch SNR. The SNR fluctuation at the receiver side for distributed-STBC is more sensitive to the large scale parameters such as the distance between transmitter and receiver than to slow fading. In addition, if the channel gains are available at the transmitter side, the maximum ratio combining is optimal as mentioned in [90].

The effect of our proposal on the SCU of the *SCN* is illustrated in the BER in Fig. 5.7,

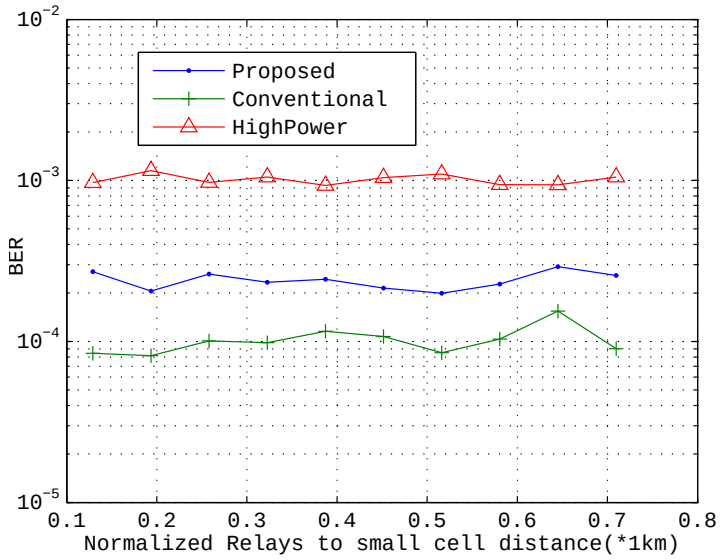

Fig. 5.7 BER at the SCU in the *SCN*.

the PER in Fig. 5.8 and the SIR for different power allocation schemes in Fig. 5.9. The x-axis on the three figures represents the ratio of the distance between the closest relay to the SCU of the *SCN* and the SCU, and the radius of the *SCN*. In the *SCN*, the distance between the SCU and the SBS is fixed at 5.4 m while the transmit power is 14.5 dBm. The power allocation difference between the proposed system and the benchmark induces a slight gap in the SIR, BER and PER. The SIR at the SCU of the *SCN* depicted in Fig. 5.9 shows the steadiness of the outage control. For different two-relays transmitting at different distances from the *SCN*, the SIR curves remain horizontal for the proposed system illustrated by the curve *"Proposed"*, the benchmark represented by *"Conventional"* and a third scheme with *"HighPower"*. The *"HighPower"* scheme consists of allocating the highest power computed from our proposal to both transmitting relays. Thus, it illustrates the effect of infringing the outage constraint at the *SCN* receiver by the relay assigned with the lowest power. The benchmark represented by the curves *"Conventional"* in Fig. 5.7 and Fig. 5.8 have a BER floor of 10^{-4} and a PER fluctuating between 0.03 and 0.04 respectively,

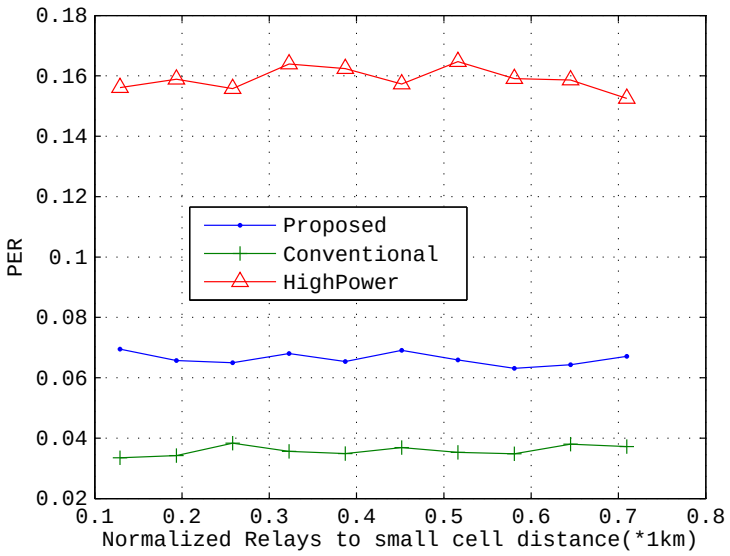

Fig. 5.8 PER at the SCU in the *SCN*.

while the proposal illustrated by the curves *"Proposed"* has a BER floor slightly above 10^{-4} and a PER fluctuating between 0.06 and 0.07. In Fig. 5.9 we can notice that the gap between the *"HighPower"* and *"Proposed"* curves is two times larger than the one between the *"Proposed"* and *"Conventional"*. Such analysis is valid for the *"HighPower"* compared to *"Proposed"* and *"Conventional"* in Fig. 5.7 and Fig. 5.8. The allocated transmit power to the transmitting relays satisfy a certain outage constraint at the *SCN*. Therefore, the performance of the *SCN* remains steady (horizontal curves) as illustrated in the figures assessing the effect of our proposal on the *SCN*.

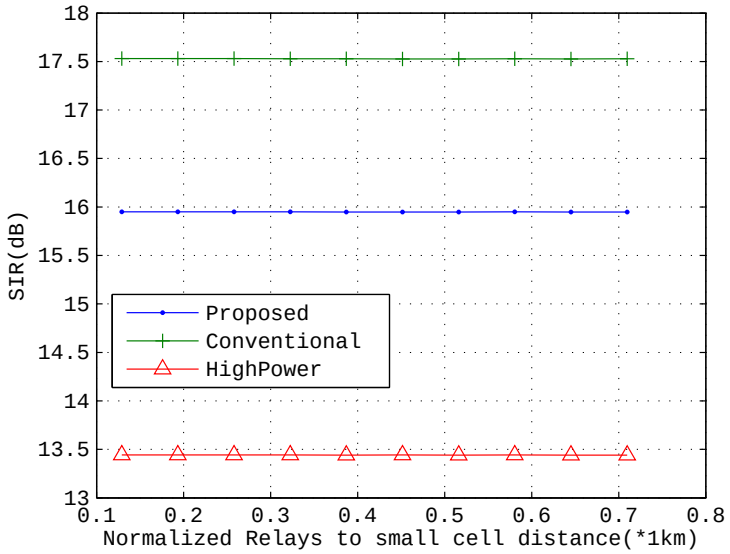

Fig. 5.9 SIR at the SCU in the *SCN*.

5.5.2 Performance evaluation at the MUE and the *SCN* including no-outage limitation scenario

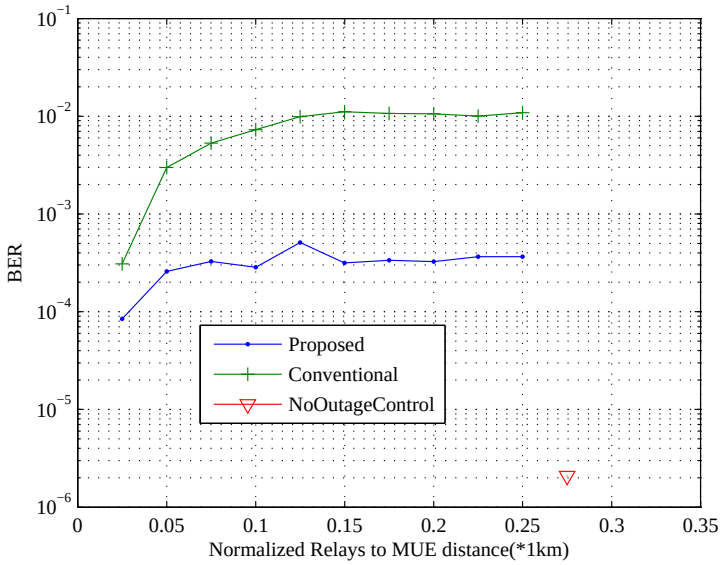

Fig. 5.10 BER at the MUE.

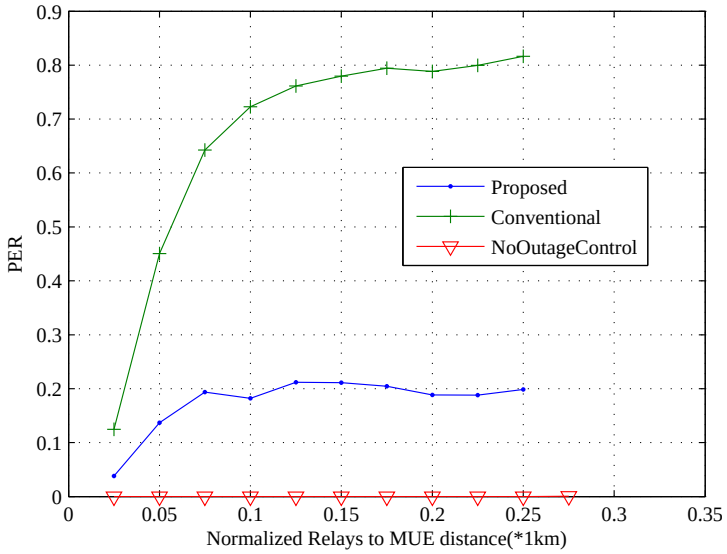

Fig. 5.11 PER at the MUE.

Another benchmark scheme denoted as *"NoOutageControl"* is considered for comparison with the previously mentioned methods. *"NoOutage"* considers only BER minimisation without taking into account the constraint from the outage at the *SCN*; in (5.13), the constraint $0 \preceq P_n \preceq Th_n, n = 1,2.$ is ignored. Thus, the relays sum-transmit power is bounded

by P_{max}. As P_{max} is superior to Th_i for $i = 1,2$, the transmit powers derived without consideration of the outage at the *SCN* cause a drastic degradation of the performance at the *SCN* while the performance at the MUE improves. Such situation is adopted in most small cell deployments because of the prioritisation of the macrocell over the small cell. In addition the concepts of self-optimised network implemented by the 3*GPP* femocells and docitive/cognitive [20, 21] small cell are based on the previously mentioned prioritisation. Such strategy yields the following results:

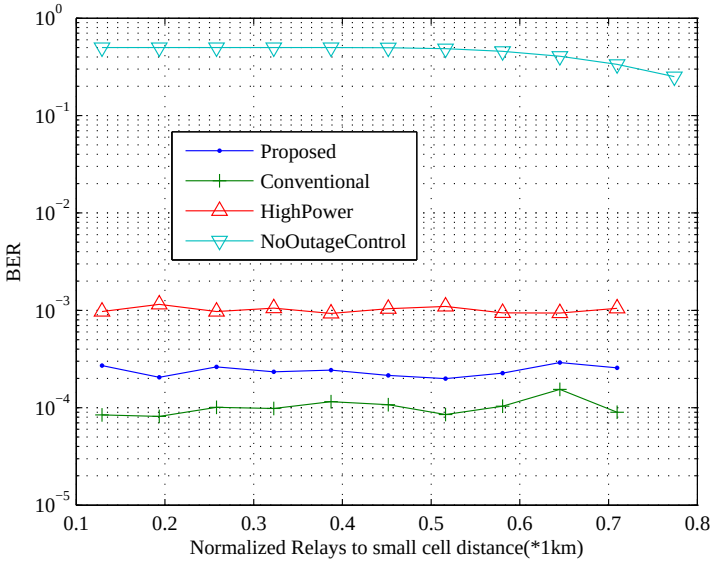

Fig. 5.12 BER at the SCU in the *SCN*.

- The outdoor MUE performance is evaluated in Fig. 5.10 for the BER and Fig. 5.11 for the PER. The *"NoOutage"* method has a bit error less than 10^{-5} occurring when the relays are beyond 250 *m* from the MUE while other methods have a higher error rate before 250 *m*.

- *"NoOutage"* outperforms the previously mentioned methods. However, the other methods offer a better performance at the *SCN* as shown on Fig. 5.12 for the BER and Fig. 5.13 for the PER evaluation at the *SCN*.

- The SIR comparison figure given in Fig. 5.14 shows the deep outage occurring at the *SCN* when the relays transmit without the transmit power limitation to allow a certain quality of signal reception at the *SCN*. While signal reception is possible with the other methods, the *"NoOutage"* puts the *SCN* in complete outage.

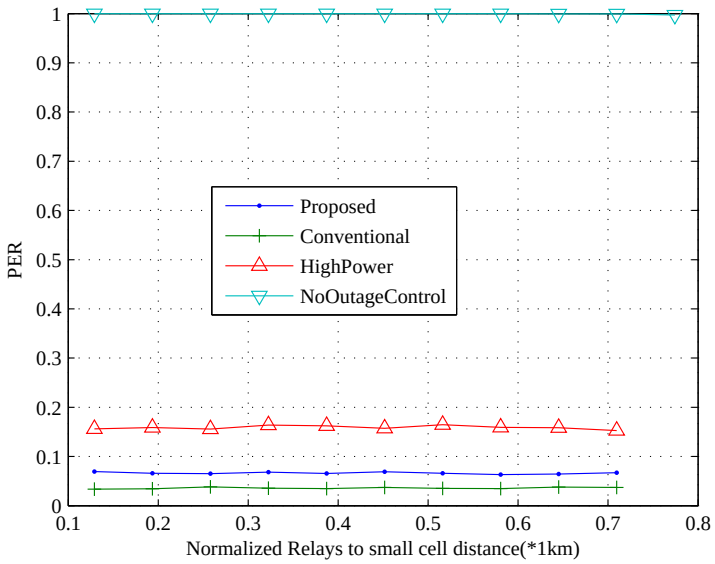

Fig. 5.13 PER at the SCU in the *SCN*.

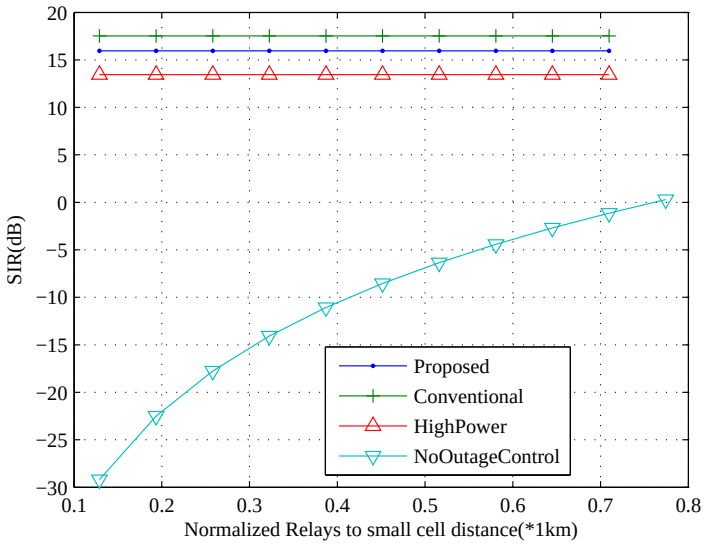

Fig. 5.14 SIR at the SCU in the *SCN*.

5.6 Conclusion

Considering the transmit power limitation imposed on outdoor relays by the outage at a neighbour small cell, we proposed a joint power allocation and two-relay selection algorithm for distributed STBC w.r.t. unequal branch SNR. Furthermore, new close-form expressions have been derived to validate the proposed BER function used in our optimisation algorithm. Our proposal gains in BER and PER over the same power allocation STBC scheme compel

to the adoption of such indoor outage precluding design for cognitive small cell networks.

Chapter 6

Conclusion and Future Work

6.1 Conclusion

This thesis has addressed several multi-tier network deployment issues by considering the main system performance limiting factor namely, cross-tier interference. The thesis studied primarily the design of small cell networks sharing the same frequency and cellular region as the macrocell. Chapter 3 presented an interference cancellation scheme for LTE-based femtocell which uses information feedback via the backhaul from the MBS. The small cell base station can recover the symbols sent by its mobile user for the aggregated signal resulting from the combination of the small cell user and the MUE signals. In Chapter 4, we leveraged the interference cancellation scheme discussed in Chapter 3 to propose a distributed cross-tier interference management using multicast feedback information to a virtual femtocell cluster which can perform interference cancellation. Chapter 3 and 4 system models are based on uplink transmission. In Chapter 5, we used a new approach to cross-tier interference mitigation by proposing a joint relay selection and adaptive power allocation for cognitive small cell networks in downlink. This thesis delved in the rising research field of distributed-STBC small cell networks considering unequal SNR branch.

6.2 Future Work

In future, our proposal on distributed STBC, by proposing resource allocation scheme based on the mobility of the MUE and the cross-tier interference from the outdoor MUE to the SCNs. We would like to consider Bayesian compressive sensing to estimate the wireless channel in mobile communications. Channel estimation requirement rises from the need to feedback the CSI to base stations and relays for best transmitter selection and/or trans-

mit power allocation. Considering the velocity of a mobile terminal, the CSI might change within the set of time slots where it is supposed to be constant. We propose to use Bayesian inference to estimate the channel in such situation. Our system model is a two-tier cellular network with cognitive small networks overlaid onto legacy macrocell such as in LTE or DAS networks. The CSI can be used to propose a switching-based channel and adaptive power allocation for heterogeneous cognitive small cell networks. The switching-based channel consists of allocating a different channel to a terminal because the cross-tier interference at the considered terminal has reached a certain threshold. Such cross-tier interference can be mitigated by adaptive transmit power allocation.

We would also like to consider a cognitive wireless cloud implementation of coexisting networks (system model mentioned in the previous paragraph) such as DAS/LTE embedding small cells using tools such as GNUradio. The concept of small cell networks leads to a densification of the wireless cellular network grid. Therefore, concepts such as cognitive wireless cloud and software defined networking are crucial to the spectrum efficiency improvement without resorting to a change in the infrastructure. We propose that the cognitive wireless cloud concept focuses on the sharing possibilities of such heterogeneous cellular network infrastructure by multiple operators while software defined networking implements resource allocations policies based on the cross-tier interference level. We propose to implement the policies which are network event-based programs in the small cell base stations. The cross-tier interference is the main issue to mitigate for spectrum efficiency improvement.

References

[1] M. Bennis, M. Simsek, A. Czylwik, W. Saad, S. Valentin, and M. Debbah, "When cellular meets wifi in wireless small cell networks," *IEEE Communications Magazine*, vol. 51, June 2013.

[2] ETSI, "Overview of 3gpp release 12 v0.0.4," 2012.

[3] T. Q. S. Quek, S. S. Yong, and M. Kountouris, "Hybrid division duplex for cognitive small cell networks," in *15th International Symposium on Wireless Personal Multimedia Communications (WPMC)*, pp. 609–613, September 2012.

[4] http://www.thedasforum.org/ 2014.

[5] W. Choi and J. G. Andrews, "Downlink performance and capacity of distributed antenna systems in a multicell environment," *IEEE Transactions on Wireless Communications*, vol. 6, pp. 69–73, 2007.

[6] L. Mailaender, "Indoor network mimo performance with regularized zero-forcing transmission," in *IEEE 10th International Symposium on Spread Spectrum Techniques and Applications*, pp. 124–128, August 2008.

[7] H. Liping, W. Dongming, and W. Xiangyang, "User cooperation communication based on cognitive radio in das," in *International Conference on Wireless Communications and Signal Processing (WCSP)*, pp. 1–5, November 2011.

[8] M. Ndong and T. Fujii, "Cross-tier interference management with a distributed antenna system for multi-tier cellular networks," *EURASIP Journal on Wireless Communications and Networking*, vol. 2014, pp. 1–12, May 2014.

[9] Z. Shi, M. C. Reed, and M. Zhao, "On uplink interference scenarios in two-tiers macro and femto co-existing umts networks," *EURASIP Journal on Wireless Communications and Networking*, vol. 2010, pp. 1–8, April 2010.

[10] O. M. Bucci, G. Pelosi, and S. Selleri, "The work of marconi in microwave communications," *IEEE Antennas and Propagation Magazine*, vol. 45, pp. 46–53, October 2003.

[11] D. Emerson, "The work of jagadis chandra bose: 100 years of mm-wave research," in *IEEE MTT-S International Microwave Symposium Digest*, vol. 2, pp. 553–556, June 1997.

[12] C. E. Shannon, "Communication in the presence of noise," *Proceeding of the IRE*, vol. 37, pp. 10–21, January 1949.

[13] J. G. Proakis and M. Salehi, "Digital communications," in *Fadings channels I : Characterization and Signaling*, pp. 872–876, New York, NY 10020: McGraw Hill, 5th ed., 2008.

[14] A. Goldsmith, "Performance of digital modulation over wireless channels," in *Wireless communications*, pp. 187–197, New York, USA: Cambridge university press, 1st ed., 2005.

[15] M. L. Doeltz, E. T. Heald, and D. L. Martin, "Binary data transmission techniques for linear systems," *Proceeding of the IRE*, vol. 45, pp. 656–661, May 1957.

[16] B. R. Saltzberg, "Performance of an efficient parallel data transmission system," *IEEE Transactions on Communications*, vol. 15, pp. 805–811, December 1967.

[17] S. B. Weinstein and P. M. Ebert, "Data transmission by frequency division multiplexing using the discrete fourier transform," *IEEE Transactions on Communications Technology*, vol. 19, pp. 628–634, October 1971.

[18] J. G. Andrews, A. Ghosh, and R. Muhamed, "Orthogonal frequency division multiple access," in *Fundamentals of WiMAX understanding broadband wireless networking* (T. S. Rappaport, ed.), pp. 210–211, Massachusetts: Prentice Hall, 1st ed., 2007.

[19] http://www.ict befemto.eu/ 2014.

[20] L. Giupponi, A. Galindo-Serrano, P. Blasco, and M. Dohler, "Docitive networks: an emerging paradigm for dynamic spectrum management [dynamic spectrum management]," *IEEE Wireless Communications*, vol. 17, pp. 47–54, August 2010.

[21] H. ElSawy and E. Hossain, "Two-tier hetnets with cognitive femtocells: Downlink performance modeling and analysis in a multichannel environment," *IEEE Transactions on Mobile Computing*, vol. 13, pp. 649–663, March 2014.

[22] A. J. Goldsmith in *Lecture EE359 on Wireless Communications, http://web.stanford.edu/class/ee359/*, 2014.

[23] A. Abdelnasser, E. Hossain, and I. K. Dong, "Clustering and resource allocation for dense femtocells in a two-tier cellular ofdma network," *IEEE Transactions on Wireless Communications*, vol. 13, pp. 1628–1641, March 2014.

[24] F. Jin, R. Zhang, and L. Hanzo, "Fractional frequency reuse aided twin-layer femtocell networks: Analysis, design and optimization," *IEEE Transactions on Communications*, vol. 61, pp. 2074–2085, May 2013.

[25] F. Baccelli and B. Blaszczyszyn in *Stochastic Geometry and Wireless Networks, Volume I - Theory, https://www.stat.berkeley.edu/ aldous/206-SNET/Papers/baccelli-1.pdf*, 2009.

[26] F. Baccelli and B. Blaszczyszyn in *Stochastic Geometry and Wireless Networks, Volume II - Applications, http://hal.inria.fr/inria-00403040*, 2009.

[27] H. ElSawy, E. Hossain, and S. Camorlinga, "Multi-channel design for random csma wireless networks: A stochastic geometry approach," in *IEEE International Conference on Communications (ICC)*, pp. 1656–1660, June 2013.

[28] H. ElSawy, E. Hossain, and M. Haenggi, "Stochastic geometry for modeling, analysis, and design of multi-tier and cognitive cellular wireless networks: A survey," *IEEE Communications Surveys Tutorials*, vol. 15, pp. 996–1019, March 2013.

[29] M. Haenggi, J. G. Andrews, F. Baccelli, O. Dousse, and M. Franceschetti, "Stochastic geometry and random graphs for the analysis and design of wireless networks," *IEEE Journal on Selected Areas in Communications*, vol. 27, pp. 1029–1046, September 2009.

[30] R. W. Heath, M. Kountouris, and B. Tianyang, "Modeling heterogeneous network interference using poisson point processes," *IEEE Transactions on Signal Processing*, vol. 61, pp. 4114–4126, August 2013.

[31] M. Vu, N. Devroye, and T. Vahid, "On the primary exclusive region of cognitive networks," *IEEE Transactions on Wireless Communications*, vol. 6, pp. 3380 – 3385, 2009.

[32] M. Bennis, M. Debbah, and A. Chair, "On spectrum sharing with underlaid femtocell networks," in *IEEE 21st International Symposium on Personal, Indoor and Mobile Radio Communications Workshops (PIMRC Workshops)*, pp. 185–190, September 2010.

[33] A. Ozgur, O. Leveque, and D. Tse, "Hierarchical cooperation achieves linear capacity scaling in ad hoc networks," in *IEEE International Conference on Computer Communications (INFOCOM)*, pp. 382–390, May 2007.

[34] V. Chandrasekhar and J. G. Andrews, "Spectrum allocation in two-tier networks," in *Proceedings of the 42nd Asilomar conference on Signals, Systems and Computers*, pp. 1583–1587, October 2008.

[35] A. Ghosh, N. Mangalvedhe, R. Ratasuk, B. Mondal, M. Cudak, E. Visotsky, T. A. Thomas, J. G. Andrews, P. Xia, H. S. Jo, H. S. Dhillon, and T. D. Novlan, "Heterogeneous cellular networks: from theory to practice," *IEEE Communications Magazine*, vol. 50, pp. 54–64, June 2012.

[36] M. Ndong and T. Fujii, "Joint femtocell clustering and cross-tier interference mitigation with distributed antenna system in small cell networks," in *Communication Systems, Networks Digital Signal Processing (CSNDSP), 9th International Symposium on*, pp. 652–657, July 2014.

[37] Z. Jie, Z. Rong, L. Guangjun, and L. Hanzo, "Distributed antenna in fractional frequency-reuse aided cellular networks," *IEEE Transactions on vehicular technology*, vol. 62, pp. 1340–1349, March 2013.

[38] Z. Jie, J. Fan, Z. Rong, L. Guangjun, and L. Hanzo, "Distributed antenna aided twin-layer femto-and macro-cell networks relying on fractional frequency-reuse," in *IEEE Wireless Communications and Networking Conference (WCNC)*, pp. 1586–1591, April 2013.

[39] M. Jan and G. Amirhossein, "Shared smallcell networks: Multi-operator or third party solutionsor both?," in *IEEE Wireless Communications and Networking Conference (WCNC)*, pp. 41–48, May 2013.

[40] V. Chandrasekhar, J. A. Andrews, and A. Gatherer, "Femtocell networks : a survey," *IEEE Communications Magazine*, vol. 46, pp. 59–67, 2008.

[41] V. Asghari and S. Aissa, "Adaptive rate and power transmission in spectrum-sharing systems," *IEEE Transactions on Wireless Communications*, vol. 9, pp. 3272–3280, 2010.

[42] V. Chandrasekhar, J. A. Andrews, T. Muharemovic, Z. Shen, and A. Gatherer, "Power control in two-tier femtocell networks," *IEEE Transactions on Wireless Communications*, vol. 8, pp. 4316 – 4328, 2009.

[43] H. Jo, J. Yook, C. Mun, and J. Moon, "A self-organized uplink power control for cross-tier interference management in femtocell networks," in *Proceedings of the Military Communications conference*, pp. 1–6, November 2008.

[44] B. Wang and K. J. R. Liu, "Advances in cognitive radio networks : a survey," *IEEE Journal on Selected Topics in Signal Processing*, vol. 5, pp. 5–23, 2011.

[45] M. Kim, H. Je, and F. Tobagi, "Cross-tier mitigation for two-tier ofdma femtocell networks with limited macrocell information," in *Proceedings of the IEEE Global telecommunications conference*, pp. 1–5, December 2010.

[46] V. Chandrasekhar, M. Kountouris, and A. J. G., "Coverage in multi-antenna two-tier networks," *IEEE Transactions on Wireless Communications*, vol. 8, pp. 5314–5327, October 2009.

[47] A. Adhikary, V. Ntranos, and G. Caire, "Cognitive femtocells: Breaking the spatial reuse barrier of cellular systems," in *Information Theory and Applications Workshop (ITA)*, pp. 1–10, February 2011.

[48] M. Yavuz, F. Meshkati, S. Nanda, A. Pokhariyal, N. Johnson, B. Raghothaman, and A. Richardson, "Interference management and performance analysis of umts/hspa+ femtocells," *IEEE Communications Magazine*, vol. 47, pp. 102 – 109, 2009.

[49] R. Q. Hu, Y. Qian, S. Kota, and G. Giambene, "Hetnets-a new paradigm for increasing cellular capacity and coverage[guest editorial]," *IEEE Wireless Communications*, vol. 18, pp. 8–9, June 2011.

[50] H. Jo, C. Mun, J. Moon, and J. Yook, "Self-optimized coverage coordination in femtocell networks," *IEEE Transactions on Wireless Communications*, vol. 9, pp. 2977 – 2982, October 2010.

[51] A. Tsai, J. Huang, L. Wang, and R. Hwang, "High capacity femtocells with directional antennas," in *Proceedings of the IEEE Wireless Communications and Networking conference*, pp. 1–6, April 2010.

[52] J. Gambini and U. Spagnolini, "Lte femtocell system through amplify-and-forward over cable links," in *Proceedings of the IEEE GLOBECOM Workshops*, pp. 716 – 720, December 2010.

[53] K. Balachandran, J. H. Kang, K. Karakayali, and K. M. Rege, "Nice: A network interference cancellation engine for opportunistic uplink cooperation in wireless networks," *IEEE Transactions on Wireless Communications*, vol. 10, pp. 540–549, 2011.

[54] W. C and J. Andrews, "Downlink performance and capacity of distributed antenna systems in a multicell environment," *IEEE Transactions on Wireless Communications*, vol. 6, pp. 69 –73, January 2007.

[55] M. Kim, J. Lee, and Y. Kim, "Implementation of the levinson algorithm for mmse equalizer," in *Proceedings of the International SoC Design conference*, pp. III–15 – III–16, November 2008.

[56] L. Shao-Yu, L. Hou-Hsun, S. Sung-Yin, C. Pin-Yu, and C. Kwang-Cheng, "Network synchronization among femtocells," in *GLOBECOM Workshops (GC Wkshps)*, pp. 248–252, December 2011.

[57] C. Oestges and B. Clerckx, "Introduction to multi-antenna communications," in *MIMO Wireless Communications From real-world propagation to space-time code design* (Elsevier, ed.), pp. 1–14, Oxford, OX2 8DP: Academic Press, 1st ed., 2007.

[58] A. Goldsmith, "Equalization," in *Wireless Communications*, pp. 351–368, Cambridge University Press, New York, NY 10011-4211,USA: Cambridge University Press, 1st ed., 2005.

[59] P. M. J. Torregoca, R. Enkhbat, and W. Hwang, "Joint power control, base station assignment, and channel assignment in cognitive femtocell networks," *EURASIP Journal on Wireless Communications and Networking*, vol. 2010, pp. 1–14, May 2010.

[60] L. Khalid and A. Anpalagan, "Performance analysis of a threshold-based group-adaptive modulation scheme with adaptive subcarrier allocation in ofcdm systems," *IEEE Transactions on Wireless Communications*, vol. 7, pp. 2463 – 2467, July 2008.

[61] R. Etkin, A. Parekh, and D. Tse, "Spectrum sharing for unlicensed bands," *IEEE Journal on Selected Topics in Communications*, vol. 25, pp. 517–528, 2007.

[62] V. Chandrasekhar, M. Kountouris, and J. G. Andrews, "Coverage in multi-antenna two-tier networks," *IEEE Transactions on Wireless Communications*, vol. 8, pp. 4316 – 4328, 2009.

[63] H. Claussen, L. T. W. Ho, and L. G. Samuel, "An overview of femtocell concept," *Bell Labs Technical Journal DOI: 10.1002/bltj.20292*, vol. 13, pp. 221–245, 2008.

[64] Y. Li, A. Maeder, L. Fan, A. Nigam, and J. Chou, "Overview of femtocell support in advanced wimax systems," *IEEE Communications magazine*, vol. 49, pp. 122–130, 2011.

[65] J. G. Andrews, H. Claussen, M. Dohler, S. Rangan, and M. C. Reed, "Femtocells: Past, present, and future," *IEEE Journal on Selected Areas in Communications*, vol. 30, pp. 497 –508, April 2012.

[66] H. Hu, J. Zhang, X. Zheng, Y. Yang, and P. Wu, "Self-configuration and self-optimization for lte networks," *IEEE Communications Magazine*, vol. 48, pp. 94–100, 2010.

[67] Y. Kon, M. Ito, N. Hassel, M. Hasegawa, K. Ishizu, and H. Harada, "Autonomous parameter optimization of a heterogeneous wireless network aggregation system using machine learning algorithms," in *Consumer Communications and Networking Conference (CCNC)*, pp. 894 –898, January 2012.

[68] D. Castanheira and A. Gameiro, "Distributed antenna system capacity scaling [coordinated and distributed mimo]," *IEEE Wireless Communications*, vol. 17, pp. 68–75, 2010.

[69] R. Q. Hu, Y. Qian, S. Kota, and G. Giambene, "Hetnets - a new paradigm for increasing cellular capacity and coverage," *IEEE Transactions on Wireless Communications*, vol. 18, pp. 8–9, 2011.

[70] H. Li, J. Hajipour, A. Attar, and V. C. M. Leung, "Efficient hetnet implementation using broadband wireless access with fiber-connected massively distributed antennas architecture," *IEEE Transactions on Wireless Communications*, vol. 18, pp. 72–78, 2011.

[71] Y. Peng and F. Qin, "Exploring het-net in lte-advanced system: interference mitigation and performance improvement in macro-pico scenario," in *Proceedings of the IEEE International Conference on Communications Workshops (ICC)*, pp. 1–5, June 2011.

[72] T. Alade and Z. Huiling, "Joint signal processing in femtocell based distributed antenna systems in high buildings," in *Proceedings of the IEEE 72nd Vehicular Technology Conference (VTC 2010-Fall)*, pp. 1–5, September 2010.

[73] T. Alade, Z. Huiling, and H. Osman, "Spectral efficiency analysis of distributed antenna system for in-building wireless communication," in *IEEE 22nd International Symposium on Personal Indoor and Mobile Radio Communications (PIMRC)*, pp. 2075–2079, September 2011.

[74] M. Ndong and T. Fujii, "Cross-tier interference mitigation for self organized-self optimized femtocells," in *Wireless Telecommunications Symposium*, pp. 1–6, April 2012.

[75] H. Kaibin and J. G. Andrews, "A stochastic-geometry approach to coverage in cellular networks with multi-cell cooperation," in *IEEE Global Telecommunications Conference*, pp. 1–5, December 2011.

[76] M. Chiang, C. W. Tan, D. P. Palomar, D. O'neil, and D. Julian, "Power control by geometric programming," *IEEE Transactions on Wireless Communications*, vol. 6, pp. 2640–2651, 2007.

[77] S. Lien, H. Lee, S. Shih, P. Chen, and K. Chen, "Network synchronization among femtocells," in *the second GLOBECOM workshop on femtocell networks*, pp. 248–252, December 2011.

[78] M. Wildemeersch, T. Q. S. Quek, C. H. Slump, and A. Rabbachin, "Cognitive small cell networks: energy efficiency and trade-offs," *IEEE Transactions on Wireless Communications*, vol. 61, pp. 4016–4029, September 2013.

[79] J. Tang, X. Zhang, and Q. Du, "Alamouti scheme with joint antenna selection and power allocation over rayleigh fading channels in wireless networks," in *IEEE Proceedings of the Global Telecommunications Conference*, pp. 3319–3323, December 2005.

[80] A. N. Alyahya and J. Ilow, "Power allocation in cooperative space-time coded wireless relay networks," in *Proceedings of the Vehicular Technology Conference(VTC 2012-Fall)*, pp. 1–5, September 2012.

[81] T. Fujii, "High contribution node selection method for stbc distributed arq," in *IEEE Proceedings of the Vehicular Technology Conference(VTC 2008-Spring)*, pp. 1970–1974, May 2008.

[82] H. ElSawy and E. Hossain, "On cognitive small cells in two-tier heterogeneous networks," in *IEEE Proceedings of the 11th International Symposium on Modeling and Optimization in Mobile, Ad Hoc and Wireless Networks (WiOpt)*, pp. 75–82, May 2013.

[83] Z. Lu and L. J. Cimini, "Efficient power allocation for decentralized distributed space-time block coding," *IEEE Transactions on Wireless Communications*, vol. 8, pp. 1102–1106, March 2009.

[84] M. Dohler, A. H. Aghvami, Z. Zhou, Y. Li, and B. Vucetic, "Near-optimum transmit power allocation for space-time block encoded wireless communication systems," *IEE communications proceedings*, vol. 153, pp. 459–463, June 2006.

[85] J. N. Laneman and G. W. Wornell, "Distributed space-time coded protocols for exploiting cooperative diversity in wireless networks," in *Proceedings of the Global Telecommunications Conference*, pp. 77–81, November 2002.

[86] F. A. Khan, C. Yunfei, and M.-S. Alouini, "Novel receivers for af relaying with distributed stbc using cascaded and disintegrated channel estimation," *IEEE Transactions on Wireless Communications*, vol. 11, pp. 1370–1379, April 2012.

[87] A. Razi, F. Afghah, and A. Abedi, "Power optimized dstbc assisted dmf relaying in wireless sensor networks with redundant super nodes," *IEEE Transactions on Wireless Communications*, vol. 12, pp. 636–645, March 2013.

[88] M. Z. Win and J. H. Winters, "Analysis of hybrid selection/maximal-ratio combining of diversity branches with unequal snr in rayleigh fading," in *IEEE Proceedings of the Vehicular Technology Conference*, pp. 215–220, July 1999.

[89] C. Jian, W. Haifeng, J. Lilleberg, and C. Shixin, "Unequally powered stbc for slow flat rayleigh fading channel," in *Proceedings of the Wireless Communications and Network Conference*, pp. 291–295, March 2002.

[90] S. Alamouti, "A simple transmit diversity technique for wireless communications," *IEEE Journal on Selected Areas in Communications*, vol. 16, pp. 1451–1458, October 1998.

[91] T. Q. S. Quek, S. S. Yong, and M. Kountouris, "Hybrid division duplex for cognitive small cell networks," in *IEEE Proceedings of the Wireless Personal Multimedia Communications*, pp. 609–613, September 2012.

[92] B. Soret, W. Hua, K. I. Pedersen, and C. Rosa, "Multicell cooperation for lte-advanced heterogeneous network scenarios," *IEEE Transactions on Wireless Communications*, vol. 20, pp. 27–34, March 2013.

[93] M. Wildemeersch, T. Q. S. Quek, A. Rabbachin, and C. H. Slump, "Performance limits for cognitive small cells," in *IEEE Proceedings of the Wireless Communications and Network Conference*, pp. 2807–2811, April 2013.

[94] S. Siduo and T. M. Lok, "Dynamic power allocation for downlink interference management in a two-tier ofdma network," *IEEE Transactions on Vehicular Technology*, vol. 62, pp. 4120–4125, October 2013.

[95] P. Tarasak, T. Q. S. Quek, and F. Chin, "Closed access ofdma femtocells under timing misalignment," in *Proceedings of the Global Telecommunications Conference*, pp. 1–5, December 2010.

[96] W. C. Lee, "Mobile communications engineering," in *Microcell systems*, pp. 304–308, McGraw-Hill company, 2nd ed., 1982.

[97] M. Bibinger, "Notes on the sum and maximum of independent exponentially distributed random variables with different scale parameters," *ArXiv e-prints*, vol. arXiv1307.3945B, pp. 1–9, July 2013.

[98] M. Akkouchi, "On the convolution of exponential distributions," *Chungcheong Mathematical Society*, vol. 21, pp. 501–510, December 2008.

[99] M. K. Simon and M.-S. Alouini, "Digital communication over fading channels," in *Fadings channels I : Characterization and Signaling*, pp. 45–85, USA, NY 07030: Wiley-Interscience, 2nd ed., 2005.

[100] W. C. Pao and Y. F. Chen, "Adaptive gradient-based methods for adaptive power allocation in ofdm-based cognitive radio networks," *IEEE Transactions on Vehicular Technology*, vol. 63, pp. 836–848, February 2014.

Appendix A

Convexity of the derived BER function P_b

We use Fig. A.1 and Fig. A.1 to show that 5.12 is a convex function and a strictly decreasing function of λ_1 and λ_2. Fig. A.1 illustrates the decrease of 5.12 as λ_1 decreases and λ_2 takes the two constant values 1 dB and 4 dB. Fig. A.2 illustrates the decrease of 5.12 as λ_2 decreases and λ_2 takes the two constant values 1 dB and 4 dB. In both figures, the BER is lower when the constant value is 4. The objective function considered in (5.13) is a strictly convex function for the values of λ_1 and λ_2 represented on Fig. A.1 and Fig.A.2 because the BER function decreases strictly with the increase of either λ_1 and/or λ_2. Hence the optimal value of (5.13) is achieved at a point (in $\Re^2$) in the set specified by the second constraint in (5.13) imposed by the outage at the *SCN*. This is due to the fact that the outage threshold values are inferior to P_{max}.

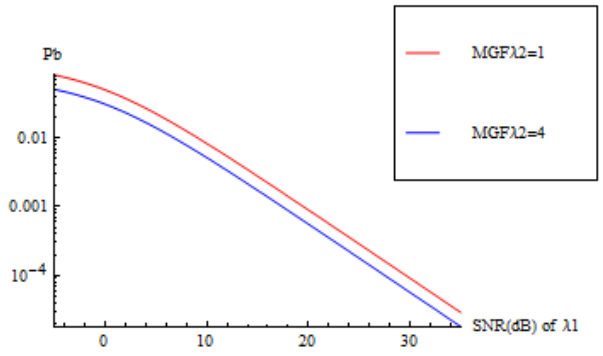

Fig. A.1 Derived unequal branch SNR BER decreasing function of λ_1.

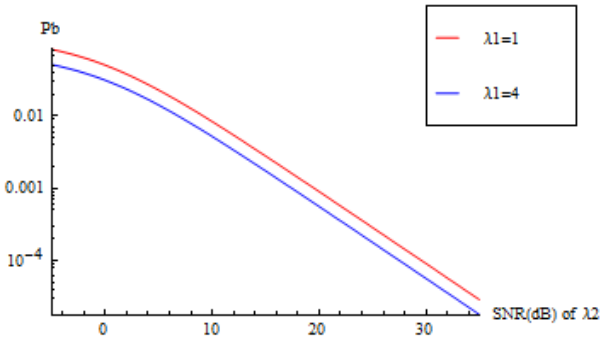

Fig. A.2 Derived unequal branch SNR BER is a decrasing function of λ_2.

Appendix B

Publication List

- Journal papers:
  [1] M. Ndong and T. Fujii, "Handling cross-tier interference in underlay macrocell system for future small cell networks", Journal of Communications and Networks (JCN), (accepted for publication), July 2014.(Related to chapter 3)
  [2] M. Ndong and T. Fujii, "Cross-tier interference management with a distributed antenna system for multi-tier cellular networks", EURASIP Journal on Wireless Communications and Networking.2014, 2014 : 73, DOI: $10.1186/1687-1499-2014-73$.(Related to chapter 4)

- Conference papers:
  [1] M. Ndong and T. Fujii," Adaptive Modulation and User Control for Cellular System with Adaptive Array Antenna based on Normalized Doppler Shift", IEICE Society Conf., $B-1-191$, Niigata (Japan), September 2009.
  [2] M. Ndong and T. Fujii, "Interference cancellation for spectrum shared femtocell networks with macrocell information feedback", in Int. Conf. on Ubiquitous and Future Netw.(ICUFN),Dallian (China), pp.$65-70$, June 2011.
  [3] M. Ndong and T. Fujii, "Cross-tier interference mitigation for self-organized self -optimized femtocells", in Wireless Telecommun. Symp. ($WTS2012$), London, April 2012.
  [4] M. Ndong and T. Fujii, "Cross-tier interference management with distributed antenna system for femtocell self-optimized networks", in Triangle Symposium on Advanced ICT (TriSAI), Tokyo, pp. $1-5$, September 2012.
  [5] M. Ndong and T. Fujii, "Distributed antenna system aided cross-tier interference management for small cell networks", In IFIP Wireless Days (WD), Dublin, pp.$1-5$,

November 2012.

[6] M. Ndong and T. Fujii, "Joint Femtocell Clustering and Cross-tier Interference Mitigation with Distributed Antenna System in Small Cell Networks", IEICE technical report, *Vol*.113, *No*.131, Shizuoka (Japan), July 2013.

[7] M. Ndong and T. Fujii,"Joint antenna selection and power allocation for distributed-STBC cognitive small cell networks", IEICE technical report, *SR*2013 – 109, Tokyo, March 2014.

[8] M. Ndong and T. Fujii," Joint Femtocell Clustering and Cross-tier Interference Mitigation with Distributed Antenna System in Small Cell Networks", 9*th* IEEE/IET International Symposium on Communication Systems, Networks and Digital Signal Processing (CSNDSP) , July 2014.

[9] M. Ndong and T. Fujii", Joint antenna selection and power allocation for distributed-STBC cognitive small cell networks," 17*th* International Symposium on Wireless Personal Multimedia Communications (WPMC), September 2014. (Related to chapter 5)